2017

Brazilian Surface and Upper-level Wind Characteristics Based on Ground and Model Observations from 1980–2014

Joshua M. Gilliland
Louisiana State University and Agricultural and Mechanical College, jgilli7@lsu.edu

BRAZILIAN SURFACE AND UPPER-LEVEL WIND CHARACTERISTICS BASED ON GROUND AND MODEL OBSERVATIONS FROM 1980–2014

A Dissertation

Submitted to the Graduate Faculty of the
Louisiana State University and
Agricultural and Mechanical College
in partial fulfillment of the
requirements for the degree of
Doctor of Philosophy

in

The Department of Geography and Anthropology

by
Joshua M. Gilliland
B.S., The Ohio State University, 2009
M.S., Western Kentucky University, 2011
August 2017

I dedicated this dissertation in memory of my grandparents, Ed and Rose Martof, aunt, Vicki Wilt, uncle, Joe Giampapa, and golden retriever, Cody.

ACKNOWLEDGMENTS

I would like to acknowledge my parents, Hank and Rita. Thank you for allowing me the opportunity to continue my education at Louisiana State University. Without your continued support and sacrifices, I would have never of gotten to this point in my life. The values and lessons that you instilled in me from a young age have encouraged me to continue to reach for the stars and never settle for anything less. Thank you and I love you very much!

To my brothers, Nick and Adam, I would like to thank you for your continual support through this part of my journey here in Louisiana. I could not ask for any better brothers whom to share my problems and concerns. I would like to also acknowledge my entire extended family for their support and guidance throughout the years.

I would like to thank my advisor, Dr. Barry D. Keim, for sharing his expertise and mentoring me through my research and guiding me through my final part of my graduate education process. In addition, I would to acknowledge my committee members, Drs. Aly-Mousaad Aly, Joshua D. Durkee, Robert V. Rohli, and Jill C. Trepanier, for their advice and guidance through the dissertation process.

TABLE OF CONTENTS

LIST OF TABLES

LIST OF FIGURES

ABSTRACT

The examination of temporal changes in surface winds has been analyzed by scientists for a variety of physical, biological, climatological, and socioeconomic reasons. This research uses surface and upper-level wind data from historical *in-situ* and climate models to examine the geographical and climatological characteristics of wind across Brazil during 1980–2014.

Overall linear and quantile regression shows that surface wind speed trends are changing regionally across Brazil. Wind speeds across northeastern Brazil are increasing, while a decreasing trend is documented for interior and southeastern Brazil. The spatial and temporal trends found are possibly related to alterations in the physical landscape (urbanization and land-cover change) and the seasonal relationship between the Intertropical Convergence Zone and the South Atlantic Anticyclone. To further examine the role of the South Atlantic Anticyclone, an additional analysis was performed to show how the position of high pressure system affects surface conditions across Brazil. Results show that surface winds across northern Brazil are affected by an equatorward shift of the semi-permanent high pressure, while southern Brazil is more influenced by migrating anticyclones that were passing through the South Atlantic Basin.

A spatial and temporal analysis of upper-level wind speed trends was conducted to examine how surface and marco-scale features have evolved over Brazil. An overall vertical profile shows a decreasing trend in lower-level winds (1000–850 hPa) that switches to a positive trend in the upper portions of the atmosphere (400–200 hPa). A geographical interpretation of upper-level wind trends was performed based on a three-dimensional model. The model depicts that seasonal wind trend patterns across Brazil

occur within the proximity of the Bolivian high and subtropical jet (400–200 hPa). A regional analysis confirms the role of these two synoptic features.

CHAPTER 1
INTRODUCTION AND LITERATURE REVIEW

1.1 Introduction

Earth's climate is an ever-changing and developing complex system that greatly affects physical, biological, and socioeconomic environments. Wind is an essential component of Earth's climate at micro-, meso-, and synoptic scales. Recent studies note that near-surface and upper-level atmospheric conditions have been influencing wind speeds across the globe (McVicar and Roderick 2010; Vautard et al. 2010; McVicar et al. 2012). Therefore, a present debate among scientists is whether macro-scale synoptic circulation is the lone factor for causing wind trends to change over time or if some unknown or misunderstood variable(s) (e.g., land-cover change, urbanization, etc.) may also play a role. Regardless, wind is a physical component associated with many weather-related (e.g., tropical and mid-latitude cyclones, tornadoes, downbursts, storm surge, etc.) and socioeconomic (energy, soil erosion, aviation, etc.) phenomena, which are known to result both in catastrophic events and impact the human condition.

Hazard studies have shown that wind-related events are capable of producing human causalities and major socioeconomic losses (Ashley and Black 2008; Changnon 2009; Schmidlin 2009; Black and Ashley 2010; Schoen and Ashley 2011; Barthel and Neumayer 2012). Table 1.1 depicts the number of wind-related fatalities by meteorological type in the United States. This table demonstrates how vulnerable humans are to meteorological hazards despite technological advancements and warning system upgrades. Interestingly, Kahn (2005) analyzed natural disaster deaths for 73 countries from 1980 to 2002 and found that nearly half were attributed to wind-related events (i.e., cyclones, hurricanes, storms, tornadoes, tropical storms, typhoons, and winter

storms). Changnon (2009) documented 176 wind-driven storms in the U.S. that produced more than $15 billion dollars in total losses between 1952 and 2006. Barthel and Neumayer (2012) found that global (U.S.) average insured loss per windstorm during 1990–2008 (1973–2008) was $21.1 ($33.6) million dollars. These findings demonstrate near-surface winds are problematic to humans and require further research.

Table 1.1. Number of wind-related fatalities in the U.S. based on meteorological hazard type.

Original Paper	Period	Tornado	Convective/ Nontornadic	Nonconvective	Tropical Cyclone
Ashley and Black (2008)	1980–2005	1388	696	616	181
Schmidlin (2009)	1995–2007	28	165	143	57
Black and Ashley (2010)	1975–2005	1710	1195	635	181
Schoen and Ashley (2011)	1998–2007	634	191	–	–

1.2 Literature Review

Climatologists and meteorologists still have many unanswered questions about surface winds. Studies have focused on understanding and evaluating the characteristics of surface winds based on three basic principles: socioeconomics, anthropogenic activity, and synoptic variability. The main focus of those studies has examined variations in synoptic and anthropogenic to help explain changes occur in near-surface winds across Earth. Therefore, this literature review provides a comprehensive overview on surface wind speeds and trends at different spatial and temporal scales to understand how changes in atmospheric conditions could be affecting these changes on Earth's surface.

1.2.1 Global

Several studies have performed general global wind trend analysis using various observational records, meteorological gridded datasets, and climatic models (Vautard et al. 2010; Zhao et al. 2011; Bichet et al. 2012). Vautard et al. (2010) found that observed surface winds are weakening over the period from1979 to 2008 across North America, eastern and central Asia, and Europe. McVicar et al. (2012) established a similar pattern to Vautard et al. (2010) when conducting a global review on relationships between wind speed and evaporation. When these results are compared to National Center for Environmental Prediction/National Center for Atmospheric Research reanalysis dataset (NCEP/NCAR), however, the negative trend disappears for each region, likely because NCEP/NCAR modeling does not include land-cover change as a parameter (Vautard et al. 2010). The study further explains that NCEP/NCAR model assimilates near-surface winds from a fixed climatological land scheme and extrapolation method.

Table 1.2. Total number of wind trend (i.e., positive and negative) studies from 1989 to 2011 conducted for each region identified by McVicar et al. (2012).

Region	Number of Studies	Positive	Negative
North America	27	6	21
Central and South America	7	2	5
Europe	24	4	20
Asia	38	0	38
Sub-continent	6	0	6
Middle-East	14	6	8
Africa	21	5	16
Oceanic	9	2	7
Antarctica	2	2	0
	148	27	121

Table 1.2 shows that 82% (121) of all studies examined found a negative temporal trend in the annual mean wind speed (McVicar et al. 2012). The only regions showing a consistent positive upward trend were located in polar latitudes, a result that could be

related to the shift of mid-latitude cyclones to higher latitudes over time (McVicar et al. 2012). A regional breakdown is necessary to understand how wind speeds have changed over time.

1.2.2 North America

Klink (1998) constructed a 30-year mean wind speed, variance, and direction climatology for the month of January using 216 U.S. observations stations between 1961 and 1990. Klink (1998) showed the highest (lowest) mean wind speeds are experienced in the central plains and northeastern part of the United States (southwest and Appalachian Mountains). The study also documented four primary cardinal direction groupings: a westerly component (i.e., west, northwest, and southwesterly) from the Great Plains to the northeast, a northeasterly wind orientation for the Gulf Coast, a southeasterly flow for the West Coast, and a highly variant flow around the Rocky Mountain range. Klink (1999a; 1999b) further expanded the study to include all other months and additional statistical parameters (i.e., minimum and maximum) which determined that the strongest (weakest) mean wind speeds occur during winter and spring (summer). Similarly, Pryor et al. (2007) documented a wind trend and speed relationship for 157 weather stations from 1973 to 2005 and found that the highest wind speeds are observed in the eastern (western) U.S. during winter (spring and summer). Klink (1999a) explained that a strong equator-to-polar temperature and pressure gradient affect surface wind speeds in particular regions across the United States. The study showed that cardinal wind directions across the central and northeastern (southeastern) U.S. become more (less) variable during the spring and eventually shift to a southerly direction during summer. Klink (1999a; 1999b) suggested that local topography, atmospheric circulation,

and air mass origin contribute to wind variability across the United States. The findings also demonstrate that western (southeastern) stations observe relatively high (low) wind speed variance (Klink 1999a).

Time-series analysis was performed to understand how atmospheric patterns are affecting near-surface wind velocities across the United States. For example, Abhishek et al. (2010) found that Cincinnati, Ohio; Indianapolis, Indiana; and Little Rock, Arkansas, all demonstrated a negative wind trend during the 20th century. A significant indicator of the downward trend is the number of calm wind reports observed, from 3% in the 1940s to almost 10% in 2008 (Abhishek et al. 2010). The study proposed that the amplified frequency in calm reports is interconnected with macro-scale synoptic and teleconnections (i.e., Pacific North American (PNA); Wallace and Gutzler 1981) pattern. However, when analyzing wind observations for 41 northeastern stations, DeGaetano (1998) found that the increase in calm reports between 1960s and 1990s is associated with human reporting bias and instrumentation error.

Despite conflicting findings between Abhishek et al. (2010) and DeGaetano (1998), other research has shown that the overall surface mean wind speed has declined across the United States (Klink 1999b; Klink 2002; Pryor et al. 2007). In a wind speed trend climatology for the contiguous U.S., Pryor et al. (2007) found statistically significant (p<0.05) negative wind trends for 71% (111) of the stations, with the highest concentration occurring in the Midwest. In a similar way, Klink (2002) documented a decreasing trend in wind speeds for seven observations stations in Minnesota. However, Klink (1999b) found that the overall mean minimum monthly wind speeds have declined for 176 stations during 1961–1990. Klink (1999b; 2002) suggested that microscale,

mesoscale, and global factors (i.e., surface temperature, seasonal cyclonic activity, urbanization, instrumentation, etc.) are contributing to the continual fluctuation in wind trends and speeds across the United States. However, Pryor et al. (2007) found that no major changes occurred in the 50^{th} and 90^{th} percentile wind speeds with the implementation of Automated Surface Observation Systems (ASOS) installed during the 1990s. This result supports findings of Klink (1999b; 2002) that atmospheric variables rather than instrumental issues may be prompting the decline in recent wind speeds across the United States.

Recent studies have shifted from investigating surface winds (10 m) to analyzing trends in modeled wind speeds at 80 m above the ground to assess the potential for wind energy production (Li et al. 2010: Greene et al. 2012; Holt and Wang 2012). Li et al. (2010) used wind data from the National American Regional Reanalysis (NARR; Mesinger et al. 2006) to understand wind characteristics of the Great Lakes region from 1979 to 2008. During the 30-year period, Li et al. (2010) found that the strongest (weakest) 80 m wind observations occurred during November–January (July–September). The study explained that these wind patterns are primarily driven by seasonal temperature and pressure gradient changes. However, Li et al. (2010) argued that seasonal wind magnitude and variability could be possibly related to El Niño/ Southern Oscillation (ENSO). The study found that during warm phases (El Niño) of ENSO, wind speeds are weaker which occurs from a greater frequency of calm periods observed across the Great Lakes region during spring and winter (Li et al. 2010). Cold phases (La Niña) of ENSO are more prone to influence wind speeds (i.e., higher variability) across the Great Lakes during summer and winter (Li et al. 2010). Despite

the phase of ENSO, Lin et al. (2010) calculated positive linear trends over both water (0.14 m s^{-1} $decade^{-1}$) and land (0.09 m s^{-1} $decade^{-1}$) for the Great Lakes region.

Following this idea further, Greene et al. (2012) used extrapolation 80 m wind data from North American Regional Climate Change Assessment Program (NARCCAP; Mearns et al. 2009) to describe the negative wind speed trend across the western High Plains from 1971 to 2000. Greene et al. (2012) identified a seasonal wind trend pattern similar to Li et al. (2010), in which the largest (smallest) wind speed variations occurred during winter and spring (summer and fall). A spatial analysis demonstrated that the greatest decreases (7%) occurred in southeastern Wyoming and western Nebraska during the 30-year period (Greene et al. 2012). Greene et al. (2012) constructed two arguments for the wind decline over the western High Plains: fewer and weaker cold fronts and a northward migration of synoptic systems.

However, Holt and Wang (2012) found increasing wind speed trends at 10 m (0.15 m s^{-1} $decade^{-1}$) and 80 m (>0.1 m s^{-1} $decade^{-1}$) for a majority of the continental U.S., including an increase up to 0.3 m s^{-1} $decade^{-1}$ for the central Plains and upper Midwest during 1979–2009. The study (2012) also found a similar wind pattern for the Great Lakes as described by Li et al. (2010) and hypothesized about the role of mid-latitude jet over the region. These results suggest that numerical models and observational datasets need to be scrutinized before any conclusive results can be drawn from them (Pryor et al. 2009). Table 1.3 summarizes the overall wind trends found for the U.S based on different record periods, study regions, and data types.

Table 1.3. Previous work conducted with land-based and numeric model data over U.S. and the wind speed trend magnitudes (m s^{-1} $decade^{-1}$) calculated for each study of interest.

Original Paper	Region	Period	Data Type	Height (m)	Trend (m s^{-1} $decade^{-1}$)
Klink (1999b)	Lower 48	1961–1990	Surface	6.1	-0.04
Klink (2002)	Minnesota	1962–1993	Surface	8	-0.05
Abhishek et al. (2010)	Midwest	1948–2008	Surface	10	-0.07
Li et al. (2010)	Great Lakes	1979–2008	Model	80	Land: 0.14 Lake: 0.09
Pryor and Ledolter (2010)	Lower 48	1973–2001 1973–2005	Surface	10	-0.32 – -0.14
Holt and Wang (2012)	Lower 48	1979–2009	Model	10	0.15
				80	>0.10

Wan et al. (2010) provided a near-surface wind trend analysis for 117 Canadian observation stations from 1953 to 2006. The study found that wind speeds declined (increased) over western and southern Canada (Canadian Arctic and Atlantic Maritimes) for all seasons (Wan et al. 2010). Table 1.4 provides a regional breakdown of the monthly linear trends described by Wan et al. (2010). This general trend is in agreement with Tuller (2004), who found a general negative wind speed trend for three west coast Canadian observation sites. Hundecha et al. (2008) concurred, finding that 69% (9) of all stations located along the Gulf of St. Lawrence showed a decline in wind speed from 1979–2004.

A seasonal time series shows wind trends (i.e., mid-1970s and early 1980s) are positively correlated with Pacific Decadal Oscillation (PDO) and PNA across Canada (Tuller 2004). Wan et al. (2010) noted that the increase in wind speeds for the central Canadian Arctic for all seasons and in Maritime Atlantic for fall and spring and suggest various atmospheric circulations (i.e., Arctic Oscillation (AO), North Atlantic Oscillation (NAO), PDO, and ENSO) are responsible for the short-term and long-term wind patterns

experienced throughout Canada. St. George and Wolfe (2009) analyzed long-term wind speed observations across the southern Canadian Prairies from 1953 to 2006 and found a significantly statistical relationship (p=0.003) between a positive phase of Southern Oscillation Index (SOI, Ropelewski and Jones 1987) and weak surface winds during winter. However, Griffin et al. (2010) suggested that the geographic heterogeneity (i.e., coastal and inland stations) and topography can influence temporal wind trends for the Canadian Pacific Northwest. The study analyzed 179 weather stations during 1950 to 2008 and found that coastal sites show a fluctuating temporal pattern (8–10 year periods), while mainland locations show a negative wind trend for the Pacific Northwest (Griffin et al. 2010). Griffin et al. (2010) proposed that the cyclical pattern found along coastal stations could be explained by an unknown macro-scale climate oscillation.

Table 1.4. Canadian regional linear mean trend estimates (m s^{-1} $decade^{-1}$) and p-values during 1979–2004 based on Wan et al. (2010).

Region	Trend (m s^{-1} $decade^{-1}$)	p-value
Central Canadian Arctic	0.023	0.027
Yukon- Northwest Territories	-0.042	>0.001
British Columbia	-0.048	>0.001
Prairies	-0.065	>0.001
Ontario	-0.061	>0.001
Quebec and Baffin Island	-0.059	>0.001
Maritimes	0.008	0.165
Newfoundland and Labrador	-0.017	0.072

1.2.3 Europe

Studies across northern and western Europe examined surface wind characteristics at a variety of temporal and spatial scales (Jönsson and Fortuniak 1995; Pryor and Barthelmie 2003; Hewston and Dorling 2011; Wever 2012). Jönsson and Fortuniak (1995) analyzed surface wind directions from 1741 to1990 for an observation station in southern Sweden. The study found three stages or phases (continental low-

zonality, an immediate maritime, and maritime high-zonality) to describe wind characteristics at Lund, Sweden (Jönsson and Fortuniak 1995). Wever (2012) established a statistically significant (p<0.05) negative linear trend (-0.06 m s^{-1} $decade^{-1}$) in wind speed for 59 Swiss stations between 1982 and 2009 using European Climate Assessment and Dataset (Klein Tank et al. 2002). A regional breakdown by Wever (2012) described the spatial and temporal mean wind speed trends for six northern and western European countries (Table 1.5).

Pryor and Barthelmie (2003) analyzed wind speeds at 850 hPa from 1953 to 1999 and determined that the annual mean wind speed has linearly increased over the Baltic region. Annual and winter mean wind speed trends indicated that the largest increase developed in the southwest part of the Baltic basin at a rate of 0.25 m s^{-1} $decade^{-1}$ (Pryor and Barthelmie 2003). The study also found that extreme wind observations increased by as much as 5 m s^{-1} during a 50-year period. Pryor and Barthelmie (2003) explained this positive temporal wind trend by connecting the increase in seasonal and extreme wind events to a positive NAO phase. However, Wever (2012) evaluated the effects of surface roughness on wind speeds from 1962 to 2009. Wever (2012) concluded that wind speeds over the Netherlands diminished linearly on average by 3.1% (0.13 m s^{-1}) per decade due to the doubling of surface roughness since 1981. Wever (2012) then developed a boundary layer model to simulate the effects of surface roughness on wind speeds and found that 70% of the wind speed decline was contributed by changes in the surface roughness associated with land redevelopment (i.e., urbanization, forestation, and pasture land).

Table 1.5. Linear trend (m s^{-1} $decade^{-1}$) analysis of the annual mean wind speed for six European countries during 1982–2009 from Wever (2012). A * indicates linear trend is statistically significant (p<0.05).

Country	Stations	Trend (m s^{-1} $decade^{-1}$)
Switzerland	59	-0.06*
Germany	28	0.10*
Estonia	2	-0.36*
Ireland	11	-0.09
Netherlands	34	-0.34*
Norway	15	0.01

Hewston and Dorling (2011) conducted a gust climatology for 43 United Kingdom Meteorological Office stations from 1980 to 2005 and found a statistically significant (p<0.05) decline of 5% (0.2 m s^{-1} $decade^{-1}$) in the daily maximum gust speed (DMGS) and a decrease of 8% (0.8 m s^{-1} $decade^{-1}$) in extreme DGMS (i.e., top 2% of all DMGS). A seasonal breakdown indicated that long-term variations are evident in the study, with the largest (smallest) decrease in DGMS occurring in fall (winter) since 1980. As a result, Hewston and Dorling (2011) proposed that a decadal macro-scale atmospheric circulation relationship exists between NAO and DGMS and extreme DGMS in the United Kingdom.

A similar decline in wind speeds and trends is described for eastern and southern Europe (Brázdil et al. 2009). The study found an overall decline in monthly, seasonal, and annual wind speeds for 23 climatological stations in the Czech Republic from 1961 to 2005. This decrease in mean wind speed is a product of the increase in frequency of anticyclonic activity over Europe between 1960 and 1990, which was followed by a rise in cyclonic circulation (Brázdil et al. 2009). However, Wever (2012) found an annual linear increase (0.06 m s^{-1} $decade^{-1}$) in wind speeds for 11 Czech Republic sites during

1982–2009. These conflicting findings may result from different methods used to calculate mean wind speeds (daily, monthly, or annual) or length of record used.

Other studies have focused on the effects of wind across the Mediterranean and Adriatic regions of southern Europe (Pirazzoli and Tomasin 1999; 2003). Pirazzoli and Tomasin (1999) analyzed three-hourly surface wind data from four Italian meteorological stations between 1951 and 1996 and found a sharp decline in the magnitude and number of Bora winds. The study attributes the decline to a climate and synoptic shift of anticyclonic and cyclonic activity in central and southern Europe (Pirazzoli and Tomasin 1999). As a result, an increase in calm wind reports indicates that a change is developing at the surface and in the atmosphere. Pirazzoli and Tomasin (1999) found that calm wind reports have increased from 26% in the 1950s to 44% in the 1990s. This dramatic rise in reports is troubling and warrants further investigation.

In another study, Pirazzoli and Tomasin (2003) investigated 17 coastal Italian stations along the Adriatic and Tyrrhenian basins to determine if any relationships exist between wind speed and sea surface temperature. The research determined that two wind trends existed: a linear decline of wind speeds from 1951 to 1975 and an increasing linear trend after 1975 (Pirazzoli and Tomasin 2003). Pirazzoli and Tomasin (2003) proposed that wind speeds are positively correlated with temperature changes experienced during the study period. Liuzzo et al. (2016) analyzed evapotranspiration for 10 southern Italian observation stations and found that 6 (1) sites show statistically significant (p<0.10) linear wind trend increases (decreases) during 1968–2004. Similarly, Liuzzo et al. (2016) identified a positive relationship between wind speed and temperature based on evapotranspiration forecast scenarios.

More recently, wind speed analysis was performed for Spain and Portugal (Moratiel et al. 2011; Azorin-Molina et al. 2014). Azorin-Molina et al. (2014) examined wind speeds for 54 (67) observation stations during 1961–2011 (1979–2008) and found a linear decline in wind speeds across the Iberian Peninsula. A seasonal breakdown determined a negative (positive) linear wind trend over winter and spring (summer and fall) for both study periods (Azorin-Molina et al. 2014). As a result, Azorin-Molina et al. (2014) evaluated three macro-scale atmospheric circulations (i.e., NAO, Mediterranean oscillation index–MOI; Palutikof 2003, and western Mediterranean oscillation index–WEMOI; Martin-Vide and Lopez-Bustin 2006) and urban-rural sites differences to explain the seasonal, annual, and long-term variability that currently exists across Spain and Portugal. However, Moratiel et al. (2011) found that wind speeds have linearly increased at both annual and monthly intervals over the northwest Iberian Peninsula during 1980–2009.

1.2.4 Middle East

Limited research has been conducted to understand surface winds across Middle East. McVicar et al. (2012) describes mixed trend results due to the limited results (i.e., number of observations and period of record) and paucity of studies conducted for the region. Recently, Dadaser-Celik and Cengiz (2014) investigated wind speed trends for 206 Turkish weather stations between 1975 and 2006 and found that the majority of sites are observing a negative linear temporal trend at monthly, seasonal, and annual intervals. Dadaser-Celik and Cengiz (2014) found that the wind speed changes across Turkey are (are not) related to alterations in macro-scale atmospheric circulations and air temperatures (data quality and land-cover type). The study found that annual linear wind

trends showed a strong correlation between atmospheric conditions (temperature and atmospheric circulation), while a small annual mean standard deviation (0.29 m s^{-1} $decade^{-1}$) and a nonsignificant paired *t*-test (p=0.11) among urban and rural wind stations was found for Turkey.

1.2.5 Asia

During the past decade, climatologists and meteorologists focused on analyzing wind trends in China (Xu et al. 2006; Jiang et al. 2010; Fu et al. 2011; Guo et al. 2011; Yang et al. 2012; Lin et al. 2013; Cheng et al. 2013; You et al. 2014). Table 1.6 shows a consistent overall linear decline in the annual mean wind speed over China ranging between 0.12 and 0.24 m s^{-1} $decade^{-1}$. Fu et al. (2011) found that 81% (481) of observation sites across China are showing negative wind trends, of which 66% (392) are statistically significant (p<0.05). Similarly, Xu et al. (2006) examined surface wind data for 305 weather observation sites and found that the annual mean wind speed has decreased by 28%, with the number of high-wind days (>5 m s^{-1}) also declining by 58%. The study explains that simultaneous significant warming (cooling) in the northern (southern) region of China was responsible for the weakening of meridional pressure gradient and therefore the wind speeds commonly associated with East Asian monsoons (Xu et al. 2006). You et al. (2014) documented a statistically significant (p<0.01) negative correlation between wind speed and temperature across the Tibetan Plateau from 1980 to 2005. Jiang et al. (2010) argued a similar concept but further explained that contrasts in sea level pressure and surface temperature between Asia and the Pacific Ocean have disrupted the macro-scale atmospheric circulation (i.e., meridional and zonal flow), resulting in an amplitude change of East Asian monsoons.

Table 1.6. As in Table 1.3 except from surface observation data for China.

Original Paper	Period	Region	Stations	Trend ($m\ s^{-1}\ decade^{-1}$)
Chen et al. (2013)	1971–2007	Contiguous China	540	-0.17
Fu et al. (2011)	1961–2007	Contiguous China	597	-0.13
Guo et al. (2011)	1969–2005	Contiguous China	652	-0.18
Jiang et al. (2010)	1956–2004	Contiguous China	535	-0.12
Lin et al. (2013)	1960–2009	Contiguous China	–	-0.10
Shenbin et al. (2006)	1961–2000	Tibetan Plateau	101	-0.13
Yang et al. (2012)	1969–2009	Southwestern China	110	-0.24
You et al. (2014)	1980–2005	Tibetan Plateau	71	-0.24

Guo et al. (2011) found that 72% (469) of the observation sites evaluated from 1969–2005 exhibited a statistically significant ($p<0.05$) decline in wind speeds. Guo et al. (2011) recognized tropospheric modifications (i.e., pressure gradient force) and urbanization as the primary factors in the reduction of wind speeds across China. Additionally, Fu et al. (2011) determined that wind speeds are highly correlated with the phase of Interdecadal Pacific Oscillation (IPO, Mantua et al. 1997). Chen et al. (2013) compared observations from 540 weather stations to the NCEP/NCAR reanalysis dataset during 1961–2007 and found that macro-scale oscillations are influencing mean wind speeds across certain geographical regions of China. In particular, Chen et al. (2013) found that during a positive AO phase, a large portion of China experiences lower mean wind speeds. However during a positive ENSO (Niño 3.4 region) phase, the highest (lowest) wind speeds are observed in the northern (southern) part of the country (Chen et al. 2013). As a result, these studies demonstrated that various macro-scale conditions and circulations are affecting wind trends in China.

Studies have also observed various wind speed patterns (i.e., short-term and long-term) over the last century in China (Shenbin et al. 2006; Jiang et al. 2010; Fu et al. 2011; Guo et al. 2011; Chen et al. 2013; You et al. 2014). Specifically, Guo et al. (2011) found

a prominent fluctuation in wind speed based on seasonality for China. The largest linear decreasing (smallest) trends between 1969 and 2005 occurred during spring (summer) at a rate of 0.21 m s^{-1} $decade^{-1}$ (0.15 m s^{-1} $decade^{-1}$, Guo et al. 2011). However, Jiang et al. (2010) explained that the peak wind speed change developed during winter (-0.151 m s^{-1} $decade^{-1}$) rather in in spring (-0.149 m s^{-1} $decade^{-1}$) between 1956 and 2004. This variation in seasonalityis likely due to the difference of time period and surface observation data used to conduct each study. Similarly, Fu et al. (2011) described the removal of observations from its study prior to 1960 due to the lack of available station data and gaps and discrepancies found in the records. These variances may contribute or explain the disparity found between Jiang et al. (2010) and Guo et al. (2011). Likewise, Chen et al. (2013) suggested that anemometer height changes could be exacerbating the annual wind speeds and observations across China during the 1970s because the European Center for Medium-Range Weather Forecasts 40 years Re-Analysis (ERA-40) does not show any significant trends for 10 m wind speeds during 1971–2007.

Another component of detecting wind trend variations is evident from a time series perspective (Xu et al. 2006; Jiang et al. 2010; Fu et al. 2011; Guo et al. 2011; Chen et al. 2013; Lin et al. 2013). Fu et al. (2011) established four distinct temporal wind phases for China: two steady wind periods from 1961 to 1968 and 1969 to 1974, a sharp decline in 1974–1990s, followed by another constant wind speed era from 1990s to 2007. The study explains that the trends are derived from instrument relocation, land use and land-cover change, and synoptic parameters (Fu et al. 2011). Lin et al. (2013) also noted two wind speed increases during the early 1970s and middle 2000s over China. Chen et

al. (2013) found a similar pattern and attributed the trend to a change in the upper 90^{th} (95^{th}) wind speed percentile by -0.39 m s^{-1} $decade^{-1}$ (-0.50 m s^{-1} $decade^{-1}$).

Urbanization is another factor possibly influencing wind records and trends across China (Xu et al. 2006; Jiang et al. 2010; Guo et al. 2011). Jiang et al. (2010) analyzed wind speeds from 174 urban and 180 rural observation sites and found two major results: urban stations tend to record weaker annual mean wind speeds with a distinct negative mean wind speed trend denoted from 1956 to 2004 due to urban development in China. Yang et al. (2012) identified a statistically significant (p<0.05) linear decrease of wind speeds (i.e., during seasonal and annual intervals) in urban vs. rural sites in southwestern China from 1969 to 2000. On the other hand, Guo et al. (2011) determined that urban and rural stations follow a comparable negative wind speed trend until 1990 when a positive shift is noted in urban observations. An explanation of this upward trend in urban stations is not provided and contradicts the effect of frictional drag on wind speed in urban development (Guo et al. 2011). Lin et al. (2013) support the idea that urbanization and land-cover change are not influencing surface wind speeds and suggest that atmospheric processes are the major factor contributing to the downward trend across China. However, You et al. (2014) explained that a combination of anthropogenic (i.e., surface roughness, land-cover change, urbanization, etc.) and natural (i.e., synoptic, atmospheric circulations, topography, etc.) causes may possibly be leading to the overall wind speed changes occurring across China.

Recent work also describes the spatial heterogeneity of linear temporal wind trends across China (Xu et al. 2006; Jiang et al. 2010; Fu et al. 2011; Guo et al. 2011; Yang et al. 2012). The largest wind speed decreases are observed in northern China,

Tibetan Plateau, and coastal China (Xu et al. 2006; Shenbin et al. 2006). Xu et al. (2006) suggested that recent temperature increases from solar radiation has resulted in the weakening of monsoonal winds which greatly influences wind speed within these regions. This concept is supported by You et al. (2014) who found a negative correlation between sunshine hours and wind speed at an annual and seasonal (i.e., spring, summer, and autumn) basis in Tibetan Plateau. In addition, Yang et al. (2012) described sunshine radiation as a possible cause of surface wind speed decreases but suggested that other atmospheric, anthropogenic, and topographic influences may be contributing to the decline for southwestern China.

Wind speed trends have also been conducted to understand relationships between evaporation or potential evapotranspiration (PET) and other atmospheric variables in China (Zheng et al. 2009; Liu et al. 2010; Liu et al. 2011; Yin et al. 2010a; 2010b; Tang et al. 2011). Table 1.7 shows that annual wind speed magnitudes have declined during the late 20th century. Many of these studies establish a relationship evaporation and PET to wind speed changes in China. Yin et al. (2010b) explained that the decline results from changes in macro-scale atmospheric circulations (i.e., East Asian monsoon and Siberian high) in northern China and Tibetan Plateau. The weakening (strengthening) of meridional (zonal) circulation is related to the evolving location of the Siberian high which maybe influencing the relationship between evaporation and wind speed across China (Yin et al. 2010b). Zheng et al. (2009) found that evaporation increases due to atmospheric warming were offset by other climatic variables (i.e., wind speed, solar radiation, and vapor pressure) in the Haihe River Basin. Therefore, wind speed is not the only atmospheric variable affecting evaporation and PET in China.

Table 1.7. Studies investigating changes in evaporation and potential evapotranspiration for China using wind speed as a variable (m s^{-1} $decade^{-1}$). A *(**) indicates linear trend is statistically significant at 95% (99%) confidence-level.

Original Paper	Period	Study Region	Stations	Trend (m s^{-1} $decade^{-1}$)
Zheng et al. (2009)	1957–2001	Haihe River	45	-0.14*
Liu et al. (2010)	1961–2006	Yellow River	89	-0.09*
Liu et al. (2011)	1960–2007	Contiguous China	518	-0.12**
Yin et al. (2010a)	1961–2008	Contiguous China	595	-0.09
Yin et al. (2010b)	1960–2009	Contiguous China	603	-0.12
Tang et al. (2011)	1961–2000	Haihe River	34	-0.14*

1.2.6 India

Jaswal and Koppar (2013) analyzed the wind characteristics for 171 Indian weather sites between 1961 and 2008. The study reported that monthly and annual wind trends are declining linearly across the study region. Overall monthly and annual linear trends were found to be statistically significant (p<0.01) with an overall mean wind speed trend decreasing at a rate of 0.24 m s^{-1} $decade^{-1}$ for India (Jaswal and Koppar 2013). Bandyopadhyay et al. (2009) found that 85% (113) of observation stations were detecting a decrease in wind speeds during 1971–2002. As a result, Jaswal and Koppar (2013) examined several possible reasons that surface winds are slowing across India. Jaswal and Koppar (2013) discussed the decrease frequency of cyclonic activity in the Bay of Bengal has led to the decline in the annual average wind speed across India as one possible reason. Jaswal and Koppar (2013) also analyzed sea surface temperature (SST) and urbanization as other motives connected to the decline in wind speeds across India.

1.2.7 Australia

McVicar et al. (2008) performed a wind speed climatology for Australia based on daily u wind data at 2 m from 1975 to 2006. The study found on average a linear trend of -0.09 m s^{-1} $decade^{-1}$ for 88% of the observation stations in Australia. Interestingly, a

positive wind speed trend was determined for three regions: central Australia, southeast Queensland, and northeast New South Wales and southern Victoria and Tasmania (McVicar et al. 2008). However, the study explained that the positive wind trend in arid central Australia resulted from above-average precipitation during the mid-1970s (McVicar et al. 2008). McVicar et al. (2008) concluded that if the study would have started after 1980, then the positive wind trend in central Australia would not exist. McVicar et al. (2008) also determined the highest (lowest) wind speeds were observed during summer (winter) at 2.3 m s^{-1} (1.7 m s^{-1}) in Australia.

In a similar way, Troccoli et al. (2012) conducted a 59-year study analyzing long-term wind linear trends using observations at 2 m and 10 m in Australia. Troccoli et al. (2012) established that wind speed trends are sensitive to the height of the station during two periods: 1975–2006 and 1989–2006. A negative (positive) wind speed trend is directly observed at 2 m (10 m) for both periods (Troccoli et al. 2012). Troccoli et al. (2012) identified that surface observations are greatly influenced by topographical features and do not accurately describe and represent macro-scale synoptic patterns. Donohue et al. (2010) found a statistically significant (p=0.002) negative trend (-0.1 m s^{-1} $decade^{-1}$) of 2 m wind speeds during 1981–2006. Troccoli et al. (2012) suggested that 10 m wind data should be used to understand any relationships between the surface and atmosphere is valid.

1.2.8 South America

The wind characteristics of Brazil are primarily driven by a macro-scale atmospheric circulation system (i.e., Intertropical Convergence Zone – ITCZ and South Atlantic Anticyclone – SAA) and topographic features (Ratisbona 1976). Consequently,

the seasonality of surface winds is affected by these two previously mentioned features. During winter (JJA), the SAA is dominant and the wind fields follow a counter-clockwise rotation outward around the SAA across Brazil. Ratisbona (1976) classified wind direction into three major groupings: southeasterly flow for the east, northeasterly direction for the north and northwest, and a westerly flow for high altitudes and extreme portions of southern Brazil (Figure 1.1).

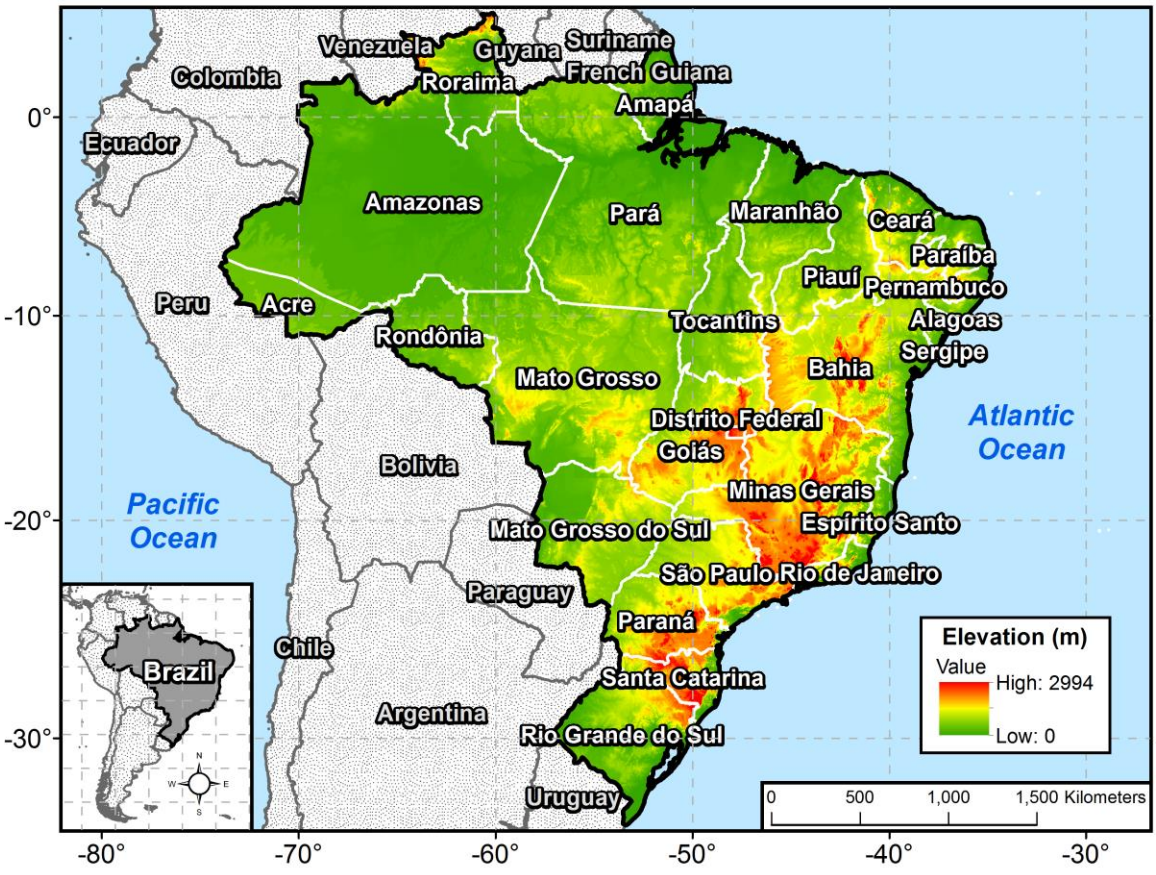

Figure 1.1. A map showing the 26 states and one federal district that constitutes the country of Brazil and the countries that border it. Digital elevation (m) map data is provided by GLOBE database (Hastings et al. 1999).

Ratisbona (1976) explained the overall mean wind speed pattern for Brazil based on seasonal fluctuations. During austral winter, coastal lowlands, equatorial, and Amazonian regions experience calm or weak wind speeds, while the central portion of

the Brazilian Highlands exhibits higher winds, ranging from 5 to 10 m s^{-1}, primarily driven by altitude change within the region (Ratisbona 1976). However, the strongest wind speeds are experienced in southern Brazil, where mid-latitude cyclones and anticyclones pass through the region. In summer (DJF), continental heating results in the overall decline of wind speeds across Brazil. The only exception to this geographic pattern occurs at high altitudes, where climatological mean wind speeds are observed during winter (Ratisbona 1976).

During the past several years, scientists have started to focus on understanding the impact of wind trends on energy production in Brazil (Lucena et al. 2010; Pereria et al. 2013; Santos and Silva 2013). Numerical models suggest that wind power production should increase for coastal and northern Brazil by the end of the 21st century based on current land-cover figurations (Lucena et al. 2010). Similarly, Pereria et al. (2013) simulated future wind power density based on the HadCM3 (Hadley Centre Coupled Model, version 3; Gordon et al. 2000) model and expect increases in wind productivity for northeastern and southern parts of Brazil. However, Pereria et al. (2013) also analyzed historic wind records for 15 stations during 1960–2007 and found decreasing and non-significant linear trends for a majority (11) of those observation sites. Santos and Silva (2013) analyzed 47 weather stations based on five station groupings for northeastern Brazil from 1986–2011 and determined that three of the five groups are observing statistically significant (p<0.01) decreasing linear trends for annual and seasonal wind speeds (Santos and Silva 2013). Santos and Silva (2013) found that linear wind trends across northeastern Brazil are positively correlated with the different phases of ENSO.

Similar to Brazil, wind characteristics of Argentina, Paraguay, and Uruguay can be explained by major macro-scale atmospheric circulations. Prohaska (1976) showed the interaction between the South AA and Pacific anticyclone, a quasi-stationary low in northern Argentina, and prevailing westerlies of the middle latitudes affect the magnitude and direction of the wind speeds across the region. Prohaska (1976) documented that the strongest wind speeds are observed in the southern portion of the continent, where westerlies are dominant. The strong winds that develop within the Roaring Forties (40°–50° S) of the Southern Hemisphere result from an absence of landmass which minimizes friction. On average, coastal and inland weather stations record wind speeds of 7–8 m s^{-1} (3–6 m s^{-1}) during austral winter (summer). Next, Prohaska (1976) explained the effect of the SAA over the area in the context of two broad wind groups: northeasterly winds for central Argentina and southwestern Uruguay and easterly and southeasterly winds for eastern Paraguay, northeastern Argentina, and northeastern Uruguay. Wind speeds found in this region are usually dependent on the position and strength of the nearby SAA (Prohaska 1976). In addition, a northerly migration of maximum wind speeds is experienced from early spring to summer due to heating and pressure contrast between the continent and Atlantic Ocean. Finally, wind speeds associated with the quasi-stationary low follow a similar pattern found across central Argentina and southwestern Uruguay.

1.3 Research Questions

Wind speed trends have been researched and investigated throughout the world using different statistical methods, historic datasets, and climatic models. However,

scientists still have many unanswered questions about which variables are influencing surface and upper-level winds at different spatial and temporal scales. The motivation of this research is derived from the limited amount of research on the surface (McVicar et al. 2012) and upper-level (Vautard et al. 2010) wind speed characteristics for the Southern Hemisphere, especially with regard to Brazil described by McVicar et al. (2012). Recent several studies have analyzed wind speeds for the northeastern part of Brazil for potential wind energy production (Lucena et al. 2010; Pereria et al. 2013; Santos and Silva 2013). However, a complete analysis of surface and upper-level wind characteristics for the entire country of Brazil has not yet been conducted. As a result, this dissertation addresses these issues in a three-part study.

The first manuscript (Chapter 2) provides a climatological assessment of linear wind speed trends over Brazil using historical surface wind and climatic model datasets from 1980 to 2014. Seasonal and annual linear trends are determined to understand how wind speeds vary across the country at various temporal and spatial scales. Studies have already shown that changes in surface winds were related to synoptic and surface-based conditions (land-cover change and urbanization; Vautard et al. 2010). It is hypothesized that surface winds are changing differently across portions of Brazil. To address these issues, this study investigates the following questions:

- How do seasonal and annual mean wind speeds vary across Brazil from 1980 to 2014?
- How do surface wind speeds compare to each other from a seasonal and overall perspective based on the Weibull distribution?

- Are any of the seasonal or annual linear wind trends statistically significant (p<0.05) from a geographical and temporal perspective for station and climate reanalysis datasets?
- Are extreme near-surface winds following these same linear trends across different percentiles (i.e., 5%, 25%, 50%, 75%, and 95%) from 1980 to 2014?
- How do *in-situ* surface wind trend patterns compare to those of climate model datasets?

The second manuscript (Chapter 3) evaluates the role of SAA and its effect on the surface conditions (wind speed, sea-level pressure (SLP), and temperature) across Brazil using reanalysis data. Studies have examined temporal changes in monthly, seasonal, and annual position of the SAA to explain modification in near-surface and upper-level atmospheric conditions across the South Atlantic Basin (SAB; Hastenrath 1985; Mächel et al. 1998; Degola 2013). Ratisbona (1976) explained that wind speeds across Brazil were under the control of the SAA and ITCZ. As a result, it is expected that any shift in the latitudinal or longitudinal position of SAA could impact surface conditions across Brazil. To address this relationship between SAA and surface conditions across Brazil, this study addresses the following questions:

- How have seasonal and annual surface winds changed spatially and temporally across the SAB?
- What are the seasonal and annual linear SLP trends of the latitudinal and longitudinal center of the SAA in the SAB?
- What is the geographical relationship between the position of the SAA and wind speed across Brazil?

- To what extent does the position of the SAA affect the regional relationships of surface wind speed, SLP, and temperature?
- Are there any regional anomalies between the relationships of surface wind, SLP, and temperature based on the position of the SAA relative to Brazil?
- How does the spatial location of the SAA in the SAB affect surface wind anomalies geographically across Brazil?

The last manuscript (Chapter 4) examines linear temporal trends in upper-level winds across Brazil during 1980–2014. Vautard et al. (2010) found that upper-level wind (850–200 hPa) trends did not match changes in near-surface winds for the Northern Hemisphere during 1979–2008. It is hypothesized that surface and upper-level wind trends across Brazil could be connected to each other through alternations in macro-scale atmospheric conditions. The remaining questions that will be addressed in this study include the following:

- What is the overall vertical relationship of upper-level wind patterns at the mandatory pressure levels (1000, 925,850, 700, 600, 500, 400, 300, 250, 200, 150, and 100 hPa) of the atmosphere across Brazil?
- How do the overall and regional seasonal and annual surface wind trends compare to upper-level wind trends?
- How has upper-level wind speed changed over time from a three-dimensional visualization (coordinate system) perspective?
- What atmospheric circulations are related to the upper-level wind speed trends found over Brazil?

1.4 Summary

Overall surface wind speed characteristics described by Ratisbona (1976) provide an important foundation of what type of climatological and meteorological research has been conducted in Brazil. However, this region has not been fully investigated as described by McVicar et al. (2012). In a study using data from 1986 to 2011, Santos and Silva (2013) is the only major study of Brazilian wind climatology to find that surface wind speeds have decreased across the majority of northeastern stations. Besides this regional study, no other formal research has been conducted to understand the surface and upper-level wind trends of Brazil from a climatological and geographical approach.

The purpose of this dissertation is to understand and expand our background about Brazilian surface and upper-level wind characteristics. To understand more completely the implications of how surface and upper-level winds have changed, this dissertation performs nonparametric statistics and quantile regression of historical and reanalysis datasets. Results from this dissertation will provide a broader understanding of how surface and upper-level wind speed characteristics across Brazil have changed between 1980 and 2014.

1.5 References

Abhishek A, Lee J-Y, Keener TC, Yang YJ. 2010. Long-term wind speed variations for three Midwestern U.S. cities. *Journal of the Air and Waste Management Association* **60**: 1057–1064. doi: 10.3155/1047-3289.60.9.1057.

Ashley WS, Black AW. 2008. Fatalities associated with nonconvective high-wind events in the United States. *Journal of Applied Meteorology and Climatology* **47**: 717–725. doi: http://dx.doi.org/10.1175/2007JAMC1689.1.

Azorin-Molina C, Vicente-Serrano SM, McVicar TR, Jerez S, Sanchez-Lorenzo A, López-Moreno J-I, Revuelto J, Trigo RM, Lopez-Bustins JA, Espírito-Santo F. 2014. Homogenization and assessment of observed near-surface wind speed trends over Spain and Portugal, 1961–2011. *Journal of Climate* **27**: 3692–3712. doi: 10.1175/JCLI-D-13-00652.1.

Bandyopadhyay A, Bhadra A, Raghuwanshi NS, Singh R. 2009. Temporal trends in estimates of reference evapotranspiration over India. *Journal of Hydrologic Engineering* **14**: 508–515. doi: http://dx.doi.org/10.1061/(ASCE)HE.1943-5584.0000006.

Barthel F, Neumayer E. 2012. A trend analysis of normalized insured damage from natural disasters. *Climatic Change* **113**: 215–237. doi 10.1007/s10584-011-0331-2.

Bichet A, Wild M, Folini D, Schär C. 2012. Causes for decadal variations of wind speed over land: Sensitivity studies with a global climate model. *Geophysical Research Letters* **39**: L11701. doi: 10.1029/2012GL051685.

Black AW, Ashley WS. 2010. Nontornadic convective wind fatalities in the United States. *Natural Hazards* **54**: 355–366. doi: 10.1007/s11069-009-9472-2.

Brázdil R, Chromá K, Dobrovolný P, Tolasz R. 2009. Climate fluctuations in the Czech Republic during the period 1961–2005. *International Journal of Climatology* **29**: 223–242. doi: 10.1002/joc.1718.

Changnon SA. 2009. Temporal and spatial distributions of wind storm damages in the United States. *Climatic Change* **94**: 473–482. doi: 10.1007/s10584-008-9518-6.

Chen L, Li D, Pryor SC. 2013. Wind speed trends over China: Quantifying the magnitude and assessing causality. *International Journal of Climatology* **33**: 2579–2590. doi: 10.1002/joc.3613.

Dadaser-Celik F, Cengiz E. 2014. Wind speed trends over Turkey from 1975 to 2006. *International Journal of Climatology* **34**: 1913–1927. doi: 10.1002/joc.3810.

DeGaetano AT. 1998. Identification and implications of biases in U.S. surface wind observation, archival, and summarization methods. *Theoretical and Applied Climatology* **60**: 151–162. doi: 10.1007/s007040050040.

Degola TSD. 2013. Impactos e variabilidade do Anticiclone Subtropical do Atlântico Sul sobre o Brasil no clima presente e em cenários futuros. Institute of Astronomy, Geophysics and Atmospheric Sciences, University of São Paulo, São Paulo, pp. 91.

Donohue RJ, McVicar TR, Roderick ML. 2010. Assessing the ability of potential evaporation formulations to capture the dynamics in evaporative demand within a changing climate. *Journal of Hydrology* **386**: 186–197. doi: 10.1016/j.jhydrol. 2010.03.020.

Fu G, Yu J, Zhang Y, Hu S, Ouyang R, Wenbin L. 2011. Temporal variation of wind speed in China for 1961–2007. *Theoretical and Applied Climatology* **104**: 313–324. doi: 10.1007/s00704-010-0348-x.

Gordon C, Cooper C, Senior CA, Banks H, Gregory JM, Johns TC, Mitchell JFB, Wood A. 2000. The simulation of SST, sea ice extents and ocean heat transports in a version of the Hadley Centre coupled model without flux adjustments. *Climate Dynamics* **16**: 147–168. doi: 10.1007/s003820050010.

Greene SJ, Chatelain M, Morrissey M, Stadler S. 2012. Estimated changes in wind speed and wind power density over the western High Plains, 1971–2000. *Theoretical and Applied Climatology* **109**: 507–518. doi: 10.1007/s00704-012-0596-z.

Griffin BJ, Kohfeld KE, Cooper AB, Boenisch G. 2010. Importance of location for describing typical and extreme wind speed behavior. *Geophysical Research Letters* **37**: L22804. doi: 10.1029/2010GL045052.

Guo H, Xu M, Hu Q. 2011. Changes in near-surface wind speed in China: 1969–2005. *International Journal of Climatology* **31**: 349–358. doi: 10.1002/joc.2091.

Hastenrath S. 1985. Regional circulation systems. *Climate and Circulation of the Tropics*. Reidel, D (ed.). Dordrecht. 107–209.

Hewston R, Dorling S. 2011. An analysis of observed daily maximum wind gusts in the UK. *Journal of Wind Engineering and Industrial Aerodynamics* **99**: 845–856. doi: http://dx.doi.org/10.1016/j.jweia.2011.06.004.

Holt E, Wang J. 2012. Trends of wind speed at wind turbine height of 80 m over the contiguous United States using the North American Regional Reanalysis (NARR). *Journal of Applied Meteorology and Climatology* **51**: 2188–2202. doi:10.1175/JAMC-D-11-0205.1.

Hundecha Y, St-Hilaire A, Ouarda TBMJ, El Adlouni S, Gachon P. 2008. A nonstationary extreme value analysis for the assessment of changes in extreme annual wind speed over the Gulf of St. Lawrence, Canada. *Journal of Applied Meteorology and Climatology* **47**: 2745–2759. doi: http://dx.doi.org/10.1175 /2008JAMC1665.1.

Jaswal AK, Koppar AL. 2013. Climatology and trends in near-surface wind speed over India during 1961–2008. *Mausam* **64**: 417–436.

Jiang Y, Luo Y, Zhao Z, Tao S. 2010. Changes in wind speed over China during 1956–2004. *Theoretical and Applied Climatology* **99**: 421–430. doi: 10.1007/s00704-009-0152-7.

Jönsson P, Fortuniak K. 1995. Interdecadal variations of surface wind direction in Lund, Southern Sweden, 1741–1990. *International Journal of Climatology* **15**: 447–461. doi: 10.1002/joc.3370150407.

Kahn ME. 2005. The death toll from natural disasters: The role of income, geography, and institutions. *The Review of Economics and Statistics* **87**: 271–284. doi: 10.1162/0034653053970339.

Klein Tank, AMG, Wijngaard JB, Können GP, Böhm R, Demarée G, Gocheva A, Mileta M, Pashiardis S, Hejkrlik L, Kern-Hansen C, Heino R, Bessemoulin P, Müller-Westermeier G, Tzanakou M, Szalai S, Pálsdóttir T, Fitzgerald D, Rubin S, Capaldo M, Maugeri M, Leitass A, Bukantis A, Aberfeld R, van Engelen AFV, Forland E, Mietus M, Coelho F, Mares C, Razuvaev V, Nieplova E, Cegnar T, Antonio López J, Dahlström B, Moberg A, Kirchhofer W, Ceylan A, Pachaliuk O, Alexander LV, Petrovic P. 2002. Daily dataset of 20th-century surface air temperature and precipitation series for the European Climate Assessment. *International Journal of Climatology* **22**: 1441–1453. doi:10.1002/joc.773.

Klink K. 1998. Complementary use of scalar, directional and vector statistics with an application to surface winds. *The Professional Geographer* **50**: 3–13. doi: 10.1111/0033-0124.00099.

----------. 1999a. Climatological mean and interannual variance of United States surface wind speed, direction and velocity. *International Journal of Climatology* **19**: 471–488. doi: 10.1002/(SICI)1097-0088(199904)19:5<471::AID-JOC367>3.0.CO;2-X.

----------. 1999b. Trends in mean monthly maximum and minimum surface wind speeds in the coterminous United States, 1961 to 1990. *Climate Research* **13**: 193–205. doi: 10.3354/cr013193.

----------. 2002. Trends and interannual variability of wind speed distributions in Minnesota. *Journal of Climate* **15**: 3311–3317. doi: http://dx.doi.org/10.1175 /1520 0442(2002)015<3311:TAIVOW>2.0.CO; 2.

Li X, Zhong S, Bian X, Heilman WE. 2010. Climate and climate variability of the wind power resources in the Great Lakes region of the United States. *Journal of Geophysical Research* **115**: D18107. doi: 10.1029/2009JD013415.

Lin C, Yang K, Qin J, Fu R. 2013. Observed coherent trends of surface and upper-air wind speed over China since 1960. *Journal of Climate* **26**: 2891–2903. doi: http://dx.doi.org/10.1175/JCLI-D-12-00093.1.

Liu Q, Yang Z, Sun T. 2010. The temporal trends of reference evapotranspiration and its sensitivity to key meteorological variables in Yellow River Basin, China. *Hydrological Processes* **24**: 2171–2181. doi: 10.1002/hyp.7649.

Liu X, Luo Y, Zhang D, Zhang M, Liu C. 2011. Recent changes in pan-evaporation dynamics in China. *Geophysical Research Letters* **38**: L13404. doi: 10.1029/2011GL047929.

Liuzzo L, Viola F, Noto LV. 2016. Wind speed and temperature trends impacts on reference evapotranspiration in southern Italy. *Theoretical and Applied Climatology* **123**: 43–62. doi: 10.1007/s00704-014-1342-5.

Lucena AFP, Szklo AS, Schaeffer R, Dutra RM. 2010. The vulnerability of wind power to climate change in Brazil. *Renewable Energy* **35**: 904–912. doi: 10.1016/j.renene.2009.10.022.

Mächel H, Kapala A, Flohn, H. 1998. Behaviour of the centres of action above the Atlantic since 1881. Part I: Characteristics of seasonal and interannual variability. *International Journal of Climatology* **18**: 1–22. doi: 10.1002/(SICI)1097-0088(199801)18:1<1::AID-JOC225>3.0.CO;2-A.

Mantua NJ, Hare SR, Zhang Y, Wallace JM, Francis RC. 1997. A Pacific Interdecadal Climate Oscillation with impacts on salmon production. *Bulletin of the American Meteorological Society* **78**: 1069–1079. doi: http://dx.doi.org/10.1175/1520-0477(1997)078<1069:APICOW>2.0.CO;2.

Martin-Vide J, Lopez-Bustins J-A. 2006. The Western Mediterranean Oscillation and rainfall in the Iberian Peninsula. *International Journal of Climatology* **26**: 1455–1475. doi:10.1002/joc.1388.

McVicar TR, Van Niel TG, Li LT, Roderick ML, Rayner DP, Ricciardull L, Donohue RJ. 2008. Wind speed climatology and trends for Australia, 1975–2006: Capturing the stilling phenomenon and comparison with near-surface reanalysis output. *Geophysical Research Letters* **35**: L20403. doi: 10.1029/2008GL035627.

----------, Roderick ML. 2010. Atmospheric science: Winds of change. *Nature Geoscience* **3**: 747–748. doi: 10.1038/ngeo1002.

----------, Roderick ML, Donohue RJ, Li, LT, Van Niel TG, Thomas A. Grieser J, Jhajharia D, Himri Y, Mahowald NM, Mescherskaya AV, Kruger AC, Rehman S, Dinpashoh Y. 2012. Global review and synthesis of trends in observed terrestrial near-surface wind speeds: Implications for evaporation. *Journal of Hydrology* **417**: 182–205. doi: http://dx.doi.org/10.1016/j.jhydrol.2011.10.024.

Mearns LO, Gutowki W, Jones R, Leung R, McGinnis S, Nunes A, Qian Y. 2009. A regional climate change assessment program for North America. *Eos Transactions* **90**: 311–311. doi: 10.1029/2009EO360002.

Mesinger F, DiMego G, Kalnay E, Mitchell K, Shafran PC, Ebisuzaki W, Jović D, Woollen J, Rogers E, Berbery EH, Ek MB, Fan Y, Grumbine R, Higgins W, Li H, Lin Y, Manikin G, Parrish D, Shi W. 2006. National American Regional Reanalysis. *Bulletin of American Meteorological Society* **87**: 343–360. doi: 10.1175/BAMS-87-3-343.

Moratiel R, Snyder RL, Durán JM, Tarqius AM. 2011. Trends in climatic variables and future reference evapotranspiration in Duero Valley (Spain). *Natural Hazards and Earth System Sciences* **11**: 1795–1805. doi: 10.5194/nhess-11-1795-2011.

Palutikof JP. 2003. Analysis of Mediterranean climate data: Measured and modelled. *Mediterranean Climate: Variability and Trends*. Bolle, H-J. (ed.). Springer-Verlag. Berlin. 125–132.

Pereira EB, Martins FR, Pes MP, Segundo EID, Lyra AD. 2013. The impacts of global climate changes on the wind power density in Brazil. *Renewable Energy* **49**: 107–110. doi: 10.1016/j.renene.2012.01.053.

Pirazzoli PA, Tomasin A. 1999. Recent abatement of easterly winds in the northern Adriatic. *International Journal of Climatology* **19**: 1205–1219. doi: 10.1002/(SICI)1097-008(199909)19:11<1205::AID-JOC405>3.0.CO;2-D.

----------, ----------. 2003. Recent near-surface wind changes in the central Mediterranean and Adriatic areas. *International Journal of Climatology* **23**: 963–973. doi: 10.1002/joc.925.

Prohaska F. 1976. The climate of Argentina. *World Survey of Climatology, Volume 12, Climates of Central and South America*. Schwerdtfeger, W (ed.). Amsterdam. 13–112.

Pryor SC, Barthelmie RJ. 2003. Long-term trends in near-surface flow over the Baltic. *International Journal of Climatology* **23**: 271–289. doi: 10.1002/joc.878.

----------, ----------, Riley ES. 2007. Historical evolution of wind climates in the USA. *Journal of Physics: Conference Series* **75**: 012065. doi: 10.1088/1742–6596/ 75/1/012065.

----------, ----------, Young, DT, Takle ES, Arritt RW, Flory D, Gutowski WJ, Nunes A, Roads J. 2009. Wind speed trends over the contiguous United States. *Journal of Geophysical Research* **114**: D14105. doi: 10.1029/2008JD011416.

----------, Ledolter J. 2010. Addendum to “Wind speeds trends over the contiguous United States”. *Journal of Geophysical Research* **115**: D10103. doi: 10.1029/2009 JD013281.

Ratisbona LR. 1976. The climate of Brazil. *World Survey of Climatology, Volume 12, Climates of Central and South America*. Schwerdtfeger, W (ed.). Amsterdam. 405–451.

Ropelewski CF, Jones PD. 1987. An extension of the Tahiti–Darwin Southern Oscillation Index. *Monthly Weather Review* **115**: 2161–2165. doi: http://dx.doi.org/10.1175/ 1520-0493(1987)115<2161:AEOTTS>2.0.CO;2.

Santos ATS, Silva CMS. 2013. Seasonality, interannual variability, and linear tendency of wind speeds in the northeast Brazil from 1986 to 2011. *The Scientific World Journal*. doi: http://dx.doi.org/10.1155/2013/490857.

Schmidlin TW. 2009. Human fatalities from wind-related tree failures in the United States, 1995–2007. *Natural Hazards* **50**: 13–25. doi: 10.1007/s11069-008-9314-7.

Schoen JM, Ashley WS. 2011. A climatology of fatal convective wind events by storm type. *Weather and Forecasting* **26**: 109–121. doi: http://dx.doi.org/10.1175/2010 WAF2222428.1.

Shenbin C, Yunfeng L, Thomas A. 2006. Climatic change on the Tibetan Plateau: Potential evapotranspiration trends from 1961–2000. *Climatic Change* **76**: 291–319. doi: 10.1007/s10584-006-9080-z.

St. George S, Wolfe SA. 2009. El Niño stills winter winds across the southern Canadian Prairies. *Geophysical Research Letters* **36**: L23806. doi:10.1029/2009GL041282.

Tang B, Tong L, Kang S, Zhang L. 2011. Impacts of climate variability on reference evapotranspiration over 58 years in the Haihe river basin of north China. *Agricultural Water Management* **98**: 1660–1670. doi: 10.1016/j.agwat.2011. 06.006.

Troccoli A, Muller K, Coppin P, Davy R, Russell C, Hirsch AL. 2012. Long-term wind speed trends over Australia. *Journal of Climate*, **25**: 170–183. doi: http://dx.doi.org/10.1175/2011JCLI4198.1.

Tuller SE. 2004. Measured wind speed trends on the west coast of Canada. *International Journal of Climatology* **24**: 1359–1374. doi: 10.1002/joc.1073.

Vautard R, Cattiaux J, Yiou P, Thépaut J-N, Ciais P. 2010. Northern Hemisphere atmospheric stilling partly attributed to an increase in surface roughness. *Nature Geoscience* **3**: 756–761. doi: 10.1038/ngeo979.

Wallace JM, Gutzler DS. 1981. Teleconnections in the geopotential height field during the Northern Hemisphere winter. *Monthly Weather Review* **109**: 784–812. doi: http://dx.doi.org/10.1175/1520-0493(1981)109<0784:TITGHF>2.0.CO;2.

Wan H, Wang, XL, Swail VR. 2010. Homogenization and trend analysis of Canadian near-surface wind speeds. *Journal of Climate* **23**: 1209–1225. doi: http://dx.doi.org/10.1175/2009JCLI3200.1.

Wever N. 2012. Quantifying trends in surface roughness and the effect on surface wind speed observations. *Journal of Geophysical Research* **117**: D11104. doi: 10.1029 /2011JD017118.

Xu M, Chang C-P, Fu C, Qi Y, Robock A, Robinson D, Zhang H. 2006. Steady decline of East Asian monsoon winds, 1969–2000: Evidence from direct ground measurements of wind speed. *Journal of Geophysical Research* **111**: D24111. doi: 10.1029/2006JD007337.

Yang X, Li ZX, Feng Q, He YQ, An WL, Zhang W, Cao WH, Yu TF, Wang YM, Theakstone W. 2012. The decreasing wind speed in southwestern China during 1969–2009 and possible causes. *Quaternary International* **263**: 71–84. doi: http://dx.doi.org/10.1016/j.quaint.2012.02.020.

Yin Y, Wu S, Chen G, Dai E. 2010a. Attribution analyses of potential evapotranspiration changes in China since the 1960s. *Theoretical and Applied Climatology* **101**: 19–28. doi: 10.1007/s00704-009-0197-7.

————, ————, Dai E. 2010b. Determining factors in potential evapotranspiration changes over China in the period 1971–2008. *Chinese Science Bulletin* **55**: 3329–3337. doi: 10.1007/s11434-010-3289-y.

You Q, Fraedrich K, Min J, Kang S ,Zhu X, Pepine N, Zhanga L. 2014. Observed surface wind speed in the Tibetan Plateau since 1980 and its physical causes. *International Journal of Climatology* **34**: 1873–1882. doi: 10.1002/joc.3807.

Zhao Z, Luo Y, Jiang Y. 2011. Is global strong wind declining?. *Advances in Climate Change Research* **2**: 225–228. doi: 10.3724/SP.J.1248.2011.00225.

Zheng X, Liu X, Liu C, Dai X, Zhu R. 2009. Assessing contribution to panevaporation trends in Haihe River Basin, China. *Journal of Geophysical Research* **114**: D24105. doi: 10.1029/2009JD0112203.

CHAPTER 2
SURFACE WIND SPEED: TREND AND CLIMATOLOGY OF BRAZIL FROM 1980–2014

2.1 Introduction

Regional wind climatologies across North America (Klink 1999; 2002; Tuller 2004; Pryor et al. 2007; 2009; Hundecha et al. 2008; Abhishek et al. 2010; Griffin et al. 2010; Li et al. 2010; Pryor and Ledolter 2010; Wan et al. 2010; Holt and Wang 2012; Romanić et al. 2016), Europe (Pirazzoli and Tomasin 2003; Pryor and Barthelmie 2003; Brázdil et al. 2009; Wever 2012; Azorin-Molina et al. 2014; Romanić et al. 2015; Liuzzo et al. 2016), Asia (Xu et al. 2006; Jiang et al. 2010; Fu et al. 2011; Guo et al. 2011; Yang et al. 2012; Chen et al. 2013; Lin et al. 2013; You et al. 2014; Kim and Palk 2015), and Australia (McVicar et al. 2008; Troccoli et al. 2012) have examined and identified changes in the geographical and temporal trends of surface winds during the 20th century. However, McVicar et al. (2012) identified that comprehensive wind trend studies for Central and South America are still lacking especially for Brazil where one study (i.e., Silva et al. 2010) was included as part of their analysis (Table 2.1).

Table 2.1. Total number of annual surface wind speed trend (i.e., positive and negative) studies conducted for each region based on McVicar et al. (2012).

Region	Number of Studies	Positive	Negative
North America	27	6	21
Central and South America	7	2	5
Europe	24	4	20
Asia	38	0	38
Sub-continent	6	0	6
Middle-East	14	6	8
Africa	21	5	16
Oceanic	9	2	7
Antarctica	2	2	0
	148	27	121

Much of Brazilian research conducted since Silva et al. (2010) has focused on assessing changes in surface winds with respect to present and future wind energy production (Lucena et al. 2010; Pereira et al. 2013; Santos and Silva 2013; Pes et al. 2017). Lucena et al. (2010) showed that future wind energy production should increase for coastal and northern Brazil by the end of the 21st century based on Intergovernmental Panel on Climate Change (IPCC) emission scenarios (pessimistic high and optimistic low emissions) and present land-cover using Hadley Centre Coupled Model, version 3 (HadCM3; Gordon et al. 2000) general circulation model. Pereira et al. (2013) stimulated future wind energy using HadCM3 model and concluded that energy production should also increase for northeastern Brazil by the end of the 21st century. However, their analysis further explored past wind records from 15 Brazilian weather stations and established that the majority (11) of sites is experiencing decreasing or non-significant linear wind speed trends from 1960 to 2007. Santos and Silva (2013) presented a comparable negative wind trend pattern between 1986 and 2011 based upon categorizing 47 northeastern Brazilian stations into five groups by derived using a cluster analysis. The study showed that three of the five groups observed significant (p<0.01) negative linear trends in seasonal and annual near-surface wind speeds.

Overall, the general consensus is that surface wind speeds are decreasing globally (Vautard et al. 2010; Bichet et al. 2012; McVicar et al. 2012). McVicar et al. (2012) showed that 82% (121) of all studies analyzed found declining annual trends (Table 2.1). This decreasing pattern is supported by more recent research conducted for Europe (Azorin-Molina et al. 2014; Romanić et al. 2015) and Asia (Yang et al. 2012; Chen et al. 2013; Lin et al. 2013; You et al. 2014; Kim and Palk 2015). However, certain studies

performed for North America exhibited increasing wind speeds (Holt and Wang 2012; Romanić et al. 2016). This discrepancy found between these regional studies can be attributed to measurement height differences. Holt and Wang (2012) and Romanić et al. (2016) used 80 m and sigma 0.995 level (~41 m) reanalysis data to calculate wind trends for the United States and Great Lakes region (i.e., Toronto), while studies conducted in Europe and Asia utilized 10 m surface wind measurements.

Despite this issue, the present debate among scientists has focused on identifying which surface and atmospheric variables can explain the modification of near-surface winds. Many studies attributed the decreasing temporal trends to urbanization (Xu et al. 2006; Guo et al. 2011; Li et al. 2011; Yang et al. 2012; Jaswal and Koppar 2013; Azorin-Molina et al. 2014) and land-cover change (Vautard et al. 2010; Bichet et al. 2012; Wever 2012). Using annual mean wind speeds for 12 stations located in Greater Beijing, Li et al. (2011) found that urbanization accounted for 20% of the regional wind decline between 1960 and 2008. Vautard et al. (2010) estimated that 25%–60% of the decrease in surface wind trends found in the Northern Hemisphere could be related to an increase in surface roughness from vegetation. While these two factors can influence surface winds, other analyses suggest that alterations in macro-scale atmospheric circulations (Jiang et al. 2010; Guo et al. 2011; Li et al. 2011; Troccoli et al. 2012; Yang et al. 2012; Jaswal and Koppar 2013; Lin et al. 2013; Dadaser-Celik and Cengiz 2014; You et al. 2014; Romanić et al. 2015) and teleconnections (Pirazzoli and Tomasin 2003; Pryor and Barthelmie 2003; Tuller 2004; St. George and Wolfe 2009; Abhishek et al. 2010; Li et al. 2010; Pryor and Ledolter 2010; Fu et al. 2011; Hewston and Dorling 2011; Chen et al.

2013; Lin et al. 2013; Azorin-Molina et al. 2014; You et al. 2014) are responsible for the decreasing trends being documented across the globe.

Surface wind climatologies have evaluated other potential causes of wind speed change including the spatial role of elevation (Griffin et al. 2010; Yang et al. 2012; You et al. 2014), surface temperature (Xu et al. 2006; Jiang et al. 2010; Yang et al. 2012; Dadaser-Celik and Cengiz 2014; You et al. 2014), solar radiation (Yang et al. 2012), solar activity (Romanić et al. 2016), and evapotranspiration (Zuo et al. 2005; Gao et al. 2006; Burn and Hesch 2007; Zheng et al. 2009; Liu et al. 2010; Yin et al. 2010a; 2010b; Liu et al. 2011; Tang et al. 2011: McVicar et al. 2012). Studies have also examined data quality and heterogeneity (e.g., anemometer relocation and height adjustment, instrument replacement, and observation bias) of wind records to explain spatial and temporal and patterns (DeGaetano 1998; Klink 1999; Pryor et al. 2007; 2009; Jakob 2010; Jiang et al. 2010; Wan et al. 2010; Dadaser-Celik and Cengiz 2014).

Previous work has suggested that wind speeds are slowing across northeastern Brazil (Silva et al. 2010; Pereira et al. 2013; Santos and Silva 2013). Yet, it has been forecasted that surface winds will increase along coastal and northeastern Brazil based on conditions implemented from IPCC emission schemes and stimulated into general climate models (Lucena et al. 2010; Pereira et al. 2013). Renewable energy is becoming an important component of the Brazilian energy production sector. Currently, wind energy accounts for 6.8% (10.4 GW) of the total electrical power capacity generated by Brazil (ANEEL 2017). Any modifications in surface or atmospheric conditions could affect surface winds across Brazil. As a result, it is important to investigate how changes

in the spatial and temporal wind patterns could impact potential wind energy production across the country.

The objectives of this study are to: (1) understand the geographic distribution of mean wind speeds, (2) identify any mean seasonal or annual surface wind speed trends across Brazil, (3) examine how seasonal and annual wind speed trends change at different percentiles (i.e., 5%, 25%, 50%, 75%, and 95%), and (4) evaluate how surface wind speeds and trends vary among surface measurements and reanalysis datasets based on linear and quantile regression. To meet these objectives, geographic and temporal characteristics of near-surface wind speeds are identified through statistical analysis of overall and individual *in-situ* and gridded observations for the study region.

2.2. Data and Methods

2.2.1 *In-situ* Winds

This study utilizes two historical wind measurement datasets to analyze the wind speed trend characteristics of Brazil during 1980–2014. The first source of surface-based measurements is provided by National Institute of Meteorology (Instituto Nacional de Meteorologia – INMET). INMET collects three daily observations (0, 12, and 18 UTC) of various meteorological variables (i.e., dry and wet bulb temperature, relative humidity, wind speed and direction, cloud coverage, and atmospheric pressure) from its manual network of 293 surface weather stations across Brazil. Santos and Silva (2013) describe that wind speed observations gathered from INMET follow and meet the anemometer height standard (10 m) set by the World Meteorological Organization (WMO). However, a setback of using observations from INMET is the lack of continuous periods of record for all given sites. INMET provides daily meteorological observations starting in 1961,

but upon further inspection, it was determined that many of the stations did not start maintaining consistent daily records until the early 1980s. Thus, many of the stations provided by INMET were not suitable for analysis and the scope of the paper limited to the period of 1980 to 2014.

A second dataset from the National Centers for Environmental Information Integrated Surface Database (NCEI-ISD) had to be included to supplement for missing daily records that existed in the original INMET dataset. NCEI-ISD is a quality-controlled global repository that collects meteorological surface observations (manual and automatic) from governmental and meteorological organizations across the world (Lott et al. 2008). Land-based stations included in the NCEI-ISD database consist of meteorological observations from two Brazilian sources: INMET and Center for Weather Forecasting and Climatic Studies and Brazilian National Institute for Space Research (CPTEC/INPE). For the purpose of this study, CPTEC/INPE wind observations are acquired for stations not included in the primary dataset from NCEI-ISD. To minimize additional error or replication bias, all NCEI-ISD observations included in this study originate from the same source and observation time as INMET. This was achieved by examining INMET and NCEI-ISD for unique identifiers (i.e., WMO number allocation), which are assigned to each weather station following the rules set by WMO.

Another issue of concern is the robustness or quality of a dataset. INMET collects three daily observations (0, 12, and 18 UTC) at each site included in its network of meteorological stations across Brazil. Santos and Silva (2013) utilize a single daily observation time (12 UTC) from INMET to construct and analyze surface wind speed trends across northeastern Brazil from 1986 to 2011**.** The study recognized that a greater

frequency of daily observations would improve their wind analysis. This statement is supported by Jakob (2010), who found that the number of observations (eight vs two reports) used to calculate daily mean wind speeds impacted seasonal and annual averages for three Australian weather stations. It is also important to document the physical environment (e.g., land-cover, urbanization, etc.) of each station. A visual inspection of aerial imagery of INMET sites shows that many of the anemometers are located in urban or vegetated environments.

Based on these concerns, supplementary resources were consulted to identify stations that contain a sufficient number of reports within study period of interest and located in more desirable settings (i.e., open terrain) to comprise the standard baseline or proxy to investigate the spatial and temporal wind speed trends of Brazil. More specifically, NCEI-ISD collects wind records from military and airport stations (i.e., Brazilian Department of Airspace Control – DECEA) across Brazil as part of its global repository. Weather stations situated at these sites tend to report a higher frequency of wind observations and be positioned in open terrain surroundings in compliance with WMO specifications. A second wind dataset was constructed based on the records from Brazilian military and airport stations by NCEI-ISD during 1980–2014. This dataset (NCEI-ISD) is used as the proxy to understand the wind speed trend characteristics of Brazil. The daily observations acquired from NCEI-ISD improve the characterization of the changes in wind speeds across Brazil despite the geographical limitations of stations included in this study.

Recent literature further shows a broad range of techniques used to identify and select stations for regional (Pryor et al. 2007, 2009; St. George and Wolfe 2009; Griffin

et al. 2010; Jakob 2010; Fu et al. 2011; Troccoli et al. 2012; Chen et al. 2013; Lin et al. 2013; Santos and Silva 2013; Azorin-Molina et al. 2014) and global (Vautard et al. 2010) studies based on the number of observations. Sites in Brazil where over 500 observations were recorded annually with each season containing more than 50 valid records during 1980–2014 were selected for analysis, following guidelines of Pryor et al. (2007) for INMET and NCEI-ISD datasets. This methodology maximizes the number of study sites in Brazil while maintaining data quality. Based on this criterion, 56 INMET and 35 NCEI-ISD stations were selected to characterize the surface wind trends of Brazil (Figure 2.1).

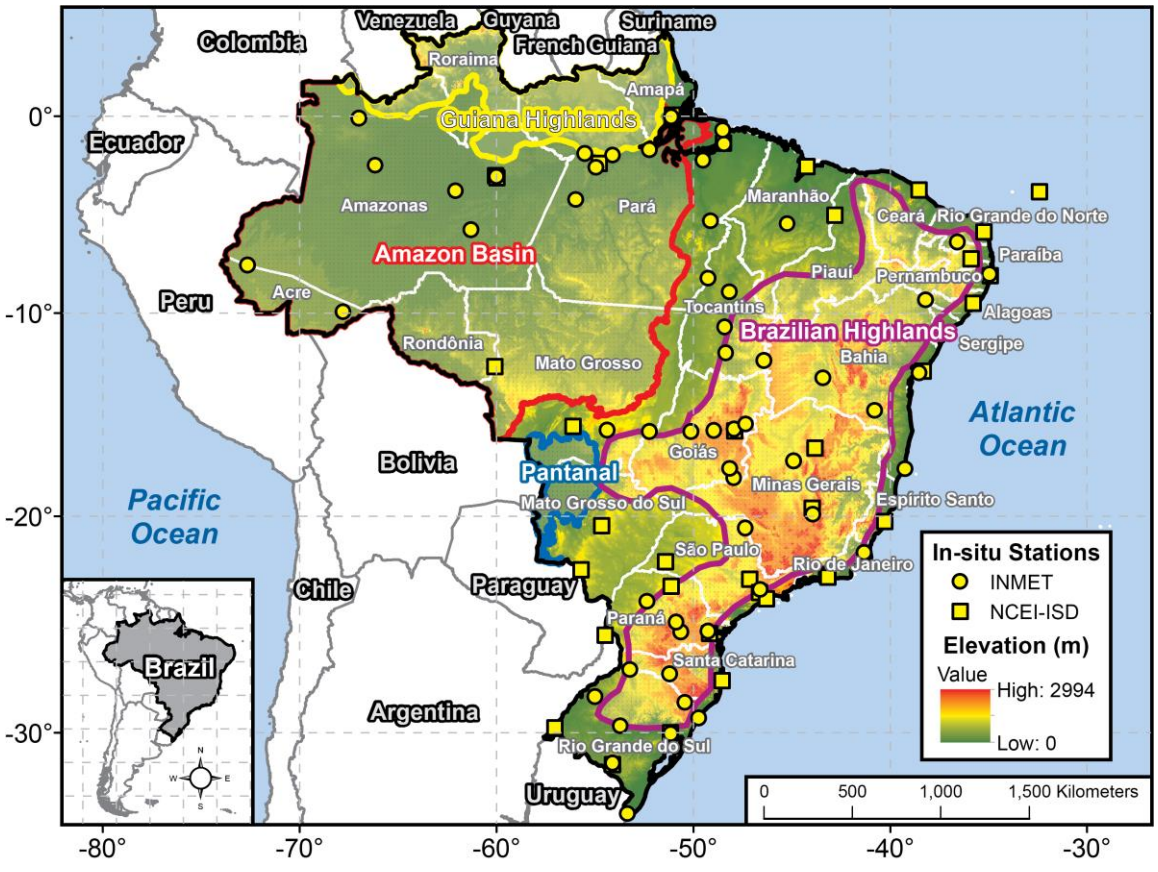

Figure 2.1. Spatial distribution of the 56 INMET and 35 NCEI-ISD stations used in the study. Digital elevation (m) map data are provided by GLOBE database (Hastings et al. 1999).

2.2.2 Reanalysis Winds

Surface zonal (*u;* west–east) and meridional (*v*; south–north) wind components (10 m) from three climate models were used to infer the wind speed trend characteristics of Brazil during 1980–2014. The first dataset used in the study is from the National Center for Environmental Prediction/National Center for Atmospheric Research (NCEP/NCAR) reanalysis dataset (i.e., referred to as Reanalysis 1), which is a global climate model that assimilates surface and atmospheric variables at a spatial resolution of 2.5° x 2.5° (T62 model) for 28 vertical levels of the atmosphere every six hours (0, 6, 12, and 18 UTC; Kalnay et al. 1996). Reanalysis 1 designates surface wind records with a B-class distinction, which specifies that surface winds are integrated into the reanalysis but the model has a greater influence over the grid point value of each wind observation. Near-surface wind observations from Reanalysis 1 are determined through the downward extrapolation of *u* and *v* winds at the sigma 0.995 level using Monin-Obukhov similarity theory (Obukhov 1971) and not through the assimilation of land-based historical records. A global land-based surface roughness climatology is also implemented to control *u* and *v* wind speed outputs for Reanalysis 1 (Dorman and Sellers 1989).

The second climate dataset utilized is the National Center for Environmental Prediction and Department of Energy (NCEP-DOE) reanalysis dataset (i.e., Reanalysis 2) is an updated version of Reanalysis 1, which contains the equivalent spectral resolution of 28 vertical levels, six-hourly interval (0, 6, 12, and 18 UTC), and similar raw observation data but with additional records (Kanamitsu et al. 2002). These improvements to Reanalysis 2 include the implementation of higher spatial resolution (1.875° x 1.875°), improved algorithms for processing errors, and adjustments made to forecast models and

data assimilated systems. Near-surface wind (*u* and *v*) components are constructed using the same processing technique of extrapolating winds at the sigma 0.995 level based on Monin-Obukhov similarity theory and global roughness length described by Pryor et al. (2009).

The final reanalysis dataset used in the study is the European Centre for Medium-Range Weather Forecasts (ECMWF) Interim (i.e., ERA-Interim) is a six-hourly interval (0, 6, 12, and 18 UTC) global assimilated model that is constructed at 60 vertical levels with a grid resolution of 0.75° x 0.75° (T255) for the period of 1979 to present (Dee et al. 2011). Surface wind records from automatic and manual land stations, Meteorological Terminal Aviation Routine (METAR) reports, ships, and drifting buoys are included in ERA-Interim. Dee et al. (2011) describes how the selection process is applied to select and remove convectional surface data from the model. After this quality control, *u* and *v* winds are constructed by the interpolation of upper-level atmospheric winds and Tiled ECMWF Scheme for Surface Exchanges over Land (TESSEL) surface scheme (Viterbo and Beljaars 1995).

2.2.3 Statistical Analysis

Wind data (*u* and *v* components) extracted from Reanalysis 1, Reanalysis 2, and ERA-Interim are used to calculate the actual wind speeds (V) modelled for each grid point (Equation 1). Geographical information systems (GIS) is utilized to select reanalysis grid points that overlay the study area of Brazil. Overall and individual mean wind speeds are determined for each *in-situ* and reanalysis climate product used in this analysis.

$$V(u,v) = \sqrt{u^2 + v^2} \tag{1}$$

The data is then fitted to the Weibull distribution (Davenport 1963) to understand how the seasonal and annual wind speed histograms differ among the *in-situ* and climate reanalysis datasets. This function is used in the study to represent the wind speed frequency distribution of each dataset. Justus et al. (1978) describes five methods used to determine the two parameters [shape (k) and scale (λ)] of the Weibull distribution based on the wind statistics available. For this study, the mean ($\overline{V}$) and standard deviation (σ) from each dataset are used to estimate seasonal and annual k and scale λ values.

Nonparametric statistics and quantile regression are used to describe the surface wind trend characteristics of Brazil during 1980–2014. Mann-Kendall test (Mann 1945; Kendall 1975) and Sen's slope estimator (Sen 1968) are employed to reveal the seasonal and annual linear trends of mean wind speeds for each dataset. These two statistical methods are commonly applied in surface wind trend climatologies (e.g., Chen et al. 2013; Dadaser-Celik and Cengiz 2014; Romanić et al. 2016). However, this type of statistical analysis leaves many unanswered questions pertaining to how wind speeds vary across different percentiles. Studies have documented wind speed trends for specific quartiles (Pryor et al. 2007; 2009; Pryor and Ledolter 2010; Guo et al. 2011) based on linear regression. Here, overall and individual percentile (5%, 25%, 50%, 75%, and 95%) wind speed trends are identified for each dataset using quantile regression (Koenker and Bassett 1978). The percentiles selected follow the typical convention of a standard boxplot. Lastly, a comparative assessment of surface measurement and climate reanalysis datasets is performed to understand how wind speed trends differ geographically and temporally across Brazil.

2.3 Results

2.3.1 Wind Climatology

Four geographic regions are identified based on seasonal and annual mean wind speed climatology during 1980–2014 for Brazil (Figure 2.2). The slowest mean wind speeds are found over the Amazon, where wind speed averages less than 2 m s^{-1} for each dataset. A transition zone is located across central Brazil (Mato Grosso and Pará), where a gradual increase in elevation occurs. Reanalysis winds indicate that the mean wind speeds for this region fall between 2 and 3 m s^{-1}. The third region, largely corresponding to the Brazilian Highlands, exhibits an average wind speed of 3–4 m s^{-1}. The final wind speed region is located on the perimeter of the Brazilian Highlands (i.e., coastal, southern, and northeastern Brazil), where mean wind speeds exceed 5 m s^{-1}.

Seasonal mean wind speeds across Brazil are influenced by macro-scale atmospheric circulations. Figure 2.2a–2.2d shows that when the Intertropical Convergence Zone (ITCZ) is located south (north) of the Equator during summer and fall (winter and spring) mean wind speeds across Brazil are slower (faster). This seasonal shift in mean wind speeds is influenced by the position of the South Atlantic Anticyclone (SAA). As the ITCZ shifts seasonally, the SAA becomes a prominent feature that affects sea-level pressure (SLP) gradients over Brazil. Schwerdtfeger (1976) shows when the ITCZ moves southward (northward), SLP decreases (increases) during summer and fall (winter and spring) over Brazil. This relationship between the locations of the ITCZ and SAA controls the magnitude of wind speeds, with the fastest (slowest) observations occurring during winter and spring (summer and fall).

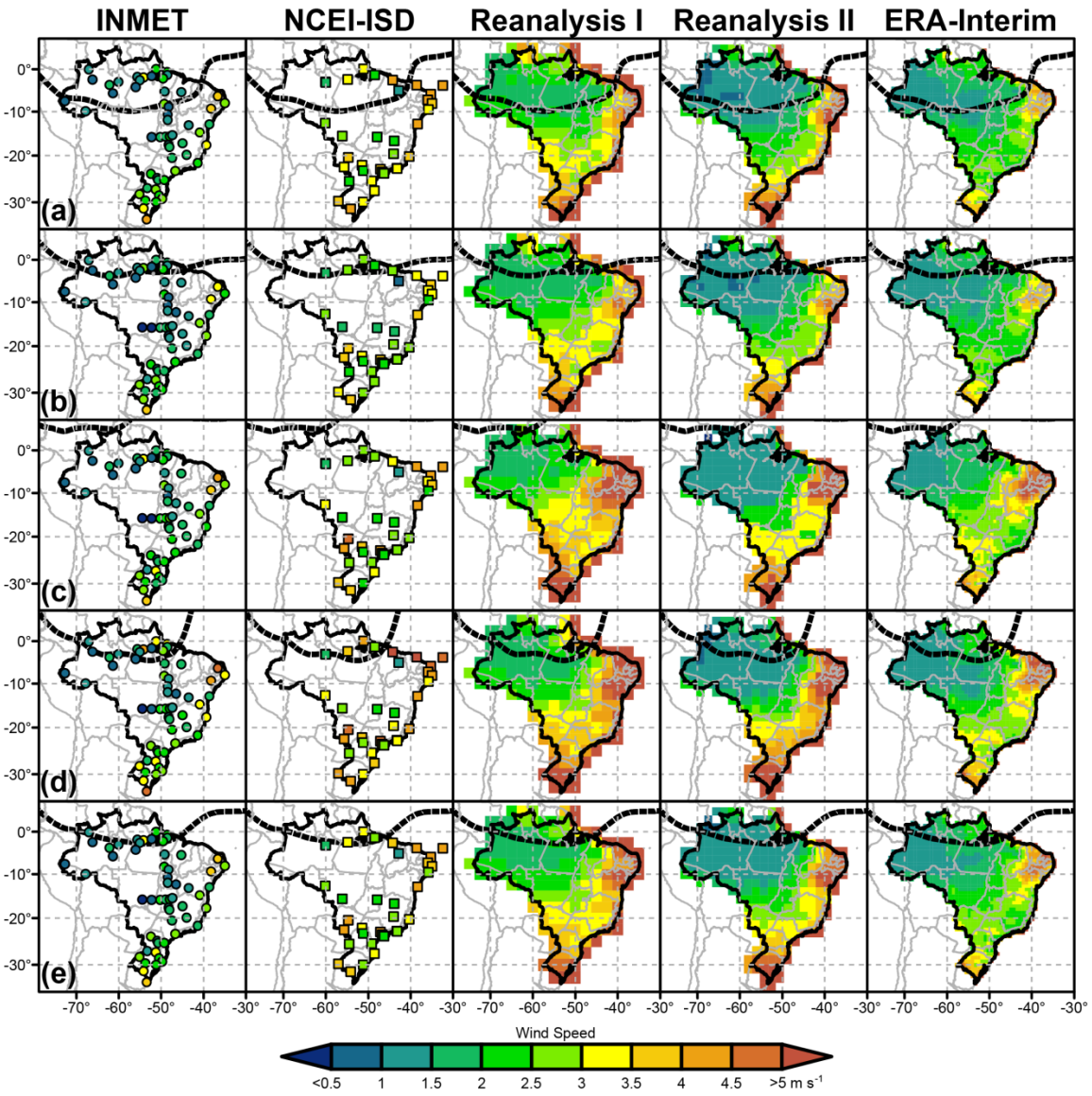

Figure 2.2. Mean wind speeds (m s^{-1}) for (a) summer (DJF), (b) fall (MAM), (c) winter (JJA), (d) spring (SON), and (e) annual based on surface measurement and reanalysis datasets during 1980–2014. Mean seasonal and annual position of the ITCZ (dash line) is derived from Waliser and Gautier (1993).

Overall annual average winds from each dataset were categorized into 4 groups (0–2, 2–4, and 4–6, and >6 m s^{-1}). INMET, Reanalysis 2, and ERA-Interim show that the majority of annual average wind speeds across Brazil are below 2 m s^{-1}, while NCEI-ISD and Reanalysis 1 exhibited mean wind speeds that range between 2 and 4 m s^{-1}. The strongest (>6 m s^{-1}) mean annual wind speeds occur with each climate reanalysis dataset.

These results demonstrate that the annual mean winds across Brazil are slow and light. This high frequency of low annual mean speeds is a result of the Amazon basin, where average wind speeds across the basin range between 1 and 2 m s^{-1} for each dataset and when located outside the Amazon basin, the average wind speed exceeds 3 m s^{-1}.

Figure 2.3 shows the seasonal and overall Weibull distribution of wind speeds by dataset. The strongest (weakest) mean wind speeds are observed during winter and spring (summer and fall). Weibull parameters display a gradual flattening (stretching) of the distribution, which supports higher (lower) wind speeds during winter and spring (summer and fall).

The surface wind speed distributions also shows a variation exists between the five datasets. INMET depicts an exponential distribution, where a low λ value indicates a higher random probability of expecting light winds (<2 m s^{-1}) to occur. In contrast, NCEI-ISD shows wind distributions more comparable to reanalysis data. The best-fit wind distribution comparison of NCEI-ISD is to Reanalysis 1, which exhibit similar k and λ values during summer, spring, and annual periods (Figure 2.3a, 2.3d, and 2.3e). The difference shown in Weibull parameters between land-based stations is likely related to the physical environment. INMET stations tend to be located in urban environments, whereas airport and military sites selected from NCEI-ISD are positioned in open terrain surroundings. The high frequency of low wind speeds observed by INMET sites could also be influencing the overall seasonal and annual distribution. Pes et al. (2017) identified data quality issues when examining minimum and maximum surface wind trends across Brazil between 1947 and 2014.

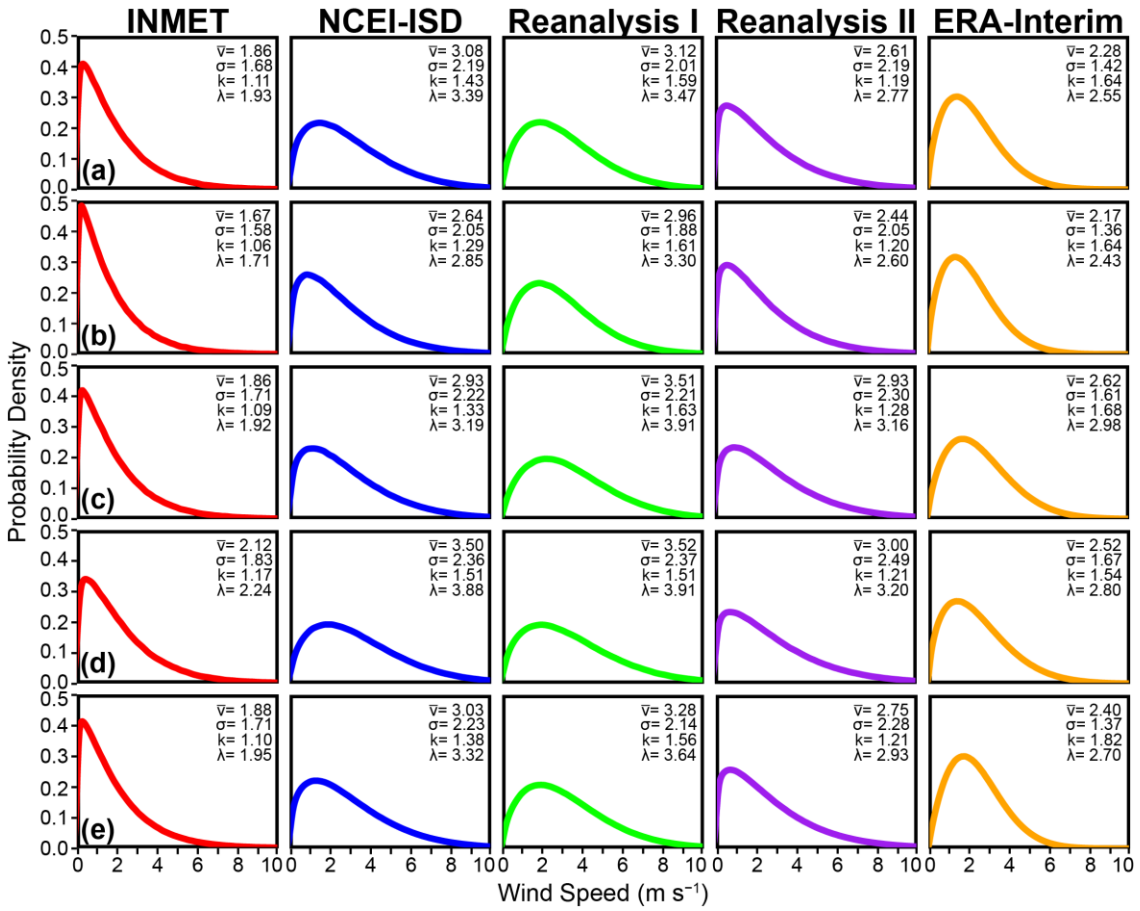

Figure 2.3. Weibull probability density plots of surface and reanalysis datasets for (a) summer (DJF), (b) fall (MAM), (c) winter (JJA), (d) spring (SON), and (e) overall during 1980–2014. Mean wind speed (m s^{-1}) [$\overline{V}$], standard deviation (σ), shape (k), and scale (λ) parameter values are provided for each Weibull plot.

The distribution of surface wind speeds for each reanalysis dataset is impacted by the type of land-cover and planetary boundary layer scheme used in the model. This is supported by Reanalysis 1 and Reanalysis 2, which use similar raw observational data to calculate surface wind speeds. Kanamitsu et al. (2002) describes that an updated planetary boundary and orographic scheme was introduced into Reanalysis 2. This improved scheme used by Reanalysis 2 shows a lower mean wind speed and a reduction (stretching) of λ (k) values for each seasonal and annual period when compared to Reanalysis 1.

2.3.2 Linear Trend Analysis

Overall linear seasonal and annual mean wind speed trends are displayed in Table 2.2, which shows a high degree of variability exists between the five datasets from 1980 to 2014. INMET shows that mean wind speeds have significantly (p<0.05) decreased during all periods except winter. This finding is in accordance with Santos and Silva (2013), who described negative linear wind speed trends for INMET stations across northeastern Brazil. However, NCEI-ISD and ERA-Interim, show positive significant (p<0.05) linear wind trends during each seasonal and annual interval. This temporal variation in trends is also described for Reanalysis 1 and Reanalysis 2, which exhibit negative (positive) wind speed trends for fall (spring). The only agreement found between the datasets occurs during spring when INMET is excluded.

Table 2.2. Statistical regression (m s^{-1} $decade^{-1}$) analysis of overall seasonal and annual mean wind speeds for *in-situ* and reanalysis datasets during 1980–2014. A * indicates the linear regression is statistically significance at the 95% confidence-level.

Dataset	Summer (DJF)	Fall (MAM)	Winter (JJA)	Spring (SON)	Annual
INMET	-0.02*	-0.03*	-0.05*	-0.02	-0.03*
NCEI-ISD	0.17*	0.16*	0.16*	0.20*	0.17*
Reanalysis 1	0.02	-0.04*	-0.02	0.05*	0.00
Reanalysis 2	0.00	-0.02	0.03	0.06*	0.02
ERA-Interim	0.05*	0.03*	0.05*	0.06*	0.05*

The differences that exist between the datasets demonstrate the importance of not interpreting trends based on overall mean wind speeds alone. McVicar et al. (2008) found that reanalysis models (Reanalysis 1, Reanalysis 2, and ERA-40) underestimated overall annual *u* linear trends when compared to Australian wind data during 1975–2006. The study suggested that modifications in the data assimilation scheme or insufficient key-boundary layer parameterizations could contribute to the *u* winds calculated for each

model. Vautard et al. (2010) showed a similar underestimated linear wind trend of Reanalysis 1, while analyzing surface wind speeds across the Northern Hemisphere between 1979 and 2008. Their analysis also indicated that wind speed changes associated with ERA-Interim were related to alterations in macro-scale circulations. Consequently, these findings suggest that geographic and meteorological variables could affect wind speeds differently across Brazil. Many of the studies reported by McVicar et al. (2012) performed their analysis on a regional scale, which allowed them to examine different factors (e.g., topography, land-cover, synoptic conditions) to explain wind speed trends observed within their study area. Therefore, a geographic analysis will allow improved assessment of the differences between the datasets for Brazil.

Seasonal and annual wind speed trends are displayed in Figure 2.4. Surface winds along coastal Brazil show varying trends by season and dataset. Stations for NCEI-ISD show positive trends, while INMET exhibits declining wind speeds for each season and annually along the coastal states of Ceará to Rio Grande do Sul. Reanalysis 1 shows a coastal concentration of positive temporal trends in wind speed north of 10° S for northern and northeastern Brazil. Reanalysis 2 suggests a positive temporal trend at coastal locations that reaches its maximum extent during spring and gradually becomes more concentrated over northeastern Brazil during summer and fall. ERA-Interim indicates a broad region of temporally increasing winds over northern Brazil, with the highest positive wind trends within the states of Pará and Maranhã. The primary focus is located north of 15° S with an exception during spring and summer, where a localized area of increasing wind speeds is identified over the wetlands of Pantanal and the state of Mato Grosso.

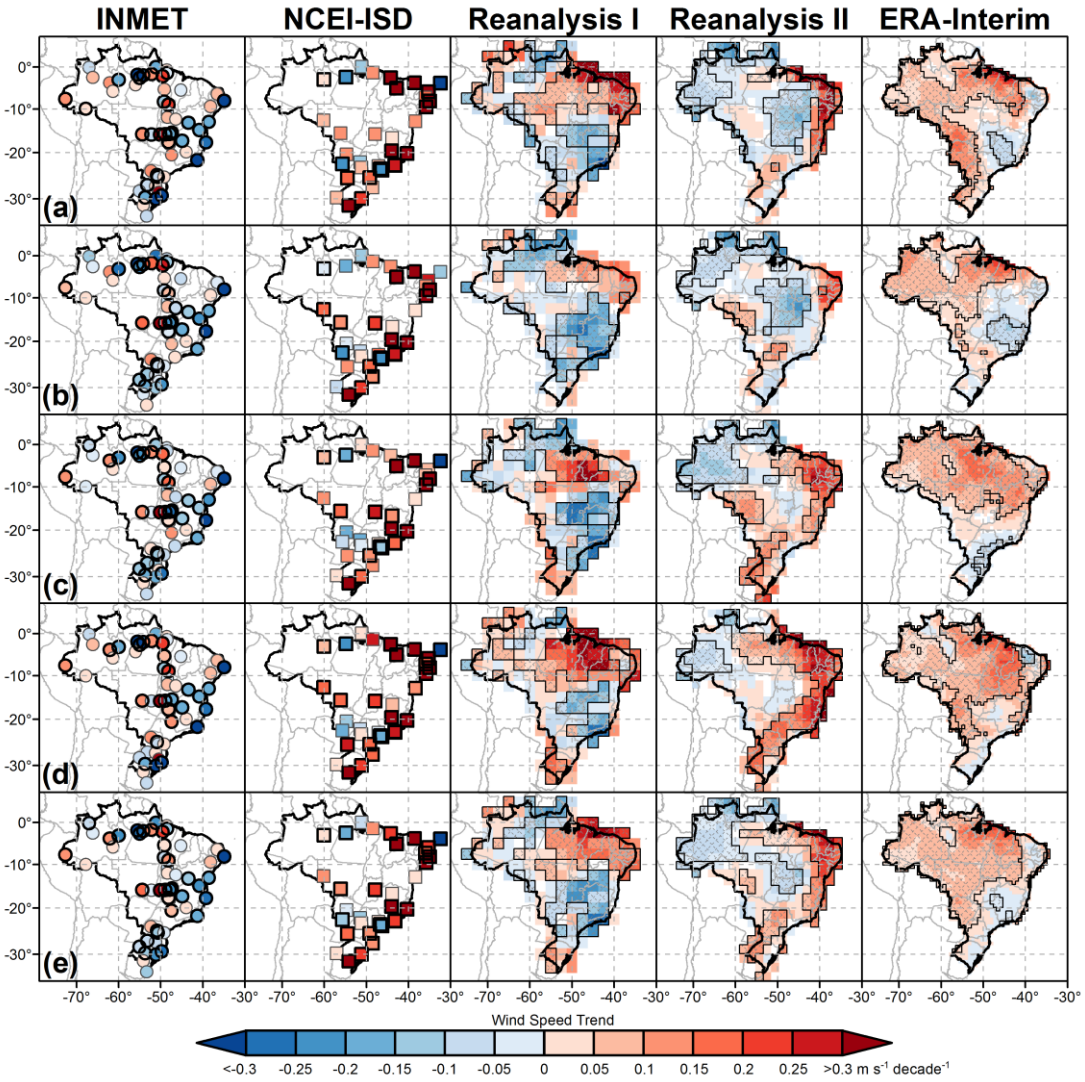

Figure 2.4. Geographic distribution of wind speed trends (m s^{-1} $decade^{-1}$) for (a) summer (DJF), (b) fall (MAM), (c) winter (JJA), (d) spring (SON), and (e) annual for INMET, NCEI-ISD, Reanalysis 1, Reanalysis 2, and ERA-Interim. Black outlines or shaded areas depict statistically significant trends at the 95% confidence-level.

Negative linear temporal trends are also present across portions of Brazil. Reanalysis 1 shows that wind speed decreases have occurred over central and southeastern Brazil. NCEI-ISD suggests a similar zonal alignment of negative wind trends that extends from Mato Grosso do Sul to São Paulo, with two localized declining patterns situated along the mouth of Amazon River and archipelago islands of Fernando de Noronha. INMET reveals that negative wind speed trends are mostly concentrated

over the states of Bahia and Minas Gerais, with a secondary axis located over Rio Grande do Sul. A similar zonal pattern is evident for southeastern Brazil with ERA-Interim during summer and fall. However, Reanalysis 2 shows the concentration of decreasing wind speeds farther north over the central Brazilian Highlands. A localized negative trend is also located along the peripheral of the Guiana Highlands during winter and spring. INMET, Reanalysis 1, and Reanalysis 2 support the decline over the Guiana Highlands but only Reanalysis 2 produces a negative surface wind speed trend into the Amazon basin.

The statistical significance of each dataset is also shown in Figure 2.4. A statistically significant ($p<0.05$) positive linear surface wind speed trend is exhibited across northeastern Brazil for Reanalysis 1, Reanalysis 2, and ERA-Interim. Likewise, a general consensus of a negative linear surface wind speed trend is found over southern and southeastern Brazil during summer and fall for all datasets excluding NCEI-ISD.

The proximity and location of both wind speed trends generate questions about the role of geographic, atmospheric, and oceanic variables for Brazil and how it is modeled. Santos and Silva (2013) suggested that wind speeds from stations located along coastal northeastern Brazil are influenced by changes in ocean-land thermal gradients and trade winds from the seasonal cycle of the ITCZ and SAA, while inland sites (i.e., Maranhão, Piauí, and Bahia) are impacted by temporally weakening SLP gradients from the equatorial low and physical topography (i.e., vegetation and elevation). Hastenrath (1976) associated stronger (weaker) than normal surface wind speeds along the coast of northeastern Brazil with dry (wet) periods. This synoptic setting develops when the ITCZ is shifted equatorward (poleward), which allows the SAA to move into lower

(higher) latitudes during austral winter (summer). As a result, sea surface temperatures (SSTs) along the coast of northeastern Brazil decrease (increase), which allows a larger (smaller) temperature gradient to develop between the land and ocean for winter (summer) in the Southern Hemisphere. As this thermal gradient increases (decreases), *u* winds located on the equatorward side of the SAA increase (decrease) and move toward the coast of northeastern Brazil. However, Vizy and Cook (2016) found that surface winds across the South Atlantic Basin (SAB) have increased despite a poleward shift of the SAA between 1982 and 2013. The study showed that an increased in latent heat transfer from the southward movement of the SAA has led to an increase in SLP. Vizy and Cook (2016) further explain that this rise in SLP intensifies near-surface winds, which in response transports more latent energy away from the area and causes a decline in SSTs to occur between 18° S and 28° S in the SAB. It is believed that the evolving position of the SAA and ITCZ is influencing the surface wind trends found across northern and northeastern Brazil.

Modifications found in land and SSTs could affect the balance between wind speed and SLP. This balance could be related to changes occurring with atmospheric temperatures being observed across South America (Skansi et al. 2013). In particular, diurnal temperature ranges (DTR) have decreased across southern Brazil during the 20th century (Marengo and Camargo 2008; Sansigolo and Kayano 2010). Both studies indicate that decreasing DTRs can be attributed to changes in land-cover and urbanization. Marengo and Camargo (2008) also examined annual SSTs between 1990–2002 and 1961–1969 for the SAB and found positive anomalies along coastal Brazil. Klink (1999) noted that decreasing surface wind speeds found across the U.S. were

related to the weakening of the pressure gradient caused by high-latitudinal hemispheric warming. This finding suggests that alternations between temperature and pressure gradient could attribute to the stilling of surface winds found across southern Brazil during 1980–2014.

2.3.3 Quantile Regression Analysis

Figure 2.5 shows the annual quantile temporal linear wind speed trends of Brazil during 1980–2014. The overall wind speed trends across the lowest percentile (i.e., 5%) exhibit minimal change (Figure 2.5a). Positive and negative geographic trends exist across portions of northeastern and southeastern Brazil of the lowest 5% and 25% quantiles (Figures 2.5a–2.5b). This finding is supported by Pes et al. (2017), who documented that weather stations located along the coast of Brazil showed changes in minimum wind speeds between 1947 and 2014. A gradual spatial expansion of wind trend magnitudes is detected with the largest changes occurring among the upper quantile wind speeds (i.e., 75% and 95%) for each dataset (Figures 2.5d–2.5e). Annual upper quantile regressions show predominately increasing (decreasing) wind speed trends over the Amazon basin for ERA-Interim (Reanalysis 2) [Figures 2.5d–2.5e]. Reanalysis 1 depicts a spatial pattern of increasing wind speeds developing over the western part of Amazonas and declining extreme wind speeds across northeastern Amazonas, Para, and Roraima. INMET shows comparable negative trends to Reanalysis 2, which are observed across the states of Amazonas and Pará.

A seasonal quantile trend analysis is also performed for austral summer (Figure 2.6) and winter (Figure 2.7). Reanalysis datasets show large areas of increasing (decreasing) lower quantile winds along the Brazilian coast (highland) during summer

(Figure 2.6a–2.6b). This suggests that the summer land-ocean thermal gradient is strengthening over northeastern Brazil. Silva (2004) documented that minimum temperatures across northeastern Brazil have increased during later part of the 20th century. This temperature modification along the coast of Brazil would allow a stronger thermal gradient to develop between the land and ocean, which would enable wind speeds to increase at the lower quantiles.

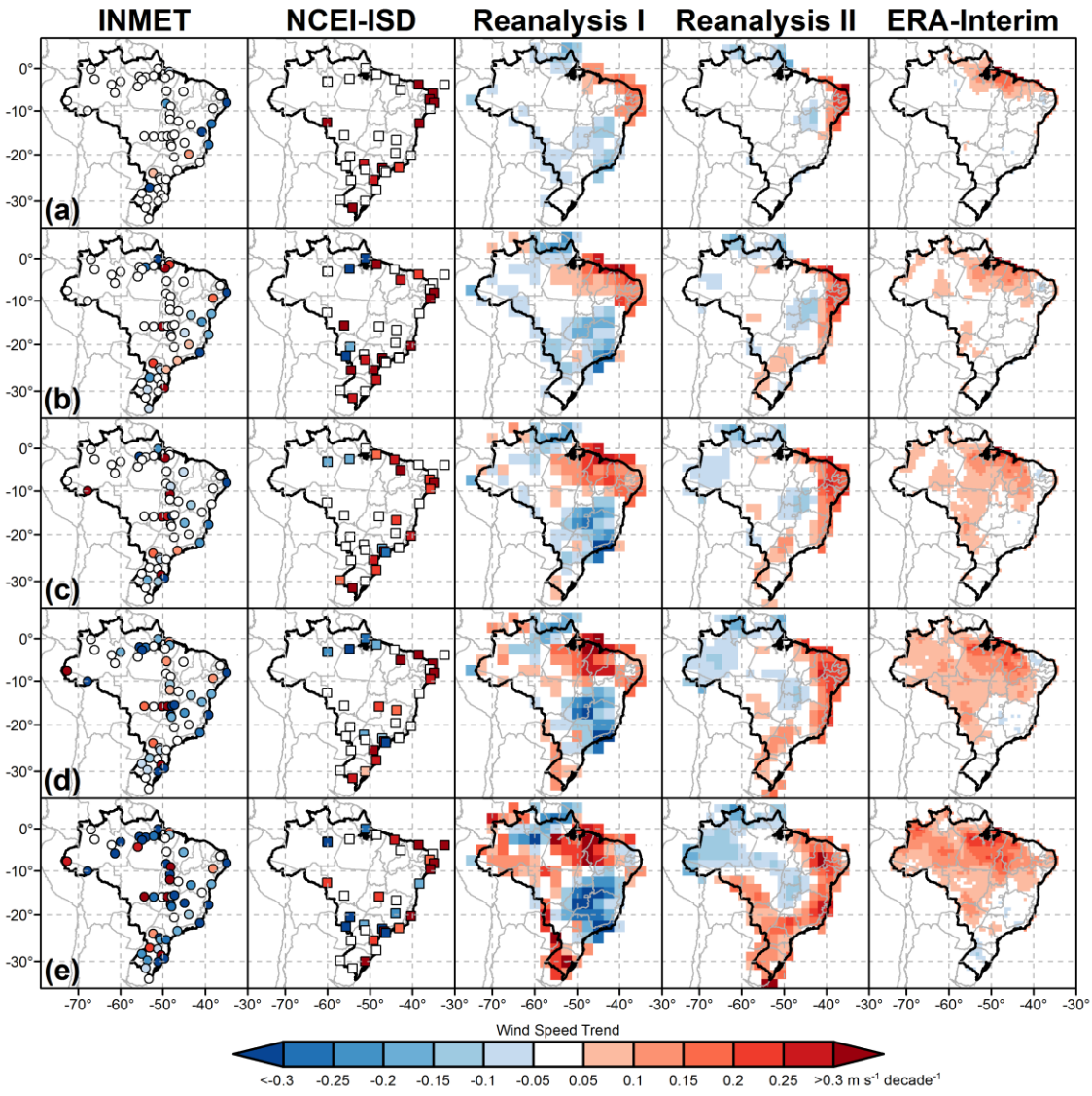

Figure 2.5. Annual quantile regression (m s^{-1} $decade^{-1}$) by percentile (a) 5%, (b) 25%, (c) 50%, (d) 75%, and (e) 95% for INMET, NCEI-ISD, Reanalysis 1, Reanalysis 2, ERA-Interim for the period of 1980 to 2014.

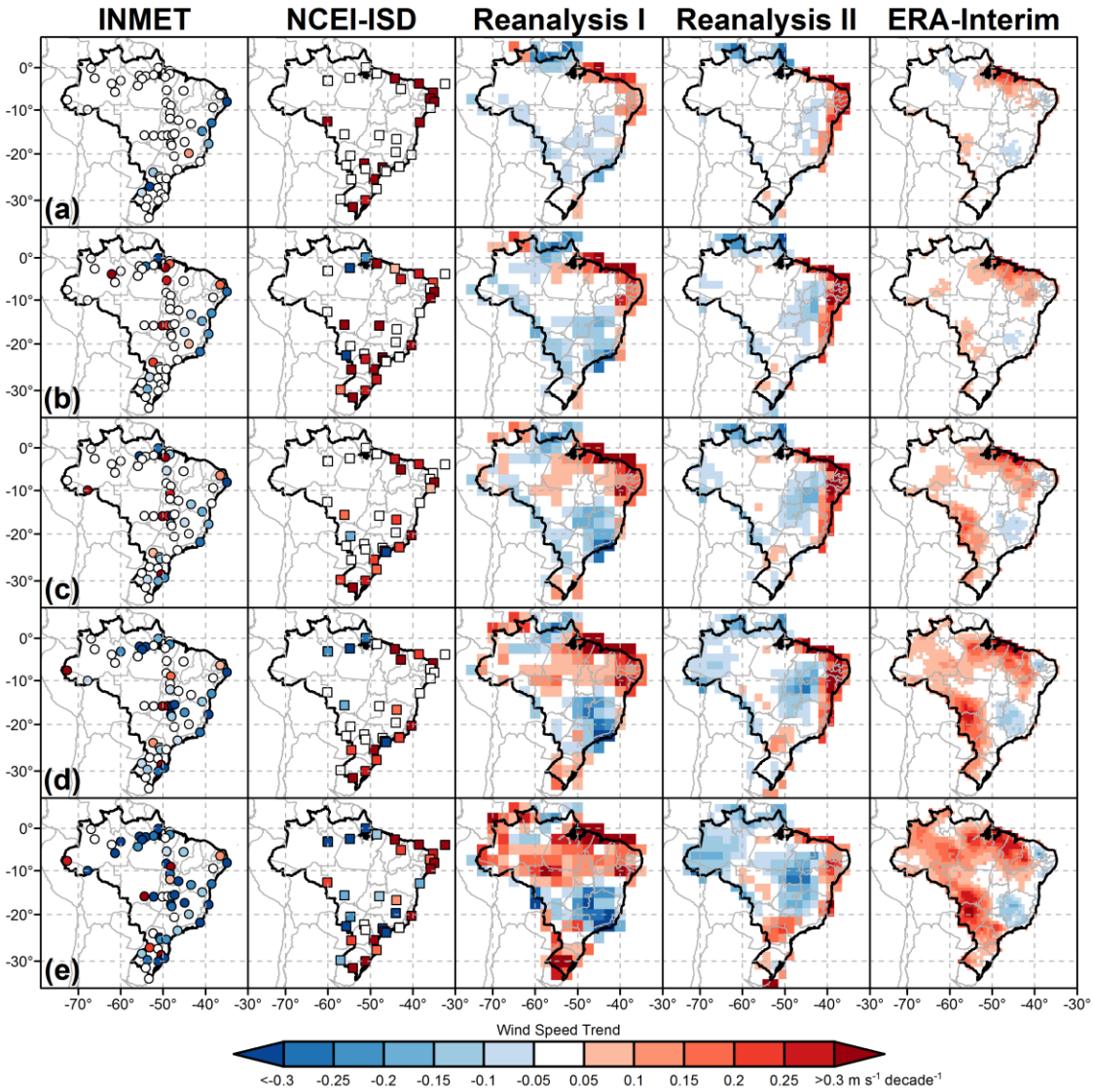

Figure 2.6. As in Figure 2.5 except for summer (DJF).

During winter, geographic trends of minimum wind speeds are present but on a broader, regional scale (Figure 2.7). Positive and negative wind trends extend farther into central Brazil and portions of the Amazon basin for each reanalysis dataset, while station data depict quantile trends along parts of eastern Brazil. This change occurring at lower wind speeds indicates that macro-scale conditions are possibly shifting across Brazil during the dry season. Degola (2013) documented that when the SAA shifts west (east) of its annual climatological mean, 10-m *u* winds increase (decrease), while temperatures

decrease (increase) across northeastern Brazil. The study further investigated the position of the SAA and found that under future warming scenarios, it is forecasted that the longitudinal center of the SAA will continually progress westward during the 21st century. It is then estimated that lower percentile wind speeds would continue to increase and impact wind energy production over northeastern Brazil.

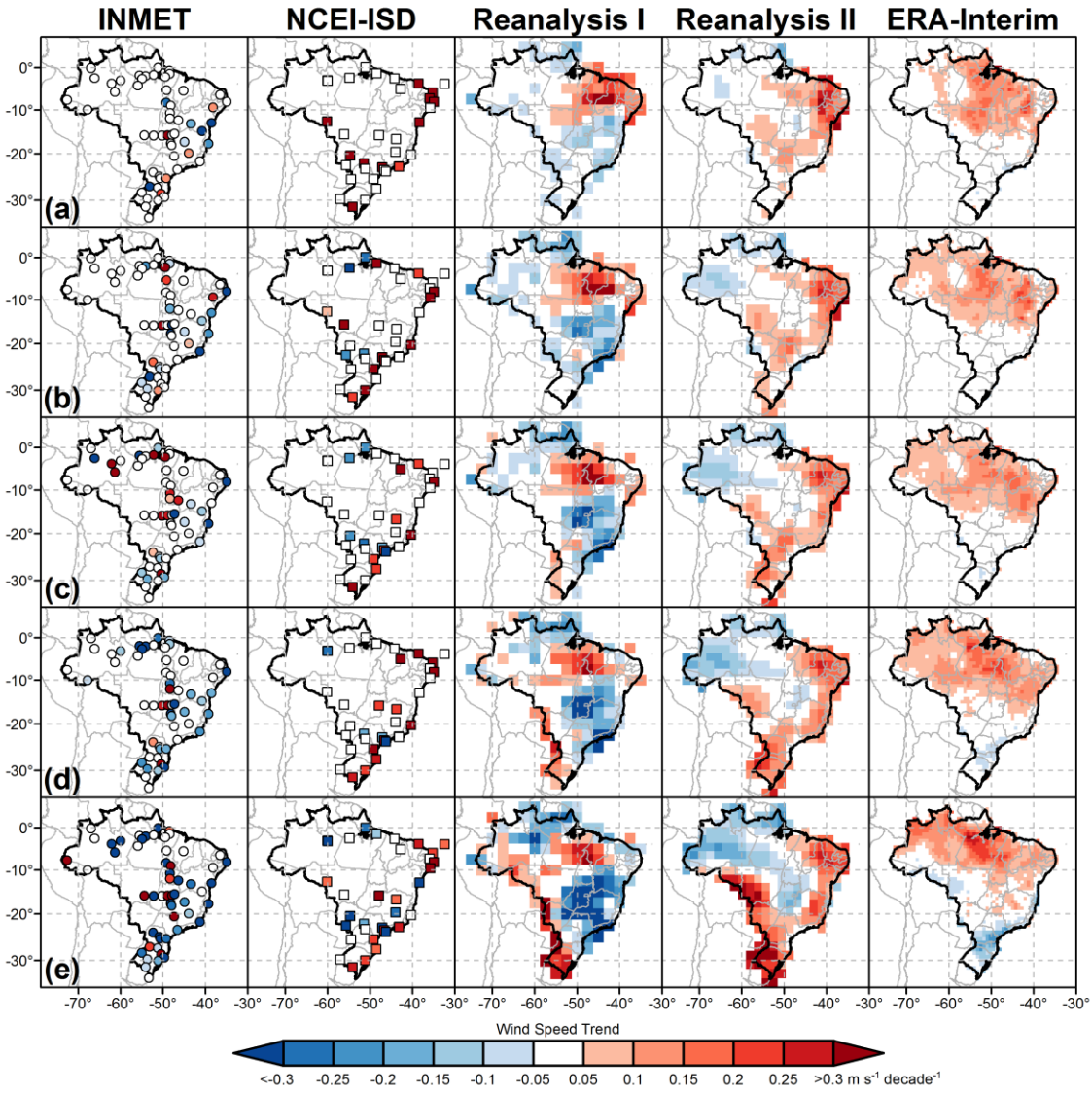

Figure 2.7. As in Figure 2.5 except for winter (JJA).

Upper quantiles (75%–95%) show that wind speeds are changing more substantially when compared to lower percentiles during austral summer (Figure 2.6) and

winter (Figure 2.7). INMET shows far more decreasing wind speeds than increasing nationwide. NCEI-ISD displays declining winds for stations located in the states of Amapá, Pará, and eastern Amazonas for each season. Reanalysis 1 depicts decreasing surface winds across portions of northern Brazil, but with largest negative trends over southeastern Brazil. However, Reanalysis 2 exhibits a defined zone of diminishing surface winds that extends from the interior of Brazil to the Brazilian Highlands, with the highest declining trends found over the state of Tocantins. ERA-Interim shows a negative concentration of upper quartile trends across southeastern Brazil during austral summer. Additionally, upper positive trends are found along the coast of Brazil for each dataset except for ERA-Interim, which exhibits an increasing pattern north of 15° S. A secondary axis of increasing quantile winds are found between the states of Rondonia and Mato Grosso do Sul during winter (summer) for Reanalysis 2 (ERA-Interim). However, INMET stations show no compatible positive quantile trends when compared to numerical data.

2.4 Conclusions

This study examines the surface wind speed trend characteristics of Brazil during 1980–2014 based on *in-situ* and climate reanalysis products. In general, the lowest (highest) seasonal and annual mean winds occur over the Amazon (coastal) states. The weakest (strongest) wind speeds develop during summer and fall (winter and spring). Density plots of the wind distributions support the seasonal wind patterns, but show differences exist between each dataset, possibly stemming from land-cover and data quality concerns associated with INMET.

Nonparametric statistics are implemented to describe the overall linear trends of seasonal and annual mean wind speeds for Brazil. INMET observation sites show that wind speeds have statistically (p<0.05) declined across seasonal and annual periods (except for winter) from 1980 to 2014. However, NCEI-ISD and ERA-Interim exhibit a statistically significant (p<0.05) increase in seasonal and annual winds across Brazil. This temporal inconsistency of the overall seasonal and annual surface wind speed trends of both *in-situ* and reanalysis datasets is concerning. It is supported by the linear trend differences that exist between Reanalysis 1 and Reanalysis 2, which use similar raw data to extrapolate surface winds across Brazil. Pryor et al. (2009) demonstrated that discrepancy exists between surface wind measurements and reanalysis products while examining surface wind speed trends across the United States. The results from this study support that outcome and suggest the concerns that occur for station observations and climate reanalysis datasets.

This study also examined how lower and upper percentile wind speeds have changed linearly through time based on quantile regression (Koenker and Bassett 1978). Lower percentile (5% and 25%) trends show that positive or negative wind speed changes that exist tend to be found along the coast of Brazil. Median quantile (50%) trends similarly follow the patterns described by mean wind speeds for *in-situ* and reanalysis products. The highest spatial distribution wind speed change is found with upper quantiles (75% and 95%), which were located in coastal and southeastern Brazil. The variation that exists among extreme wind speeds for surface wind measurements and climate models implies that other atmospheric or geographic variables are possibly changing over the study region. Degola (2013) documented using ERA-Interim that

changes in the location of the SAA were responsible for influencing surface winds for northeastern Brazil. Any modifications in wind speeds across each quantile could be related to changes in temperature and pressure gradients observed over Brazil and warrants further investigation.

It is challenging to compare and assess historical and reanalysis surface wind products to each other adequately. This conclusion is supported by Troccoli et al. (2012) who investigated three reanalysis products and found that land-based wind speed trends vary greatly between models, which made it difficult to determine which reanalysis product can replicate near-surface winds across Australia. Pryor et al. (2009) concluded that no distinct agreement could be reached when analyzing *in-situ*, regional climate, and reanalysis datasets for the contiguous United States.

The present study found some agreements between weather station and climate reanalysis models. However, reanalysis products show overall annual and seasonal mean wind speeds and trends that are comparable to NCEI-ISD than INMET. This favorable agreement of NCEI-ISD with reanalysis products may be related to the fact that INMET reporting stations tend to be located in urban environments across Brazil. Pes et al. (2017) describes three regions across Brazil that are generating wind energy, with the largest contribution coming from the northeast followed by the southeastern and southern regions. Therefore, further research is required to understand how and why differences exist between historical data and reanalysis products with the goal in mind to improve and produce better future forecasting on wind energy production for Brazil.

2.5 References

Abhishek A, Lee J-Y, Keener TC, Yang YJ. 2010. Long-term wind speed variations for three Midwestern U.S. cities. *Journal of the Air and Waste Management Association* **60**: 1057–1064. doi: 10.3155/1047-3289.60.9.1057.

ANEEL. 2017. Banco de Informacão de Geracão. Available at: National Electricity Regulatory Agency. http://www2.aneel.gov.br/aplicacoes/capacidadebrasil/capacidadebrasil.cfm. [Accessed May 2017].

Azorin-Molina C, Vicente-Serrano SM, McVicar TR, Jerez S, Sanchez-Lorenzo A, López-Moreno J-I, Revuelto J, Trigo RM, Lopez-Bustins JA, Espírito-Santo F. 2014. Homogenization and assessment of observed near-surface wind speed trends over Spain and Portugal, 1961–2011. *Journal of Climate* **27**: 3692–3712. doi: 10.1175/JCLI-D-13-00652.1.

Bichet A, Wild M, Folini D, Schär C. 2012. Causes for decadal variations of wind speed over land: Sensitivity studies with a global climate model. *Geophysical Research Letters* **39**: L11701. doi: 10.1029/2012GL051685.

Brázdil R, Chromá K, Dobrovolný P, Tolasz R. 2009. Climate fluctuations in the Czech Republic during the period 1961–2005. *International Journal of Climatology* **29**: 223–242. doi: 10.1002/joc.1718.

Burn DH, Hesch NM. 2007. Trends in evaporation for the Canadian Prairies. *Journal of Hydrology* **336**: 61–73. doi: http://doi.org/10.1016/j.jhydrol.2006.12.011.

Chen L, Li D, Pryor SC. 2013. Wind speed trends over China: Quantifying the magnitude and assessing causality. *International Journal of Climatology* **33**: 2579–2590. doi: 10.1002/joc.3613.

Dadaser-Celik F, Cengiz E. 2014. Wind speed trends over Turkey from 1975 to 2006. *International Journal of Climatology* **34**: 1913–1927. doi:10.1002/joc.3810.

Davenport AG. 1963. The relationship of wind structure to wind loading. *Proceedings of Conference: Wind Effects on Buildings and Structures*. National Physical Laboratory. London, England. 19–82.

Dee DP, Uppala SM, Simmons AJ, Berrisford P, Poli P, Kobayashi S, Andrae U, Balmaseda MA, Balsamo G, Bauer P, Bechtold P, Beljaars ACM, van de Berg L, Bidlot J, Bormann N, Delsol C, Dragani R, Fuentes M, Geer AJ, Haimberger L, Healy SB, Hersbach H, Hólm EV, Isaksen L, Kållberg P, Köhler M, Matricardi M, McNally AP, Monge-Sanz BM, Morcrette J-J, Park B-K, Peubey C, de Rosnay P, Tavolato C, Thépaut J-N, Vitart F. 2011. The ERA-Interim reanalysis: Configuration and performance of the data assimilation system. *Quarterly Journal of the Royal Meteorological Society* **137**: 553–597. doi: 10.1002/qj.828.

DeGaetano AT. 1998. Identification and implications of biases in U.S. surface wind observation, archival, and summarization methods. *Theoretical and Applied Climatology* **60**: 151–162. doi: 10.1007/s007040050040.

Degola TSD. 2013. Impactos e variabilidade do Anticiclone Subtropical do Atlântico Sul sobre o Brasil no clima presente e em cenários futuros. Institute of Astronomy, Geophysics and Atmospheric Sciences, University of São Paulo, São Paulo, pp. 91.

Dorman JL, Sellers PJ. 1989. A global climatology of albedo, roughness length and stomatal resistance for atmospheric general circulation models as represented by the Simple Biosphere Model (SiB). *Journal of Applied Meteorology and Climatology* **28**: 833–855. doi: http://dx.doi.org/10.1175/1520-0450(1989)028<0833:AGCOAR>2.0.CO;2.

Fu G, Yu J, Zhang Y, Hu S, Ouyang R, Wenbin L. 2011. Temporal variation of wind speed in China for 1961–2007. *Theoretical and Applied Climatology* **104**: 313–324. doi: 10.1007/s00704-010-0348-x.

Gao G, Chen D, Ren G, Chen Y, Liao Y. 2006. Spatial and temporal variations and controlling factors of potential evapotranspiration in China: 1956–2000. *Journal of Geographical Sciences* **16**: 3–12. doi:10.1007/s11442-006-0101-7.

Gordon C, Cooper C, Senior CA, Banks H, Gregory JM, Johns TC, Mitchell JFB, Wood A. 2000. The simulation of SST, sea ice extents and ocean heat transports in a version of the Hadley Centre coupled model without flux adjustments. *Climate Dynamics* **16**: 147–168. doi: 10.1007/s003820050010.

Griffin BJ, Kohfeld KE, Cooper AB, Boenisch G. 2010. Importance of location for describing typical and extreme wind speed behavior. *Geophysical Research Letters* **37**: L22804. doi: 10.1029/2010GL045052.

Guo H, Xu M, Hu Q. 2011. Changes in near-surface wind speed in China: 1969–2005. *International Journal of Climatology* **31**: 349–358. doi: 10.1002/joc.2091.

Hastenrath S. 1976. Variations in low-latitude circulation and extreme climatic events in the Tropical Americas. *Journal of the Atmospheric Sciences* **33**: 202–215. doi: http://dx.doi.org/10.1175/1520-0469(1976)033<0202:VILLCA>2.0.CO;2.

Hastings DA, Dunbar PK, Elphingstone GM, Bootz M, Murakami H, Maruyama H, Masaharu H, Holland P, Payne J, Bryant NA, Logan TL, Muller J-P, Schreier G, MacDonald JS. 1999. The Global Land One-kilometer Base Elevation (GLOBE) Digital Elevation Model, Version 1.0. *National Oceanic and Atmospheric Administration National Geophysical Data Center*. Boulder, CO. http://www.ngdc.noaa.gov/mgg/topo/globe.html.

Hewston R, Dorling SR. 2011. An analysis of observed daily maximum wind gust in the UK. *Journal of Wind Engineering and Industrial Aerodynamics* **99***:* 845–856. doi: 10.1016/j.jweia.2011.06.004.

Holt E, Wang J. 2012. Trends of wind speed at wind turbine height of 80 m over the contiguous United States using the North American Regional Reanalysis (NARR). *Journal of Applied Meteorology and Climatology* **51**: 2188–2202. doi: http://dx.doi.org/10.1175/JAMC-D-11-0205.1.

Hundecha Y, St-Hilaire A, Ouarda TBMJ, El Adlouni S, Gachon P. 2008. A nonstationary extreme value analysis for the assessment of changes in extreme annual wind speed over the Gulf of St. Lawrence, Canada. *Journal of Applied Meteorology and Climatology* **47**: 2745–2759. doi: http://dx.doi.org/10.1175/2008JAMC1665.1.

Jakob D. 2010. Challenges in developing a high-quality surface wind-speed data-set for Australia. *Australian Meteorological and Oceanographic Journal* **60**: 227–236.

Jaswal AK, Koppar AL. 2013. Climatology and trends in near-surface wind speed over India during 1961–2008. *Mausam* **64**: 417–436.

Jiang Y, Luo Y, Zhao Z, Tao S. 2010. Changes in wind speed over China during 1956–2004. *Theoretical and Applied Climatology* **99**: 421–430. doi: 10.1007/s00704-009-0152-7.

Justus CG, Hargraves WR, Mikhail A, Graber D. 1978. Methods for estimating wind speed frequency distributions. *Journal of Applied Meteorology* **17**: 350–353. doi: http://dx.doi.org/10.1175/1520-0450(1978)017<0350:MFEWSF>2.0.CO;2.

Kalnay E, Kanamitsu M, Kistler R, Collins W, Deaven D, Gandin L, Iredell M, Saha S, White G, Woollen J, Zhu Y, Leetmaa A, Reynolds R, Chelliah M, Ebisuzaki W, Higgins W, Janowiak J, Mo KC, Ropelewski C, Wang J, Jenne R, Joseph D. 1996. The NCEP/NCAR 40-year reanalysis project. *Bulletin of American Meteorological Society* **77**: 437–471. doi: http://dx.doi.org/10.1175/1520-0477(1996)077<0437:TNYRP>2.0.CO;2.

Kanamitsu M, Ebisuzaki W, Woollen J, Yang S-K, Hnilo JJ, Fiorino M, Potter GL. 2002. NCEP–DOE AMIP-II Reanalysis (R-2). *Bulletin of American Meteorological Society* **83**: 1631–1643. doi: http://dx.doi.org/10.1175/BAMS-83-11-1631.

Kendall MG. 1975. Rank correlation methods. 202 pp. Griffin. London, U.K.

Kim J, Palk K. 2015. Recent recovery of surface wind speed after decadal decrease: A focus on South Korea. *Climate Dynamics* **45**: 1699–1712. doi: 10.1007/s00382-015-2546-9.

Klink K. 1999. Trends in mean monthly maximum and minimum surface wind speeds in the coterminous United States, 1961 to 1990. *Climate Research* **13**: 193–205. doi: 10.3354/cr013193.

————. 2002. Trends and interannual variability of wind speed distributions in Minnesota. *Journal of Climate* **15**: 3311–3317. doi: http://dx.doi.org/10.1175/1520-0442(2002)015<3311:TAIVOW>2.0.CO;2.

Koenker R, Bassett G. 1978. Regression Quantiles. *Econometrica* **46**: 33–50.

Li X, Zhong S, Bian X, Heilman WE. 2010. Climate and climate variability of the wind power resources in the Great Lakes region of the United States. *Journal of Geophysical Research* **115**: D18107. doi: 10.1029/2009JD013415.

Li Z, Yan Z, Tu K, Liu W, Wang Y. 2011. Changes in wind speed and extremes in Beijing during 1960–2008 based on homogenized observations. *Advances in Atmospheric Sciences* **28**: 408–420. doi: 10.1007/s00376-010-0018-z.

Lin C, Yang K, Qin J, Fu R. 2013. Observed coherent trends of surface and upper-air wind speed over China since 1960. *Journal of Climate* **26**: 2891–2903. doi: http://dx.doi.org/10.1175/JCLI-D-12-00093.1.

Liu Q, Yang Z, Sun T. 2010. The temporal trends of reference evapotranspiration and its sensitivity to key meteorological variables in Yellow River Basin, China. *Hydrological Processes* **24**: 2171–2181. doi: 10.1002/hyp.7649.

Liu X, Luo Y, Zhang D, Zhang M, Liu C. 2011. Recent changes in pan-evaporation dynamics in China. *Geophysical Research Letters* **38**: L13404. doi: 10.1029/2011GL047929.

Liuzzo L, Viola F, Noto LV. 2016. Wind speed and temperature trends impacts on reference evapotranspiration in southern Italy. *Theoretical and Applied Climatology* **123**: 43– 62. doi: 10.1007/s00704-014-1342-5.

Lott JN, Vose RS, Del Greco SA, Ross TR, Worley S, Comeaux JL. 2008. The integrated surface database: Partnerships and progress. Preprints 24th Conference on Interactive Information Processing Systems for Meteorology, Oceanography, and Hydrology New Orleans, LA. *American Meteorological Society*: Paper 131387.

Lucena AFP, Szklo AS, Schaeffer R, Dutra RM. 2010. The vulnerability of wind power to climate change in Brazil. *Renewable Energy* **35**: 904–912. doi: 10.1016/j.renene.2009.10.022.

Mann HB. 1945. Nonparametric tests against trend. *Econometrica* **13**: 245–259.

McVicar TR, Van Niel TG, Li LT, Roderick ML, Rayner DP, Ricciardull L, Donohue RJ. 2008. Wind speed climatology and trends for Australia, 1975–2006: Capturing the stilling phenomenon and comparison with near-surface reanalysis output. *Geophysical Research Letters* **35**: L20403. doi: 10.1029/2008GL035627.

————, Roderick ML, Donohue RJ, Li, LT, Van Niel TG, Thomas A. Grieser J, Jhajharia D, Himri Y, Mahowald NM, Mescherskaya AV, Kruger AC, Rehman S, Dinpashoh Y. 2012. Global review and synthesis of trends in observed terrestrial near-surface wind speeds: Implications for evaporation. *Journal of Hydrology* **417**: 182–205. doi: https://doi.org/10.1016/j.jhydrol.2011.10.024.

Obukhov AM. 1971. Turbulence in an atmosphere with non-uniform temperature. *Boundary Layer Meteorology* **1**: 7–29. doi: 10.1007/BF00718085.

Pereira EB, Martins FR, Pes MP, Segundo EID, Lyra AD. 2013. The impacts of global climate changes on the wind power density in Brazil. *Renewable Energy* **49:** 107–110. doi: https://doi.org/10.1016/j.renene.2012.01.053.

Pes MP, Pereira EB, Marengo JA, Martins FR, Heineman D, Schmidt M. 2017. Climate trends on the extreme winds in Brazil. *Renewable Energy* **109**: 110–120. doi: http://doi.org/10.1016/j.renene.2016.12.101.

Pirazzoli PA, Tomasin A. 2003. Recent near-surface wind changes in the central Mediterranean and Adriatic areas. *International Journal of Climatology* **23**: 963–973. doi: 10.1002/joc.925.

Pryor SC, Barthelmie RJ. 2003. Long-term trends in near-surface flow over the Baltic. *International Journal of Climatology* **23**: 271–289. doi: 10.1002/joc.878.

————, ————, Riley ES. 2007. Historical evolution of wind climates in the USA. *Journal of Physics: Conference Series* **75**: 012065.

————,————,Young, DT, Takle ES, Arritt RW, Flory D, Gutowski WJ, Nunes A, Roads J. 2009. Wind speed trends over the contiguous United States. *Journal of Geophysical Research* **114**: D14105. doi: 10.1029/2008JD011416.

————, Ledolter J. 2010. Addendum to "Wind speeds trends over the contiguous United States". *Journal of Geophysical Research* **115**: D10103. doi: 10.1029 /2009JD013281.

Romanić D, Ćurić M, Jovičić I, Lompar M. 2015. Long-term trends of the 'Koshava' wind during the period 1949–2010. *International Journal of Climatology* **35**: 288–302. doi: 10.1002/joc.3981.

————, Hangan H, Ćurić M. 2016. Wind climatology of Toronto based on the NCEP/NCAR reanalysis 1 data and its potential relation to solar activity. *Theoretical and Applied Climatology* **In press**: 1–17. doi: 10.1007/s00704-016-2011-7.

Sansigolo CA, Kayano MT. 2010. Trends of seasonal maximum and minimum temperatures and precipitation in Southern Brazil for 1913–2006 period. *Theoretical and Applied Climatology* **101**: 209–216. doi: 10.1002/joc.3370100303.

Santos ATS, Silva CMS. 2013. Seasonality, interannual variability, and linear tendency of wind speeds in the northeast Brazil from 1986 to 2011. *The Scientific World Journal*. doi: http://dx.doi.org/10.1155/2013/490857.

Schwerdtfeger W. 1976. Introduction. *World Survey of Climatology, Volume 12, Climates of Central and South America*. Schwerdtfeger, W (ed.). Amsterdam. 1–11.

Sen PK, 1968. Estimates of the regression coefficient based on Kendall's tau. *Journal of the American Statistical Association* **63**: 1379–1389.

Silva VPR. 2004. On climate variability in northeast of Brazil. *Journal of Arid Environments* **58**: 575–596. doi: https://doi.org/10.1016/j.jaridenv.2003.12.002.

————, Silva RA, Cavalcanti EP, Braga CC, Azevedo PV, Singh VP, Pereira ERR. 2010. Trends in solar radiation in NCEP/NCAR database and measurements in northeastern Brazil. *Solar Energy* **84**: 1852–1862. doi: https://doi.org/10.1016/j.solener.2010.07.011.

Skansi MM, Brunet M, Sigró J, Aguilar E, Groening JAA, Bentancur OJ, Geier YRC, Amaya RLC, Jácome H, Ramos AM, Rojas CO, Pasten AM, Mitro SS, Jiménez CV, Martínez R, Alexander LV, Jones PD. 2013. Warming and wetting signals emerging from analysis of changes in climate extreme indices over South America. *Global and Planetary Change* **100**: 295–307. doi: https://doi.org/10.1016/j.gloplacha.2012.11.004.

St. George S, Wolfe SA. 2009. El Niño stills winter winds across the southern Canadian Prairies. *Geophysical Research Letters* **36**: L23806. doi:10.1029/2009GL041282.

Tang B, Tong L, Kang S, Zhang L. 2011. Impacts of climate variability on reference evapotranspiration over 58 years in the Haihe river basin of north China. *Agricultural Water Management* **98**: 1660–1670. doi: 10.1016/j.agwat.2011.06.006.

Troccoli A, Muller K, Coppin P, Davy R, Russell C, Hirsch AL. 2012. Long-term wind speed trends over Australia. *Journal of Climate*, **25**: 170–183. doi: http://dx.doi.org/10.1175/2011JCLI4198.1.

Tuller SE. 2004. Measured wind speed trends on the west coast of Canada. *International Journal of Climatology* **24**: 1359–1374. doi: 10.1002/joc.1073.

Vautard R, Cattiaux J, Yiou P, Thépaut J-N, Ciais P. 2010. Northern Hemisphere atmospheric stilling partly attributed to an increase in surface roughness. *Nature Geoscience* **3**: 756–761. doi: 10.1038/ngeo979.

Viterbo P, Beljaars AC. 1995. An improved land surface parameterization scheme in the ECMWF model and its validation. *Journal of Climate* **8**: 2716 –2748. doi: http://dx.doi.org/10.1175/1520-0442(1995)008<2716:AILSPS>2.0.CO;2.

Vizy EK, Cook KH. 2016. Understanding long-term (1982–2013) multi-decadal changes in the equatorial and subtropical South Atlantic climate. *Climate Dynamics* **46**: 2087–2113. doi: 10.1007/s00382-015-2691-1.

Waliser DE, Gautier C. 1993. A Satellite-derived climatology of the ITCZ. *Journal of Climate* **6**: 2162–2174. doi: http://dx.doi.org/10.1175/15200442(1993)006<2162: ASDCOT>2.0.CO;2.

Wan H, Wang, XL, Swail VR. 2010. Homogenization and trend analysis of Canadian near-surface wind speeds. *Journal of Climate* **23**: 1209–1225. doi: http://dx.doi.org/10.1175/2009JCLI3200.1.

Wever N. 2012. Quantifying trends in surface roughness and the effect on surface wind speed observations. *Journal of Geophysical Research* **117**: D11104. doi: 10.1029 /2011JD017118.

Xu M, Chang C-P, Fu C, Qi Y, Robock A, Robinson D, Zhang H. 2006. Steady decline of East Asian monsoon winds, 1969–2000: Evidence from direct ground measurements of wind speed. *Journal of Geophysical Research* **111**: D24111. doi: 10.1029/2006JD007337.

Yang X, Li ZX, Feng Q, He YQ, An WL, Zhang W, Cao WH, Yu TF, Wang YM, Theakstone W. 2012. The decreasing wind speed in southwestern China during 1969–2009 and possible causes. *Quaternary International* **263**: 71–84. doi: http://dx.doi.org/10.1016/j.quaint.2012.02.020.

Yin Y, Wu S, Chen G, Dai E. 2010a. Attribution analyses of potential evapotranspiration changes in China since the 1960s. *Theoretical and Applied Climatology* **101**: 19–28. doi: 10.1007/s00704-009-0197-7.

————, ————, Dai E. 2010b. Determining factors in potential evapotranspiration changes over China in the period 1971–2008. *Chinese Science Bulletin* **55**: 3329–3337. doi: 10.1007/s11434-010-3289-y.

You Q, Fraedrich K, Min J, Kang S ,Zhu X, Pepine N, Zhanga L. 2014. Observed surface wind speed in the Tibetan Plateau since 1980 and its physical causes. *International Journal of Climatology* **34**: 1873–1882. doi: 10.1002/joc.3807.

Zheng X, Liu X, Liu C, Dai X, Zhu R. 2009. Assessing contribution to panevaporation trends in Haihe River Basin, China. *Journal of Geophysical Research* **114**: D24105. doi: 10.1029/2009JD0112203.

Zuo H, Li D, Hu Y, Bao Y, Lü S. 2005. Characteristics of climate trends and correlation between pan-evaporation and environmental factors in the last 40 years over China. *Chinese Science Bulletin* **50**: 1235–1241. doi: 10.1007/BF03183699.

CHAPTER 3
POSITION OF THE SOUTH ATLANTIC ANTICYCLONE AND ITS IMPACT ON SURFACE CONDITIONS ACROSS BRAZIL

3.1 Introduction

The climatological position of atmospheric features (cyclones and anticyclones) have been identified and examined to understand how their spatial and temporal characteristics have changed during the 19th and 20th century (Teissereng de Bort 1883; Zishka and Smith 1980; Whittaker and Horn 1984; Harman 1987; Sahsamanoglou 1990; Sinclair 1996; 1997; Davis et al. 1997; Mächel et al. 1998; Degola 2013). Studies have highlighted changes in macro-scale atmospheric patterns as a possible cause for the wind trend patterns being observed across Earth's surface (Tuller 2004; St. George and Wolfe 2009; Abhishek et al. 2010; Jiang et al. 2010; Li et al. 2010; Pryor and Ledolter 2010; You et al. 2010; Fu et al. 2011; Hewston and Dorling 2011; Yang et al. 2012; Chen et al. 2013; Lin et al. 2013; You et al. 2014). This plausible reason may be applicable to the South Atlantic Anticyclone (SAA), which is a semi-permanent pressure system that predominately controls wind speeds across Brazil (Ratisbona 1976). Santos and Silva (2013) concluded that macro-scale atmospheric circulations and topography influence surface wind speeds and wind energy production for northeastern Brazil. Regarding wind energy, the states of northeastern Brazil currently account for 78% (332) and 94% (151) of the national operational and planned sites, respectively, which constitute 81% (8.4 GW) of all wind energy produced in the country (ANEEL 2017). Therefore, any changes in the climatological position of the SAA could impact wind speeds across Brazil which would affect wind energy production, especially for northeastern Brazil.

Previous work has closely examined the latitudinal and longitudinal position of the Intertropical Convergence Zone (ITCZ) and the SAA and their impacts on various climatological characteristics within the South Atlantic Basin (SAB) [Hastenrath 1985; Mächel et al. 1998; Degola 2013; Sun et al. 2017]. Mächel et al. (1998) documented circulation center trends based on position (latitude and longitude) and sea-level pressure (SLP) gradient and trends in the SLP core using three temporal periods (1881–1989, 1950–1989, and 1970–1989) for summer (DJFM) and fall (JJAS). The study described a relationship between the latitudinal position of the ITCZ and SAA during 1950–1989 and 1970–1989. The northward (southward) movement of both ITCA and SAA resulted in increasing (decreasing) SLP gradients over the SAB during summer (DJFM). Based on this conclusion, it is expected that modifying the location of the ITCZ and SAA can affect wind speeds across Brazil. Degola (2013) found faster (slower) than normal 10 m surface wind speeds develop for northeastern Brazil during 1989–2010 when the longitudinal center of the SAA is located west (east) of its climatological monthly mean. Both of these studies establish the relevance of investigating the latitudinal and longitudinal position of the SAA center for Brazil and the SAB. As such, the goal of this research is to construct a spatial and geographic climatology that examines the daily relationship between Brazilian surface wind characteristics and the position of the SAA within the SAB from 1980 to 2014.

3.2 Data and Methods

3.2.1 Reanalysis Datasets

Three reanalysis datasets were selected to analyze the surface wind characteristics associated with the central location of the SAA in the SAB. The period of 1980 to 2014

was chosen based on the temporal availability of each climate reanalysis used in the study. National Center for Environmental Prediction/National Center for Atmospheric Research (NCEP/NCAR) reanalysis dataset (Reanalysis 1) is a 2.5° x 2.5° (T62) global resolution model that assimilates meteorological components for 28 vertical levels of the atmosphere from 1948 to present (Kalnay et al. 1996). National Center for Environmental Prediction and Department of Energy (NCEP-DOE) reanalysis dataset (Reanalysis 2) is an improved form of Reanalysis 1, which includes an enhanced spatial resolution (1.875° x 1.875°) of surface and atmospheric conditions from 1979 to present time (Kanamitsu et al. 2002). European Centre for Medium-Range Weather Forecasts (ECMWF) Interim (ERA-Interim) is a 0.75° x 0.75° (T255) global atmospheric assimilated model constructed at 60 vertical levels for the period of 1979 to present (Dee et al. 2011). Data obtained from each reanalysis product consists of six-hourly (0, 6, 12, and 18 UTC) 10 m *u* (west–east) and *v* (south–north) wind component, SLP, and 2 m air temperature which was used to calculated daily, seasonal, and annual mean grid point values for Brazil and the SAB during 1980–2014. Resultant surface wind speeds for each grid point (V) are determined based on the *u* and *v* wind components obtained from Reanalysis 1, Reanalysis 2, and ERA-Interim (Equation 1).

$$V(u,v) = \sqrt{u^2 + v^2} \tag{1}$$

3.2.2 Identify SAA Center in the SAB

Overall daily mean SLPs (based on the 4-times daily observations) were calculated for each reanalysis grid point found within the SAB during the period of 1980 to 2014. The preliminary domain of 10° S to 50° S and 60° W to 20° E was used to identify the daily center of high pressure in the SAB, which follows similar boundaries

employed by earlier analyses (i.e., Ito and Ambrizzi 2000; Castro et al. 2015). Degola (2013) used monthly mean SLPs to determine the central location of pressure for the SAA instead of daily mean SLPs because of the concern that migrating anticyclones and fragmented pressure centers in the SAB may disrupt the analysis when approximating the true mean position of the semi-permanent SAA. Ito and Ambrizzi (2000) also found that the SAA shifts from its climatological position approximately every 4 to 5 days because of mid-latitude dynamics and frontal passages that occur in the SAB during austral winter. While these issues are acknowledged, this study still believes by identifying the daily position of the maximum pressure center in the SAB is the most appropriate method to provide a comprehensive background on the surface wind characteristics of Brazil.

Upon selecting a defined study area for conducting a daily analysis, an algorithm was developed to determine the daily mean latitude and longitude location of the maximum pressure center within the SAB for Reanalysis 1, Reanalysis 2, and ERA-Interim from 1980 to 2014. Previous studies have implemented second-order Taylor series (Murray and Simmonds 1991), nearest-neighbor (Sinclair 1997; Blender and Schubert 2000; Ito and Ambrizzi 2000; Wernli and Schwierz 2006; Zarrin et al. 2010; Degola 2013), and threshold based (Davis et al. 1997) algorithms to identify the latitudinal and longitudinal center of pressure. For this study, the daily center of the SAA is derived using a simple mean-based algorithm (Figure 3.1). The initial step of the algorithm first calculates the mean SLP based on the preliminary boundary of 10° S to 50° S and 60° W to 20° E (label A), which selects SLP grid points that are greater than the daily average for further processing (label B). This sequence is repeated for two additional computations using the remaining grid SLP values selected from the previous

step to find the location center of the SAA (labels C–D). As the final task of the algorithm, all remaining SLPs that are one standard deviation above the mean (label E) are used to calculate the daily mean latitude and longitude center of the SAA for the SAB (label F). It should be noted that passing anticyclones that typically form during austral winter and spring in the Southern Hemisphere are subject to be included in the dataset if the algorithm determines it to be the maximum pressure center for that day. With this concern, the results from this algorithm should be inferred with caution.

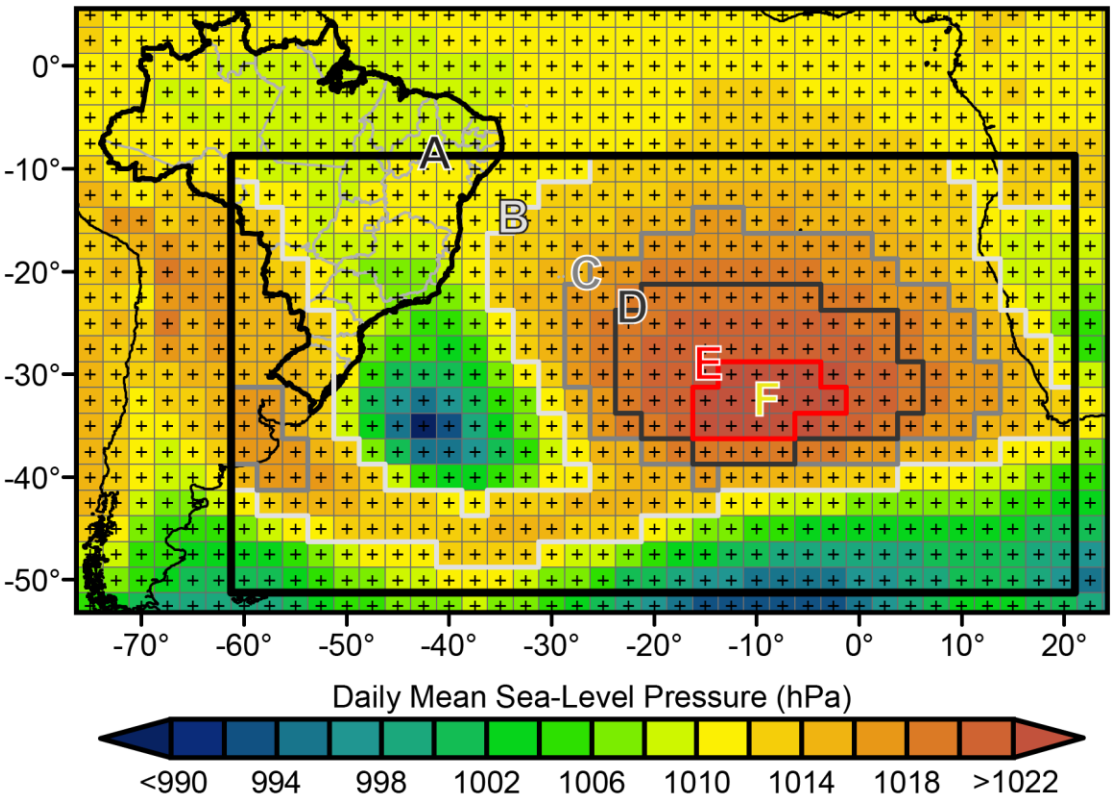

Figure 3.1. An example of the algorithm employed to identify the daily mean center of the SAB high pressure system (label F) for 1 January 1980 from Reanalysis 1. Initial black box (label A) represents the boundary used to select grid values that follow the criterion (labels B–E) set by the algorithm for each reanalysis used in the study.

3.2.3 Surface Wind Speed and SAA Characteristics of the SAB

Nonparametric statistics are used to describe the linear trends and relationships that may exist between the latitudinal and longitudinal position of the SAA and Brazilian

wind speed characteristics for each reanalysis dataset. Sen's slope estimator (Sen 1968) is utilized to evaluate seasonal and annual mean wind speed and positional trends based on spatial and temporal patterns for the SAB. Next, daily surface characteristics (wind speed, SLP, and air temperature) are correlated with the mean location of central pressure for the SAB using the Mann-Kendall test (Mann 1945; Kendall 1975) to determine if any geographic patterns exist across Brazil. It should be noted that to test the correlation of surface wind, temperature, and SLP, geographic coordinates (positive and negative) assigned to the SAA are based on the latitude and longitude spherical systems (e.g., Eastern and Western Hemisphere) maintained by each reanalysis dataset.

To further quantify the geographic correlations, wind speed, SLP, and air temperature anomalies were calculated and compared with the central location of the SAA from 1980 to 2014. Individual surface anomalies were constructed based on the annual mean of each grid point. Positive and negative anomaly boxplots identified how the annual mean latitude and longitude position of the SAA varies between the 5 regions of Brazil. Figure 3.2 shows the geographical regions used to assigned surface anomalies into one of five zones based on Instituto Brasilerio de Geografia e Estatística (IBEG). Based on these results, an average surface wind anomaly for each grid point is calculated on the position of the SAA for five different surface scenarios. The purpose of the surface wind scenarios is to relate the position of the SAA to wind speed across Brazil during the thirty-five study period.

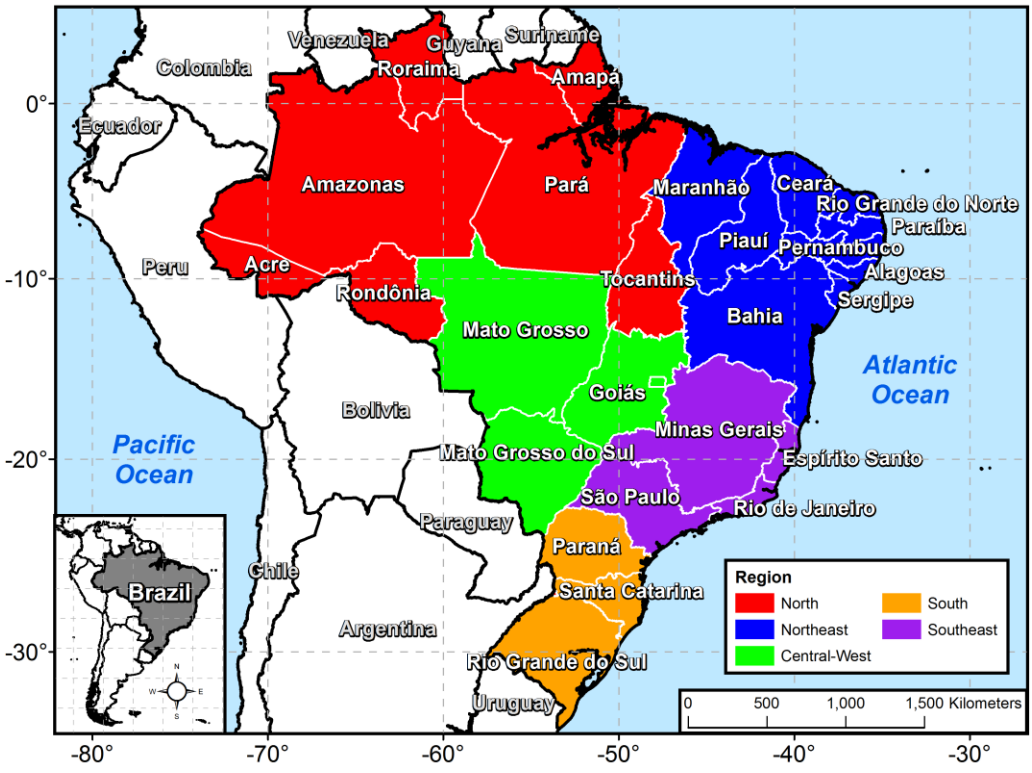

Figure 3.2. The five geographical zones of Brazil defined by the IBEG used to interpret surface wind characteristics associated with the SAA pressure center in the SAB.

3.3 Results

3.3.1 Linear Trends of Surface Wind Speed and SAA for the SAB

Figure 3.3 demonstrates seasonal and annual mean linear wind speed trends in the SAB and adjacent South America during 1980–2014. Positive wind trends found in the study are primarily located in two geographic areas**.** First, increasing surface winds are found poleward of 20° S over the SAB during summer (DJF) and fall (MAM) for Reanalysis 1 and Reanalysis 2 (Figure 3.3a–b). This positive linear wind trend detected is related to SLP and sea surface temperature changes (SST) occurring within the spatial domain of 18° S–25° S and 30° W– 0° from 1982 to 2013 (Vizy and Cook 2016). The study found that SSTs (SLPs) are linearly decreasing (increasing) within the climatological position of the SAA based on atmospheric and oceanic reanalysis products

during the dry seasons. This relationship identified between SLP and SST would result in a stronger pressure gradient to form, which would cause an increase of surface wind speeds to be observed poleward of 20° S in Reanalysis 1 and Reanalysis 2.

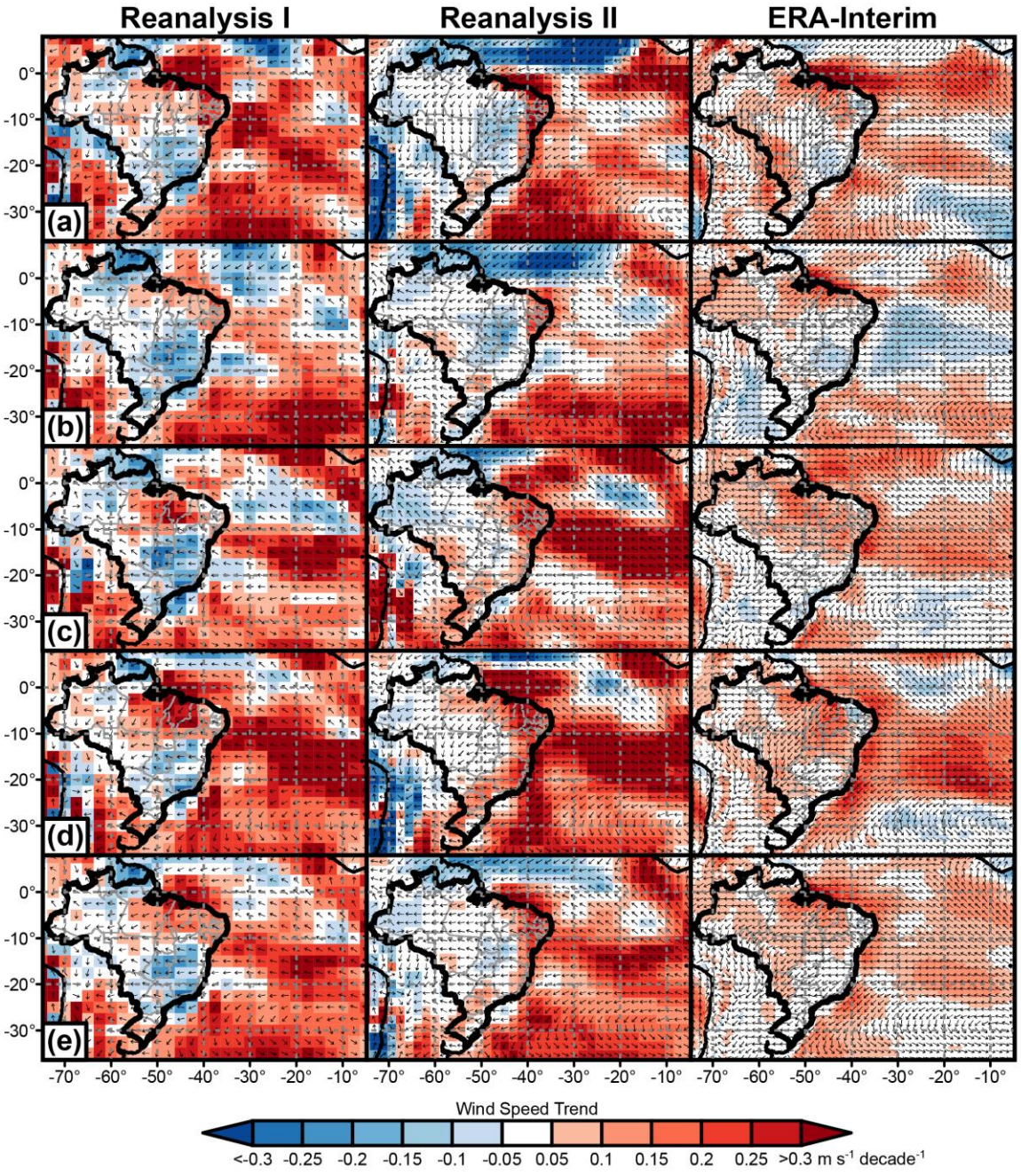

Figure 3.3. (a) Summer (DJF), (b) fall (MAM), (c) winter (JJA), (d) spring (SON), and (e) annual spatial distribution of mean wind speed trends (m s^{-1} $decade^{-1}$) with mean wind direction across the SAB for Reanalysis 1, Reanalysis 2, and ERA-Interim from 1980 to 2014.

During austral winter and spring, positive linear wind trends found are related to oceanic surface currents in the SAB (Figure 3.3 c–d). The strongest positive trends were found along the South Equatorial Current (SEC), where wind speeds have increased more than 0.3 (0.1) m s^{-1} $decade^{-1}$ for Reanalysis 1 and Reanalysis 2 (ERA-Interim). This spatial linear trend occurs because of the northward shift of the ITCZ and SAA, which relocates the orientation of SST gradients between 5º S and 15º S that transports cooler SSTs from the Benguela Current into the equatorial waters (Grodsky and Carton 2003). A temporal analysis also shows that SSTs found along the SEC have cooled based on Advanced Very High Resolution Radiometer (AVHRR) Pathfinder version 5 data from January 1985 to December 2004 (Good et al. 2007). However, Vizy and Cook (2016) found that SSTs have increased between 18° S and 25° S during winter and spring for the period of 1982 to 2013. The contrasting linear SST trends that exist between the cooling equatorial and warming subtropical waters would allow a larger thermal gradient to develop on the northward side of the SAA. With this temperature gradient change, southeastern trade winds along the SEC would increase as described by each reanalysis dataset for austral winter and spring.

While each reanalysis product shows increasing seasonal trends across the SAB, negative wind trends are still documented over the continent of South America. The primary axis of negative trends described in the study is found across southeastern and southern Brazil during summer and fall (Figure 3.3a–b). This decline in wind speed trends may be correlated to changes observed in surface air temperature. Klink (1999) explained that wind speed trends found across the U.S. were related to modifications in pressure and temperature gradient that develop at higher latitudes. Similarly, previous

studies showed that minimum surface air temperatures have increased over southern Brazil (Marengo and Camargo 2008; Sansigolo and Kayano 2010). This change in minimum surface air temperature has also been correlated with a decline in the diurnal temperature range for southern Brazil (Vincent et al. 2005). As a result, it is expected that the weakening of austral summer and fall wind speeds described by each reanalysis dataset is possibly linked to temperature (diurnal temperature range) and pressure gradient changes that have developed over southeastern and southern Brazil during the last century.

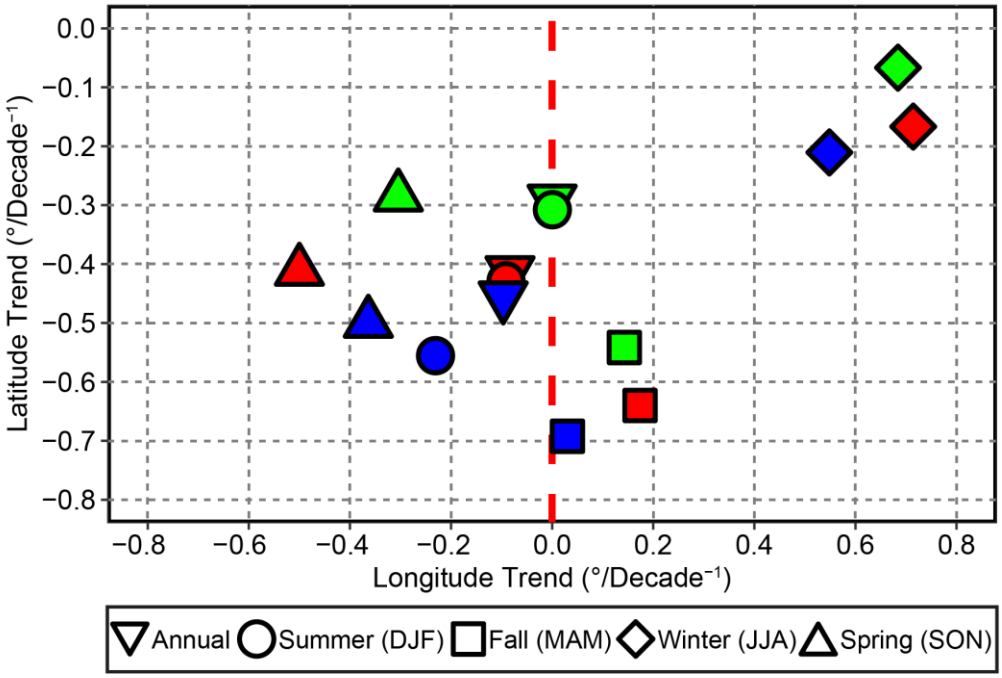

Figure 3.4. Annual and seasonal latitudinal and longitudinal trends of the SAA based on Reanalysis 1 (red), Reanalysis 2 (blue), and ERA-Interim (green) during 1980–2014.

The geographic analysis of surface wind speed trends performed from this study demonstrates that changes in macro-scale atmospheric circulation are a possible reason for decreasing and increasing winds across Brazil and the SAB. Therefore, the evolution of the climatological center of the SAA over the SAB was examined. Figure 3.4

illustrates the seasonal and annual trends based on latitudinal and longitudinal mean center of the SAA between 1980 and 2014. It is evident that two distinct patterns are documented based on latitude and longitude positions in the SAB. Reanalysis datasets show a poleward shift in the latitudinal center of the SAA for each seasonal and annual interval, with the largest (smallest) relocations developing during fall (winter). This southward shift of the SAA is supported by a linear increase of SLP occurring at higher latitudes across the SAB (Vizy and Cook 2016). With this poleward shift in SLP, Degola (2013) showed a continued southward shift of the SAA into the early portion of the 21st century based on six future warming scenarios.

However, a higher degree of seasonal variability exists when analyzing longitudinal trend position of the SAA center for the SAB. Results show that the longitudinal center for winter and spring are trending in opposite directions, while summer and fall portray marginal changes in longitude. Degola (2013) suggests that the interannual longitude variability during winter and spring is influenced by extratropical cyclone activity in the SAB. Similarly, Ito and Ambrizzi (1999) further documented that the SAA tends to be located east (west) of its climatological mean when frontal passages are frequent (less frequent to non-existent) in the SAB between 1982 and 1996. It is plausible that the frequency or intensity of extratropical cyclones in the Southern Hemisphere has changed over time which has allowed the longitudinal trends observed during spring and winter to be identified in this analysis. Reboita et al. (2015) determined the number of Southern Hemisphere extratropical cyclone occurrences has increased (remained constant) during austral winter (spring) between 1980 and 2012. The study also documented a positive temporal trend in cyclonic activity over southern Brazil during winter. This increased

frequency of extratropical cyclones developing over southern Brazil would support the eastward shift of the SAA found with Reanalysis 1, Reanalysis 2, and ERA-Interim.

3.3.2 Brazilian Surface Correlations Based on the SAA

With the continual geographic and temporal shifting of the SAA center in the SAB, it is important to understand how wind speeds change as a result of the movement of the high pressure center (Figures 3.5–3.6). Figure 3.5 shows the geographic seasonal and annual correlations between daily mean wind speed and latitudinal pressure center during the 35-year study period. When the latitudinal center shifts to lower latitudes, wind speeds across northern and northeastern Brazil increase, while southern and southeastern Brazil observe a decline in wind speeds. Central-West Brazil and eastern Amazon basin act as a transitional boundary between northern and southern Brazil which causes a lower degree of correlation to exist for each season.

A spatial pattern is also observed when analyzing daily mean wind speeds with longitudinal position of the SAA for the SAB (Figure 3.6). It shows that when the center of the SAA shifts to the east (west), wind speeds across the majority of Brazil decrease (increase), with the exception of grid points located along equatorial Brazil. This result supports findings of Degola (2013) who concluded that surface *u* winds across eastern Brazil are stronger (weaker) when the SAA is located west (east) of its climatological mean position in the SAB. The only region where the longitudinal position does not correlate with wind speed is in the western Amazon basin during austral summer (Figure 3.6a). This is a result of the equatorial trough (i.e., ITCZ) that develops over the Amazon basin, which controls the daily weather conditions observed during summer (Hastenrath 1985).

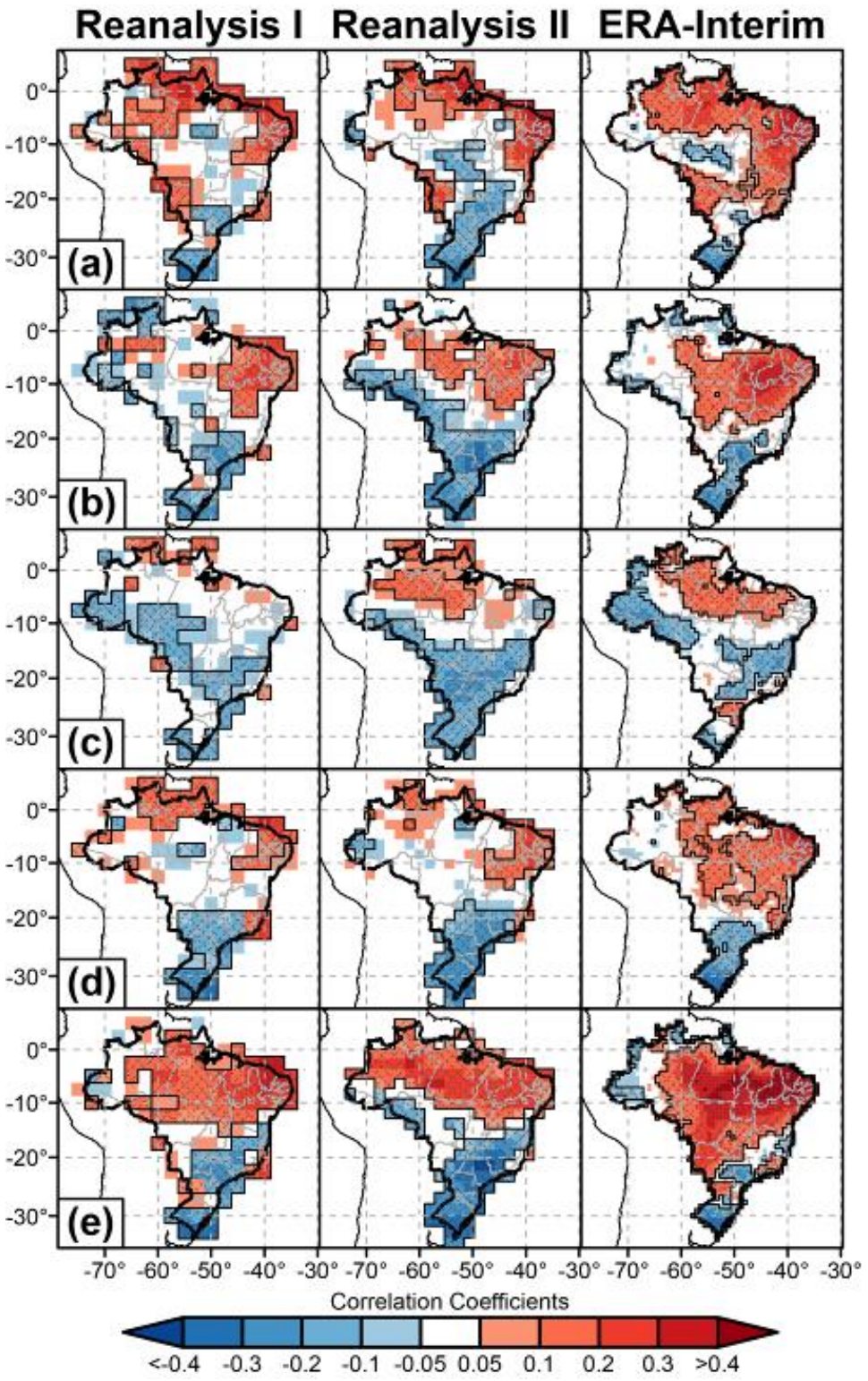

Figure 3.5. Spatial correlations between wind speed and latitudinal center of the SAA for (a) summer (DJF), (b) fall (MAM), (c) winter (JJA), (d) spring (SON), and (e) annual for Reanalysis 1, Reanalysis 2, and ERA-Interim during 1980–2014. Hatched areas indicate the correlation is statistically significant at the 95% confidence-level.

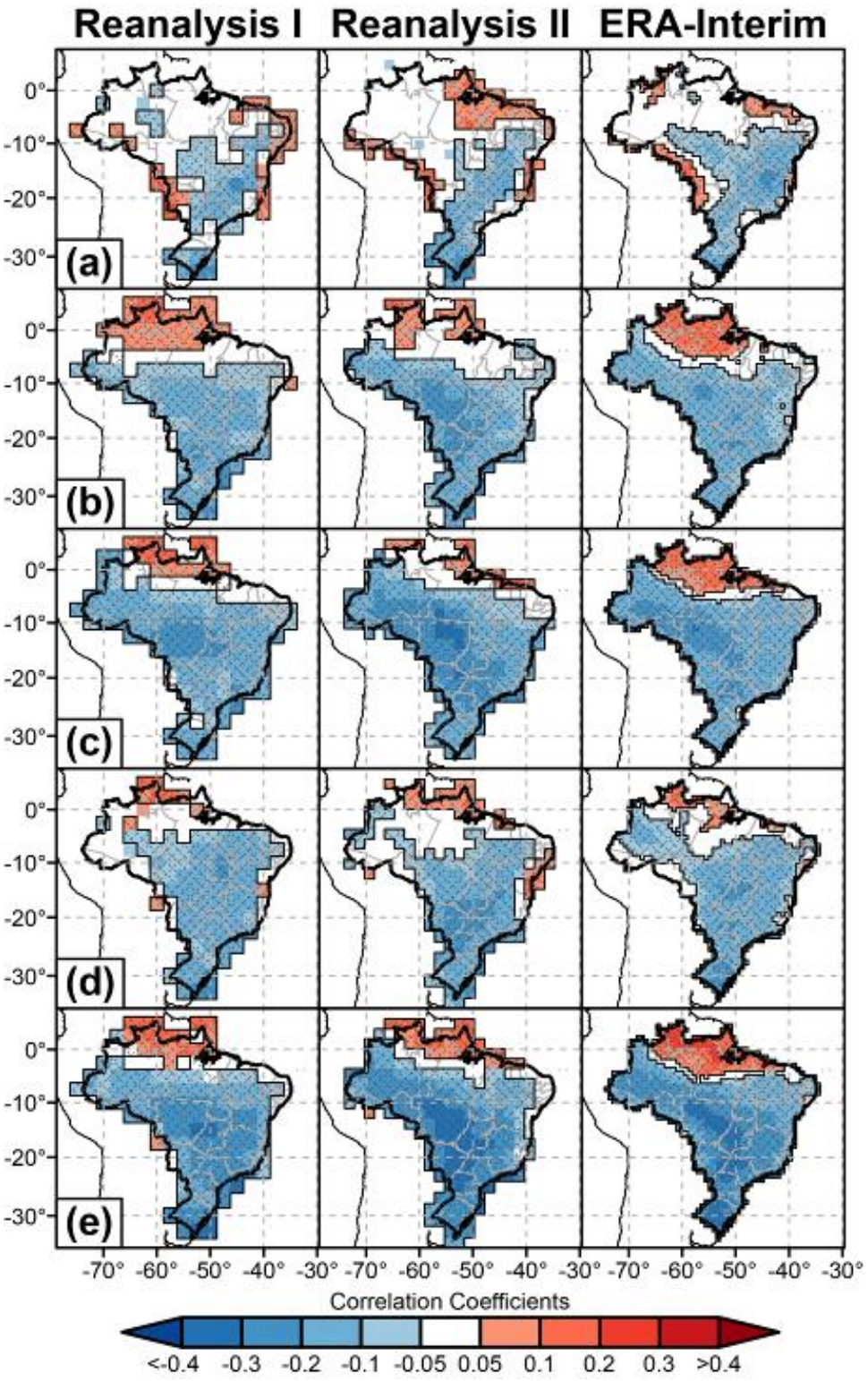

Figure 3.6. As in Figure 3.5 except for longitude.

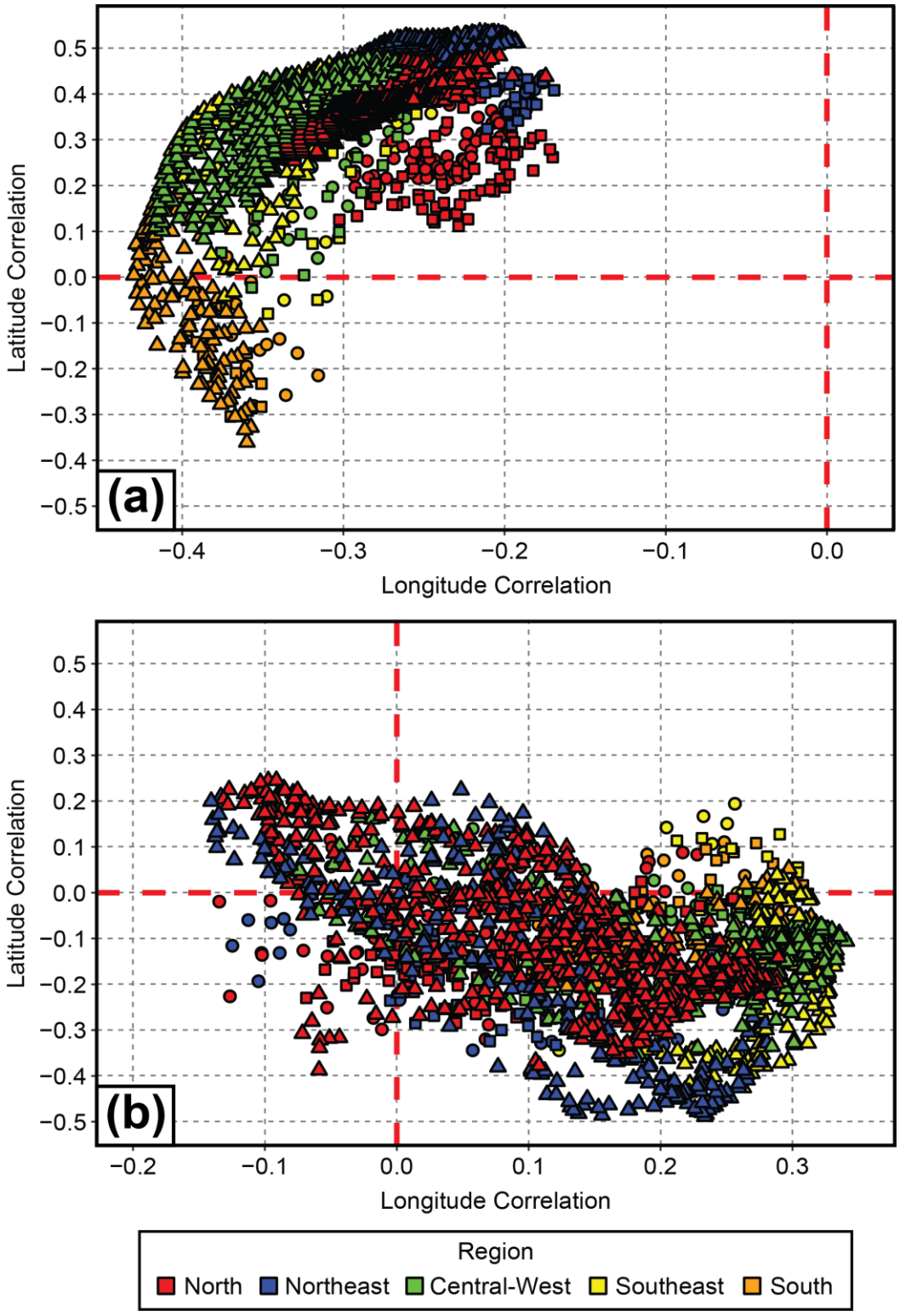

Figure 3.7. Annual regional latitudinal and longitudinal correlations between the daily mean position of the SAA and (a) SLP and (b) temperature for Reanalysis 1 (circle), Reanalysis 2 (square), and ERA-Interim (triangle).

To understand how these changes in wind speeds are linked to other atmospheric conditions as they are in turn associated with the SAA, daily mean SLP and surface air temperature were examined with respect to latitude and longitude at a regional scale. Each grid point located over Brazil was assigned to one of five zones established by IBEG. After each point was assigned to a zone, individual correlations were performed to determine how SLP and temperature are geographically related to the SAA within the SAB. Figure 3.7 shows the annual correlations for SLP and temperature based on central latitude and longitude position of the SAA across Brazil during 1980–2014. As the pressure center moves northward and westward, SLP increases (decreases) for northern and northeastern (southern) Brazil (Figure 3.7a) across each dataset. Consequently, surface temperatures across Brazil decrease (increase) when the SAA moves farther west (east) and north (south) [Figure 3.7b]. This temperature correlation is supported by the presence of moisture and clouds provided by the SAA in the SAB. Moscati and Gan (2007) found that when the SAA is located south and west of its climatological position allowed southeastern trade winds to strengthen and transports moisture into northeastern Brazil, which enabled cloud formation and precipitation to develop and a decrease in temperature to occur. As for southern and southeastern Brazil, temperature changes develop when oceanic moisture transported by the northeastern trade winds associated with the SAA and heat from the interior of Brazil converge to form convective thunderstorms (Reboita et al. 2010). Degola (2013) also found that air temperature anomalies for southern Brazil increase (decrease) when the SAA is shifted west (east) of its climatological mean. However, this analysis showed temperature increased (decreased) when the longitudinal position is shifted away (toward the continent of South

America for southern and southeastern Brazil. Therefore, it is important to further evaluate the role of latitude and longitude on surface winds, SLP, and temperature across the five different regions of Brazil.

3.3.3 SAA Characteristics Based on Surface Anomalies

Figure 3.8 displays the regional mean latitude and longitude positions of wind speed, SLP, and temperature anomalies for each reanalysis. Above (below) normal wind speeds across northern, northeastern, and central-west (southeastern and southern) Brazil occur when the SAA center is located at lower (higher) latitudes (Figure 3.8a). As expected, changes in wind speeds result because of alterations in SLP and temperature observed across each region. The northward shifting of the SAA northward causes SLP to rise across northern, northeastern, central-west, and southeastern Brazil (Figure 3.8b) and temperature to fall across all regions (Figure 3.8c). These surface conditions develop when the *u* surface winds flow across the SAB, which transports oceanic air into coastal Brazil. The resulting thermal and pressure differences established between the land and ocean cause the gradients to increase, which in response allows wind speeds to increase across the mountains and plateaus of northern and northeastern Brazil. The opposite pattern is described for southern Brazil, where SLP decreases while the SAA center is located at lower latitudes.

Longitudinally, wind speeds increase (decrease) when the central location of the SAA is located closer to (farther from) South America, which enables surface temperatures to decrease (increase) across all regions of Brazil (Figure 3.8). By contrast, Degola (2013) found that surface temperatures increase (decrease) when the SAA is west (east) of its climatological mean position for southeastern and southern Brazil based on

average synoptic conditions for September 2007 (1993). This conflicting result with Degola (2013) is related to the usage of monthly instead of daily averages which cannot distinguish migratory anticyclones in the higher latitudes of the SAB. The zonal tracking of these transient high pressure features typically bring below normal temperatures and increased barometric pressure values to southern Brazil (Satyamurty et al. 1998) which is supported by the ridge-to-trough (i.e., southwest-to-northeast in the Southern Hemisphere) propagation of Rossby waves that originate from the tropical western Pacific (Marengo et al. 2002). This relationship between air temperature and SLP causes the gradients to increase which results in the increase of wind speeds across the region. Once the migratory anticyclone shifts away from the continent, temperatures increase while SLP and wind speeds fall for the northern latitudes of Brazil. This life cycle follows the results of Sinclair (1996), which documented the initial formation of the passing anticyclone over the continent of South America, intensification off the coast of South America, and eventual dissipation on the eastern side of the SAB.

Lower (higher) spatial variability is observed in SLP anomalies of northern and northeastern (central-west, southeastern, and southern) Brazil (Figure 3.8b). Similarly, the variability of temperature is greatly dependent on the position of the SAA for southeastern and southern Brazil. The deviation between SLP and temperature anomalies for northern and southern Brazil is influenced by separate two meteorological environments. Atmospheric pressure within equatorial Brazil and Amazon basin changes minimally between summer and spring because of the influence of the ITCZ (Schwerdtfeger 1976). Any changes that develop in SLP occur when the ITCZ is seasonally displaced northward, which allows the SAA to migrate equatorward and

therefore play a more prominent role of influencing SLP characteristics for the region. On the other hand, the zonal transient anticyclones across the SAB contribute to the annual temperature patterns found, especially for southeastern and southern Brazil.

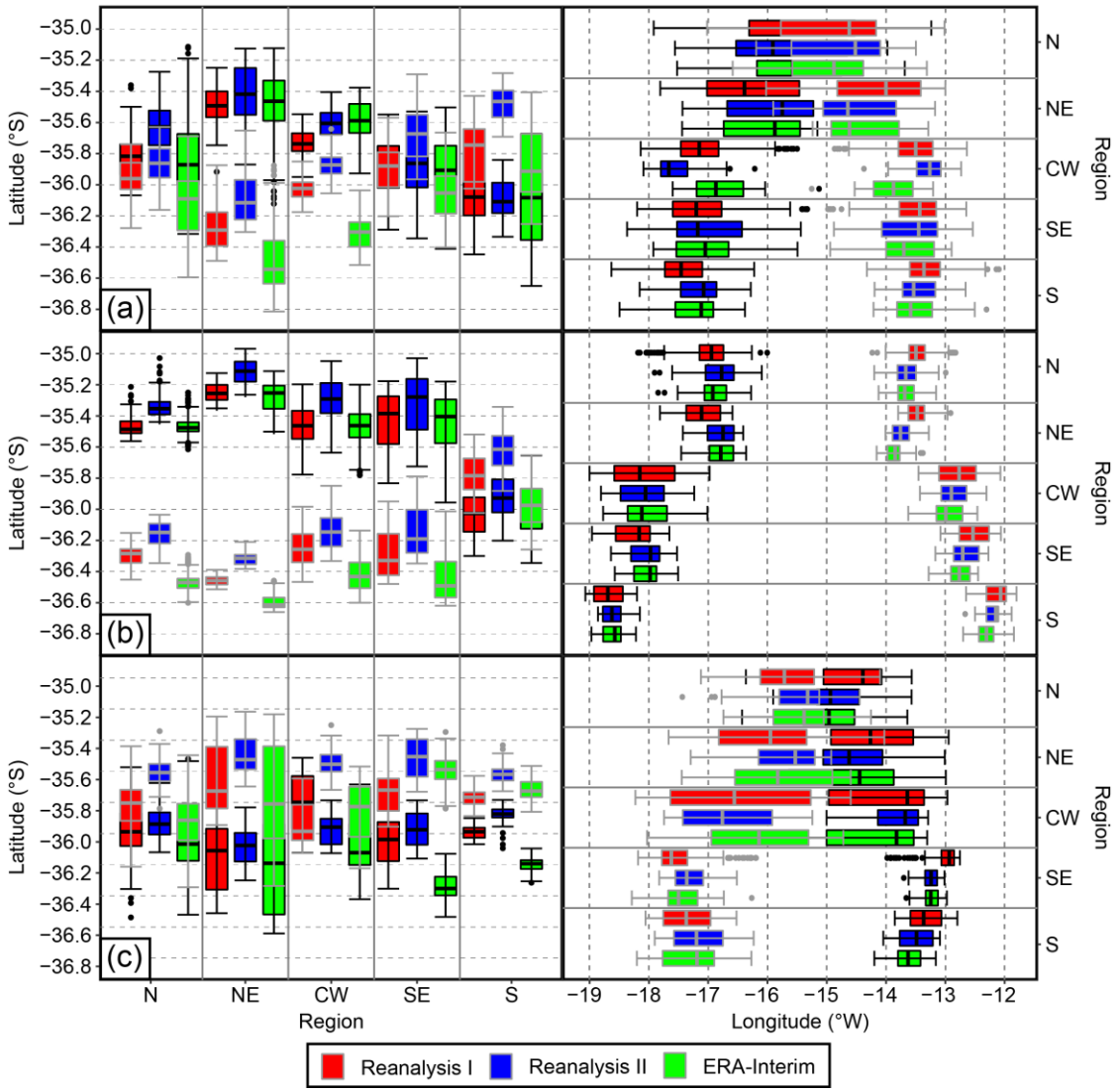

Figure 3.8. Regional latitudinal (left) and longitudinal (right) mean position boxplots of the SAA based on (a) wind speed, (b) SLP, and (c) air temperature negative (gray) and positive (black) anomalies for Reanalysis 1 (red), Reanalysis 2 (blue), and ERA-Interim (green) during 1980–2014.

This study has documented that the position of the SAA in the SAB affects surface wind characteristics observed across Brazil. Five surface map scenarios illustrate how wind speeds vary across Brazil when the location of the SAA center is situated

between a specific range of latitudes and longitudes within the SAB (Figure 3.9). First, when the latitudinal center is shifted north of its climatological mean, the average wind is above (below) normal for portions of northeastern (coastal southern) Brazil (Figure 3.9a). SLP isobars are oriented parallel to the coast of Brazil which allows a larger pressure gradient to form which enables stronger than normal winds to be observed across northeastern Brazil. If the SAA center is found off the coast of Uruguay, where on-shore flow is present, a change in pressure gradient is shown which causes wind speeds across the interior and southern Brazil to be faster than normal (Figure 3.9b). This wind anomaly pattern develops as a result of transient anticyclones that likely form on the lee side of the Andes Mountains and track across the southern portion of the SAB. The formation of the migrating system begins over the continent from low-level cooling and as the anticyclone travels over the eastern coast of South America, it undergoes rapid intensification because of intense baroclinic activity in the region (Sinclair 1996). Previous research has documented this anticyclone genesis through the "budding" mechanism, whereby the parent Pacific Ocean anticyclone cell extends a ridge downstream of the Andes Mountains which intensifies and closes off to form a new eastward high pressure cell ("cradle") over South American (Taljaard 1967; 1972; Jones and Simmonds 1994). The downstream formation of this anticyclone advects colder air northward along the Andes Mountains resulting in below normal temperatures (i.e., cold surges) to occur in southern and southeastern Brazil (Garreaud 2000; Lupo et al. 2001; Pezza and Ambrizzi 2005; Sprenger et al. 2013). While this synoptic setup is occurring, the thermal low located over central South America is displaced equatorward which

allows the SLP gradient to increase and positive wind anomalies to be observed across the interior of Brazil as described by Figure 3.9b.

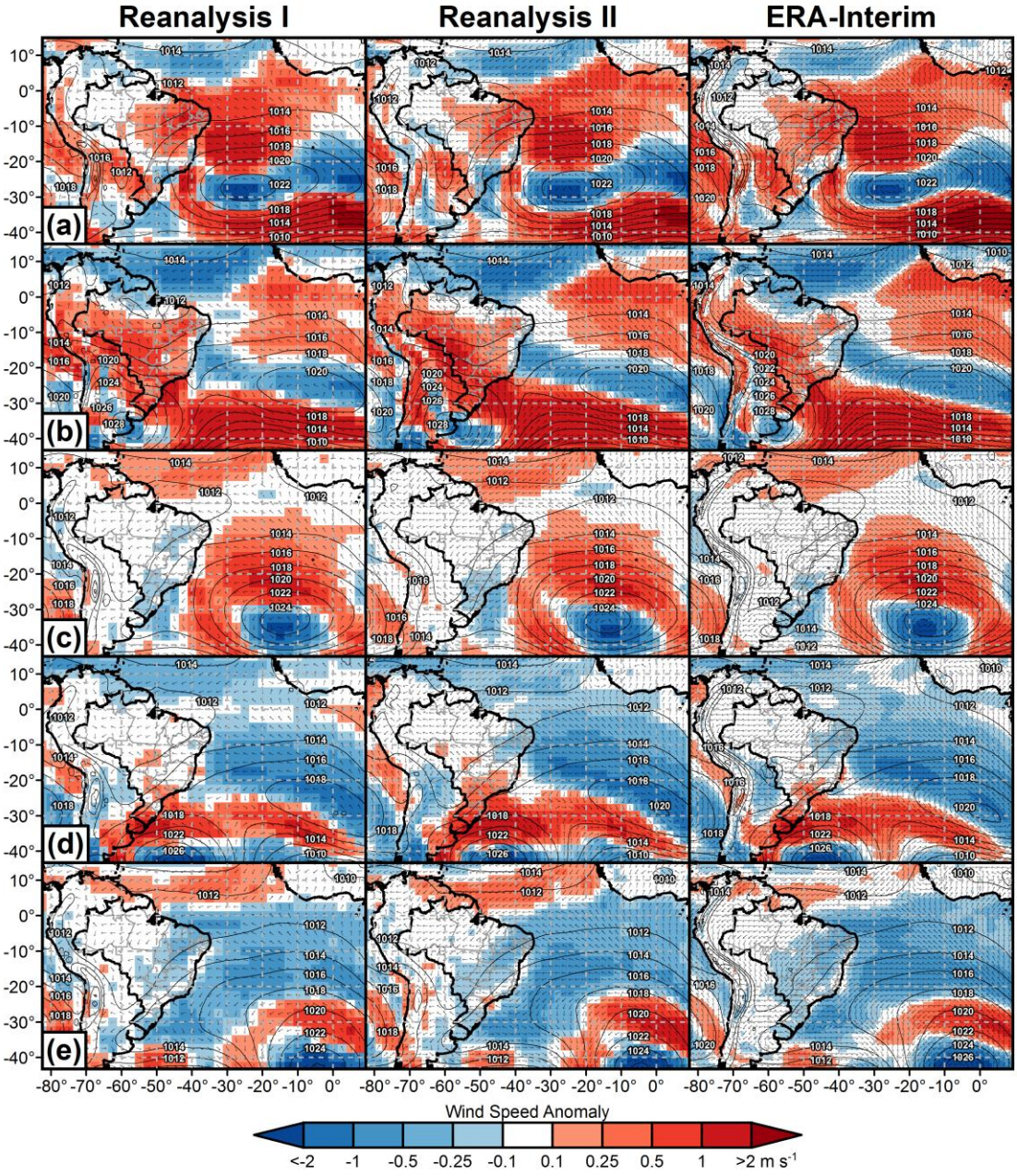

Figure 3.9. Mean wind speed anomalies (m s^{-1}) and SLP (hPa) based on the location of the SAA when located between (a) 20° S–30° S and 30° W–20° W, (b) 30° S–40° S and 60° W–50° W, (c) 30° S–40° S and 20° W–10° W, (d) 40° S–50° S and 50° W–40° W, and (e) 40° S–50° S and 10° W–0° for Reanalysis 1, Reanalysis 2, and ERA-Interim.

As the SAA shifts to its normal climatological position (35° S and 15° W) determined in the analysis, surface winds across Brazil follow their typical average with exception to southern Brazil, where a slight decline in wind speeds is observed (Figure 3.9c). It should be noted the mean position used for this study is located south and west of previous studies (Hastenrath 1985; Mächel et al. 1998; Degola 2013), which perform monthly or seasonal instead of daily analysis to identify the central location of the SAA in the SAB. It is plausible that using monthly or seasonal latitude and longitude positions could change the average wind speed anomalies found for Figure 3.9c which warrants additional analysis. Lastly, when the SAA is shifted to the south (Figure 3.9d) and east (Figure 3.9e), it reveals weaker than normal mean wind speeds across eastern Brazil. These negative wind anomalies develop because of the poleward shift of the ITCZ, which decreases SLP gradients across the country. This decrease in wind speed is also noted across the SEC, which influences surface winds observed across northern and northeastern Brazil. As a result, when the thermal and pressure gradients decline along this current, it weakens the coastal land-sea breeze, which causes negative wind anomalies to be reported across eastern Brazil.

3.4 Conclusions

This study examined the surface wind characteristics of Brazil based on the position of the SAA in the SAB using three reanalysis datasets. Temporal linear increases in wind speed across Brazil are related to the seasonal relationship between the ITCZ and SAA, especially for northern and northeastern Brazil. However, temporally decreasing linear trends in wind speed across southeastern Brazil may be related to changes in surface temperature observed during the last century. As a result of this

relationship with macro-scale atmospheric circulations, this study identified the daily position of the SAA center to determine if any seasonal or annual temporal trends exist during 1980–2014. It was documented that climatological mean position of the SAA has shifted farther east (west) during winter (spring). Previous work has shown that passing mid-latitude cyclones affect the location of the SAA in the SAB (Ito and Ambrizzi 1999; Degola 2013). Results indicate the frequency or location of extratropical cyclones passing through the SAB could be causing the opposing longitudinal trends found in austral winter and spring (Reboita et al. 2015).

Mann-Kendall test (Mann 1945; Kendall 1975) was used to show how the location of the SAA correlates with wind speed, SLP, and temperature across Brazil. When the SAA center is located at lower latitudes, SLP increases northward while temperature decreases westward, which in response, allows wind speeds to increase across northern and northeastern Brazil during summer. This surface scenario develops when the ITCZ is displaced northward, allowing higher SLPs and cooler surface conditions to be transported in from the SAB. As the ITCZ eventually shifts toward the equator, longitudinal correlations with wind speed, SLP, and temperature indicate how the position of central pressure affects conditions across Brazil differently. These results demonstrated that SLP correlations across Brazil are associated with changes in latitude, while temperature is connected to longitudinal shifts in the high pressure system.

To further quantify these results, this study analyzed the relationship of positive and negative wind, SLP, and temperature anomalies based on the location of the SAA for the SAB. For the northern half of Brazil, wind speed anomalies tend to be related to changes in SLP, while southern Brazil is more strongly connected to alterations in

temperature when examining the latitudinal and longitudinal center of the SAA for the SAB. The role of migrating anticyclones has been identified as a possible reason of influencing surface wind characteristics across southern and southeastern Brazil. These findings are further described when analyzing the average wind speed anomalies based on the location of the SAA center in different geographic locations across Brazil. Stronger (weaker) than normal wind speeds are observed when the location of the SAA center is located north and west (south and east) of its mean position in the SAB.

The location and position of the SAA in the SAB plays an important role in influencing wind characteristics across Brazil. Any latitude or longitude change in the SAA can affect the daily weather conditions observed across Brazil. The consistent wind flow across portions of northeastern Brazil has been identified by research as a potential area to develop and generate renewable wind energy (CRESESB 2001). As a result, any climatological shifting of the SAA could affect wind energy production across the region. Future wind forecasts expect that wind speeds will continue to increase by the end of the 21st century for northeastern Brazil (Lucena et al. 2010; Pereira et al. 2013). This wind forecast is based on the scenario that the longitudinal position of the SAA will shift toward the west over the next century (Degola 2013). Therefore, it is essential to continue to evaluate and understand how atmospheric features evolve across the SAB, so future climatological and socioeconomic consequences of wind on Brazil can be identified.

3.5 References

Abhishek A, Lee J-Y, Keener TC, Yang YJ. 2010. Long-term wind speed variations for three Midwestern U.S. cities. *Journal of the Air and Waste Management Association* **60**: 1057–1064. doi: 10.3155/1047-3289.60.9.1057.

ANEEL. 2017. Banco de Informacão de Geracão. Available at: National Electricity Regulatory Agency. http://www2.aneel.gov.br/aplicacoes/capacidadebrasil/capacidadebrasil.cfm/. [Accessed May 2017].

Blender R, Schubert M. 2000. Cyclone tracking in different spatial and temporal resolutions. *Monthly Weather Review* **128**: 377–384. doi: 10.1175/1520-0493(2000)128<0377%3ACTIDSA>2.0.CO%3B2.

Castro JS, Camargo R, Marone E, Sepúlveda. 2015. Using the mean pressure gradient and NCEP/NCAR reanalysis to estimate the strength of the South Atlantic Anticyclone. *Dynamics of Atmospheres and Oceans* **71**: 83–90. doi: http://doi.org/10.1016/j.dynatmoce.2015.06.003.

Chen L, Li D, Pryor SC. 2013. Wind speed trends over China: Quantifying the magnitude and assessing causality. *International Journal of Climatology* **33**: 2579–2590. doi: 10.1002/joc.3613.

CRESESB. 2001. Atlas do Potencial Eólico Brasileiro. Rio de Janeiro. Available at: Centro de Referência para Solar e Eólica Sérgio Brito. http://www.cresesb.cepel.br/publicacoes/download/atlas_eolico/Atlas%20do%20Potencial%20Eolico%20Brasileiro.pdf/. [Accessed May 2017].

Davis RB. Hayden D, Gay W, Phillips, Jones G. 1997. The North Atlantic subtropical anticyclone. *Journal of Climate* **10**: 728–744. doi: http://dx.doi.org/10.1175/1520-0442(1997)010<0728:TNASA>2.0.CO;2.

Dee DP, Uppala SM, Simmons AJ, Berrisford P, Poli P, Kobayashi S, Andrae U, Balmaseda MA, Balsamo G, Bauer P, Bechtold P, Beljaars ACM, van de Berg L, Bidlot J, Bormann N, Delsol C, Dragani R, Fuentes M, Geer AJ, Haimberger L, Healy SB, Hersbach H, Hólm EV, Isaksen L, Kållberg P, Köhler M, Matricardi M, McNally AP, Monge-Sanz BM, Morcrette J-J, Park B-K, Peubey C, de Rosnay P, Tavolato C, Thépaut J-N, Vitart F. 2011. The ERA-Interim reanalysis: Configuration and performance of the data assimilation system. *Quarterly Journal of the Royal Meteorological Society* **137**: 553–597. doi: 10.1002/qj.828.

Degola TSD. 2013. Impactos e variabilidade do Anticiclone Subtropical do Atlântico Sul sobre o Brasil no clima presente e em cenários futuros. Institute of Astronomy, Geophysics and Atmospheric Sciences, University of São Paulo, São Paulo, pp. 91.

Fu G, Yu J, Zhang Y, Hu S, Ouyang R, Wenbin L. 2011. Temporal variation of wind speed in China for 1961–2007. *Theoretical and Applied Climatology* **104**: 313–324. doi: 10.1007/s00704-010-0348-x.

Garreaud RD. 2000. Cold air incursions over subtropical South America: Mean structure and dynamics. *Monthly Weather Review* **128**: 2544–2559. doi: http://dx.doi.org/10.1175/1520-0493(2000)128<2544:CAIOSS>2.0.CO;2.

Good SA, Corlett GK, Remedios JJ, Noyes EJ, Llewellyn-Jones DT. 2007. The global trend in sea surface temperature from 20 years of Advanced Very High Resolution Radiometer data. *Journal of Climate* **20**: 1255–1264. doi: http://dx.doi.org/10.1175/JCLI4049.1.

Grodsky SA, Carton JA. 2003. The intertropical convergence zone in the South Atlantic and the Equatorial cold tongue. *Journal of Climate* **16**: 723–733. doi: http://dx.doi.org/10.1175/1520-0442(2003)016<0723:TICZIT>2.0.CO;2.

Harman JR. 1987. Mean monthly North American anticyclone frequencies, 1950–79. *Monthly Weather Review* **115**: 2840–2848. doi: http://dx.doi.org/10.1175/1520-0493(1987)115<2840:MMNAAF>2.0.CO;2.

Hastenrath S. 1985. Regional circulation systems. *Climate and Circulation of the Tropics*. Reidel, D (ed.). Dordrecht. 107–209.

Hewston R, Dorling S. 2011. An analysis of observed daily maximum wind gusts in the UK. *Journal of Wind Engineering and Industrial Aerodynamics* **99**: 845–856. doi: http://dx.doi.org/10.1016/j.jweia.2011.06.004.

Ito ERK, Ambrizzi T. 1999. Um estudo Climatológico do Anticiclone Subtropical do Atlântico Sul e sua influência em Sistemas Frontais. Institute of Astronomy, Geophysics and Atmospheric Sciences, University of São Paulo, São Paulo, pp 126.

----------, ----------. 2000. Climatologia da posição da alta subtropical do atlântico sul para os meses de inverno. Congresso Latino Americao e Iberico de Meteorologia, Metorologia Brasileria além do ano 2000. Rio de Janeiro. *Sociedade Brasileira de Meteorologia*. 860–865.

Jiang Y, Luo Y, Zhao Z, Tao S. 2010. Changes in wind speed over China during 1956–2004. *Theoretical and Applied Climatology* **99**: 421–430. doi: 10.1007/s00704-009-0152-7.

Jones DA, Simmonds I. 1994. A climatology of Southern Hemisphere anticyclones. *Climate Dynamics* **10**: 333–348. doi: 10.1007/BF00228031.

Kalnay E, Kanamitsu M, Kistler R, Collins W, Deaven D, Gandin L, Iredell M, Saha S, White G, Woollen J, Zhu Y, Leetmaa A, Reynolds R, Chelliah M, Ebisuzaki W, Higgins W, Janowiak J, Mo KC, Ropelewski C, Wang J, Jenne R, Joseph D. 1996. The NCEP/NCAR 40-year reanalysis project. *Bulletin of American Meteorological Society* **77**: 437–471. doi: http://dx.doi.org/10.1175/1520-0477(1996)077<0437:TNYRP>2.0.CO;2.

Kanamitsu M, Ebisuzaki W, Woollen J, Yang S-K, Hnilo JJ, Fiorino M, Potter GL. 2002. NCEP–DOE AMIP-II Reanalysis (R-2). *Bulletin of American Meteorological Society* **83**: 1631–1643. doi: http://dx.doi.org/10.1175/BAMS-83-11-1631.

Kendall MG. 1975. Rank correlation methods. 202 pp. Griffin. London, U.K.

Klink K. 1999. Trends in mean monthly maximum and minimum surface wind speeds in the coterminous United States, 1961 to 1990. *Climate Research* **13**: 193–205. doi: 10.3354/cr013193.

Li X, Zhong S, Bian X, Heilman WE. 2010. Climate and climate variability of the wind power resources in the Great Lakes region of the United States. *Journal of Geophysical Research* **115**: D18107. doi: 10.1029/2009JD013415.

Lin C, Yang K, Qin J, Fu R. 2013. Observed coherent trends of surface and upper-air wind speed over China since 1960. *Journal of Climate* **26**: 2891–2903. doi: http://dx.doi.org/10.1175/JCLI-D-12-00093.1.

Lucena AFP, Szklo AS, Schaeffer R, Dutra RM. 2010. The vulnerability of wind power to climate change in Brazil. *Renewable Energy* **35**: 904–912. doi: 10.1016/j.renene.2009.10.022.

Lupo AR, Nocera JJ, Bosart LF, Hoffman EG, Knight DJ. 2001. South American cold surges: Types, composites, and case studies. *Monthly Weather Review* **129**: 1021 –1041. doi: http://dx.doi.org/10.1175/1520-0493(2001)129<1021:SACSTC >2.0.CO;2.

Mächel H, Kapala A, Flohn, H. 1998. Behaviour of the centres of action above the Atlantic since 1881. Part I: Characteristics of seasonal and interannual variability. *International Journal of Climatology* **18**: 1–22. doi: 10.1002/(SICI)1097-0088(199801)18:1<1::AID-JOC225>3.0.CO;2-A.

Mann HB. 1945. Nonparametric tests against trend. *Econometrica* **13**: 245–259.

Marengo JA, Ambrizzi T, Kiladis G, Liebmann B. 2002. Upper-air wave trains over the Pacific Ocean and wintertime cold surge in tropical-subtropical South America leading to freezes in southern and southeastern Brazil. *Theoretical and Applied Climatology* **73**: 223–242. doi: 10.1007/s00704-001-0669-x.

----------, Camargo CC. 2008. Surface air temperature trends in Southern Brazil for 1960–2002. *International Journal of Climatology* **28**: 893–904. doi: 10.1002/joc.1584.

Moscati MCL, Gan MA. 2007. Rainfall variability in the rainy season of semiarid zone of northeast Brazil (NEB) and its relation to wind regime. *International Journal of Climatology* **27**: 493–512. doi: 10.1002/joc.1408.

Murray RJ, Simmonds I. 1991. A numerical scheme for tracking cyclone centres from digital data. Part I: Development and operation of the scheme. *Australian Meteorological Magazine* **39**: 155–166.

Pereira EB, Martins FR, Pes MP, Segundo EID, Lyra AD. 2013. The impacts of global climate changes on the wind power density in Brazil. *Renewable Energy* **49**: 107–110. doi: 10.1016/j.renene.2012.01.053.

Pezza AB, Ambrizzi T. 2005. Dynamical conditions and synoptic tracks associated with different types of cold surge over tropical South America. *International Journal of Climatology* **25**: 215–241. doi: 10.1002/joc.1080.

Pryor SC, Ledolter J. 2010. Addendum to "Wind speeds trends over the contiguous United States". *Journal of Geophysical Research* **115**: D10103. doi: 10.1029/2009JD013281.

Ratisbona LR. 1976. The climate of Brazil. *World Survey of Climatology, Volume 12, Climates of Central and South America*. Schwerdtfeger, W (ed.). Amsterdam. 405–451.

Reboita MS, Gan MA, Rocha RP, Ambrizzi T. 2010. Precipitation regimes in South America: A bibliography review. *Revista Brasileira de Meteorologia* **25**: 185–204. doi: http://dx.doi.org/10.1590/S0102-77862010000200004.

----------, da Rocha RP, Ambrizzi T, Gouveia CD. 2015. Trend and teleconnection patterns in the climatology of extratropical cyclones over the Southern Hemisphere. *Climate Dynamics* **45**: 1929–1944. doi: 10.1007/s00382-014-2447-3.

Sahsamanoglou HS. 1990. A contribution to the study of action centres in the North Atlantic. *International Journal of Climatology* **10**: 247–261. doi: 10.1002/joc.3370100303.

Sansigolo CA, Kayano MT. 2010. Trends of seasonal maximum and minimum temperatures and precipitation in Southern Brazil for 1913–2006 period. *Theoretical and Applied Climatology* **101**: 209–216. doi: 10.1002/joc.3370100303.

Santos ATS, Silva CMS. 2013. Seasonality, interannual variability, and linear tendency of wind speeds in the northeast Brazil from 1986 to 2011. *The Scientific World Journal*. doi: http://dx.doi.org/10.1155/2013/490857.

Satyamurty P, Nombre CA, Silva Dias PL. 1998. South America, *Meteorology of the Southern Hemisphere*. Koroly, DJ, Vincent DG (eds.). Boston, Massachusetts, 119–139.

Schwerdtfeger W. 1976. Introduction. *World Survey of Climatology, Volume 12, Climates of Central and South America*. Schwerdtfeger, W (ed.). Amsterdam. 1–12.

Sen PK, 1968. Estimates of the regression coefficient based on Kendall's tau. *Journal of the American Statistical Association* **63**: 1379–1389.

Sinclair M. 1996. A climatology of anticyclones and blocking for the Southern Hemisphere. *Monthly Weather Review* **124**: 245–263. doi: http://dx.doi.org /10.1175/1520-0493(1996)124<0245:ACOAAB>2.0.CO;2.

----------. 1997. Objective identification of cyclones and their circulation intensity, and climatology. *Weather and Forecasting* **12**: 595–612. doi: http://dx.doi.org/ 10.1175/1520-0434(1997)012<0595:OIOCAT>2.0.CO;2.

Sprenger M, Martius O, Arnold J. 2013. Cold surge episodes over southeastern Brazil – A potential vorticity perspective. *International Journal of Climatology* **33**: 2758–2767. doi: 10.1002/joc.3618.

St. George S, Wolfe SA. 2009. El Niño stills winter winds across the southern Canadian Prairies. *Geophysical Research Letters* **36**: L23806. doi:10.1029/2009GL041282.

Sun X, Cook KH, Vizy EK. 2017. The south Atlantic subtropical high: Climatology and interannual variability. *Journal of Climate* **30**: 3279–3296. doi: http://dx.doi.org/ 10.1175/JCLI-D-16-0705.1.

Taljaard JJ. 1967. Development, distribution and movement of cyclones and anticyclones in the Southern Hemisphere during the IGY. *Journal of Applied Meteorology and Climatology* **6**: 973–987. doi: http://dx.doi.org/10.1175/1520-0450(1967) 006<0973:DDAMOC>2.0.CO;2 .

----------. 1972. Synoptic Meteorology of the Southern Hemisphere. *Meteorology of the Southern Hemisphere*. Newton, CW (ed.). Boston, Massachusetts. 139–211.

Teissereng de Bort L. 1883. Etude sur l'hiver de 1879–80 et re-cherches sur la position des centres d'action de l'atmosphere dans les hivers anormaux. *Bureau Central Meteorologique de France. Annales, 1881*, **4**: 17–62.

Tuller SE. 2004. Measured wind speed trends on the west coast of Canada. *International Journal of Climatology* **24**: 1359–1374. doi: 10.1002/joc.1073.

Vincent LA, Petterson TC, Barros VR, Marino MB, Rusticucci M, Carrasco G, Ramirez E, Alves LM, Ambrizzi T, Berlato MA, Grimm AM, Marengo JA, Molion LC, Moncunill DF, Rebello E, Anunciação YMT, Quintana-Gomes J, Santos JL, Baez J, Coronel G, Garcia J, Trebejo I, Bidegain M, Haylock MR, Karoly D. 2005. Observed trends in indices of daily temperature extremes in South America 1960–2000. *Journal of Climate* **18**: 5011–5023. doi: http://dx.doi.org/10.1175/JCLI3589.1.

Vizy EK, Cook KH. 2016. Understanding long-term (1982–2013) multi-decadal changes in the equatorial and subtropical South Atlantic climate. *Climate Dynamics* **46**: 2087–2113. doi: 10.1007/s00382-015-2691-1.

Wernli H, Schwierz C. 2006. Surface cyclones in the ERA-40 Dataset (1958–2001). Part I: Novel identification method and global climatology. *Journal of Atmospheric Sciences* **63**: 2486–2507. doi: http://dx.doi.org/10.1175/JAS3766.1.

Whittaker LM, Horn LH. 1984. Northern Hemisphere extratropical cyclone activity for four mid-season months. *International Journal of Climatology* **4**: 297–310. doi: 10.1002/joc.3370040307.

Yang X, Li ZX, Feng Q, He YQ, An WL, Zhang W, Cao WH, Yu TF, Wang YM, Theakstone W. 2012. The decreasing wind speed in southwestern China during 1969–2009 and possible causes. *Quaternary International* **263**: 71–84. doi: http://dx.doi.org/10.1016/j.quaint.2012.02.020.

You Q, Kang S, Flügel W-A, PepinN, Yan Y, Huang J. 2010. Decreasing wind speed and weakening latitudinal surface pressure gradients in the Tibetan Plateau. *Climate Research* **42**: 57–64. doi: https://doi.org/10.3354/cr00864.

----------, Fraedrich K, Min J, Kang S ,Zhu X, Pepine N, Zhanga L. 2014. Observed surface wind speed in the Tibetan Plateau since 1980 and its physical causes. *International Journal of Climatology* **34**: 1873–1882. doi: 10.1002/joc.3807.

Zarrin A, Ghaemi H, Azadi M, Farajzadeh M. 2010. The spatial pattern of summertime subtropical anticyclones over Asia and Africa: A climatological review. *International Journal of Climatology* **30**: 159–173. doi: 10.1002/joc.1879.

Zishka KM, Smith PJ. 1980. The climatology of cyclones and anticyclones over North America and surrounding ocean environs for January and July, 1950–77. *Monthly Weather Review* **108**: 387–401. doi: http://dx.doi.org/10.1175/1520-0493(1980)108<0387:TCOCAA>2.0.CO;2.

CHAPTER 4
SPATIOTEMPORAL ANALYSIS OF UPPER-LEVEL WIND SPEED TRENDS OF BRAZIL DURING 1980–2014

4.1 Introduction

Surface wind climatologies have shown a general decline in wind speeds across the Earth during the 20th century (McVicar et al. 2012). Much of the research has focused on two surface variables to explain the decreasing geographic and temporal wind speed patterns found across regional and global studies. The first explanation is that changes in wind speed are related to a poleward shift in the latitude of steepest temperature and pressure gradients, leaving more of Earth's surface under the influence of weak pressure gradients (Klink 1999; Pirazzoli and Tomasin 2003; Xu et al. 2006; Jiang et al. 2010; Guo et al. 2011; Jaswal and Koppar 2013; Dadaser-Celik and Cengiz 2014; You et al. 2014; Romanić et al. 2015). The second reason is that urbanization (Xu et al. 2006; Li et al. 2011; Yang et al. 2012; Jaswal and Koppar 2013; Azorin-Molina et al. 2014) and land-cover change (Vautard et al. 2010; Bichet et al. 2012; Wever 2012) across North America, Europe, Asia, and Australia weaken surface winds by increasing surface friction. Klink (1999) suggested that modifications in the pressure gradient and surface roughness could not only affect surface winds, but also vertical mixing of atmospheric winds. In fact, analyses have examined the relationship between surface wind speeds and evapotranspiration to understand how changes in vertical forcing could impact hydrological processes (Fu et al. 2009; Zheng et al. 2009; Donohue et al. 2010; Liu et al. 2010; Yin et al. 2010a; 2010b; Liu et al. 2011; Moratiel et al. 2011; Tang et al. 2011; McVicar et al. 2012; Liuzzo et al. 2016).

Atmospheric teleconnection indices are also frequently used to explain changes in surface wind speed trends (Pirazzoli and Tomasin 2003; Pryor and Barthelmie 2003; Tuller 2004; St. George and Wolfe 2009; Abhishek et al. 2010; Li et al. 2010; Pryor and Ledolter 2010; Fu et al. 2011; Hewston and Dorling 2011; Chen et al. 2013; Lin et al. 2013; Azorin-Molina et al. 2014; You et al. 2014). For example, Chen et al. (2013) identified surface wind speed patterns based on the temporal phases of the Arctic Oscillation (AO) and El Niño–Southern Oscillation (ENSO) for China between 1971 and 2007. The study found that under a positive AO, wind speeds declined across most of China, while increased (decreased) speeds were observed over northern (southern) China during positive ENSO (Niño 3.4 region) phases. This spatial shifting of wind speeds across the continent of Asia under the different phases of ENSO could influence the position of the East Asian monsoon (Yang et al. 2002; Wu et al. 2003; Lim and Kim 2007; Zhou and Wu 2010). Therefore, studies have analyzed alterations in macro-scale atmospheric circulations to explain near-surface wind trends across the globe (Jiang et al. 2010; Guo et al. 2011; Li et al. 2011; Troccoli et al. 2012; Yang et al. 2012; Jaswal and Koppar 2013; Lin et al. 2013; Dadaser-Celik and Cengiz 2014; You et al. 2014; Romanić et al. 2015). However, many of these studies only examined a single level of the troposphere (850 or 500 hPa) to evaluate changes in macro-scale circulation and its possible relationship to surface winds.

The most complete upper-level wind trend analysis was performed by Vautard et al. (2010). It revealed positive (negative) annual mean upper-level (i.e., 850, 700, 500, and 200 hPa) wind trends for western Europe and North America (China) during 1979–2008, which does not (does) support present literature on terrestrial wind speed changes.

As a result, Vautard et al. (2010) investigated and suggested that increases in surface roughness due to vegetation could explain the reduction of surface winds observed across western Europe and North America, while changes in the Asian Monsoon from climate change and air pollution could be attributing to the decreasing surface and tropospheric winds across China.

McVicar et al. (2012) documented that wind trend climatology literature has emphasized to North America, Europe, and Asia at the expense of Central and South America over the last decade. Much of the research on Latin America has focused on evaluating the geographic and temporal surface wind speed trends and its potential implications on wind energy production for northeastern Brazil (Lucena et al. 2010; Pereira et al. 2013; Santos and Silva 2013). However, no formal studies have explored upper-level wind trends for Brazil. Vautard et al. (2010) characterized the overall vertical wind profile of wind speed trends for North America, Europe, and Asia based on monthly rawinsonde between 1979 and 2008. This provides an opportunity to analyze whether upper-level wind trend characteristics over Brazil match trends observed elsewhere. As a result, the goal of this study is to examine the spatial and temporal patterns of upper-level wind trends based on climate reanalysis datasets for Brazil. Results will show how atmospheric winds changed from a three-dimensional perspective and also provide a foundation to understand how wind speeds vary not only from a vertical, but also from a spatial (horizontal) standpoint for Brazil from 1980 to 2014.

4.2 Data and Methods

Figure 4.1 summarizes the data and methods used in the study to identify geographic and temporal upper-level wind patterns found in Brazil. Reanalysis products were selected for the analysis because of the limited temporal and spatial coverage of radiosonde data available for Brazil. Three reanalysis datasets are used to describe the upper-level wind speed trends of Brazil from 1980 to 2014. The data period selected was based on the temporal accessibility of each model. National Center for Environmental Prediction/National Center for Atmospheric Research (NCEP/NCAR) reanalysis dataset (Reanalysis 1) is a 28 vertical level global numerical model that assimilates surface and atmospheric variables at a horizontal resolution of 2.5° x 2.5° (T62) beginning in 1948 (Kalnay et al. 1996). National Center for Environmental Prediction and Department of Energy (NCEP-DOE) reanalysis dataset (Reanalysis 2) is an updated version of Reanalysis 1, with improved parameterization of physical processes and fixed errors found with Reanalysis 1 (Kanamitsu et al. 2002). Reanalysis 2 is similarly constructed at a horizontal grid scale of 2.5° x 2.5° (T62) for each pressure field (28 levels) as Reanalysis 1, but with a temporal resolution starting in 1979. Finally, European Centre for Medium-Range Weather Forecasts (ECMWF) Interim (ERA-Interim) is a global numerical model constructed at 0.75° x 0.75° (T255) resolution for 60 atmospheric pressure levels during the period of 1979 to present (Dee et al. 2011).

Data obtained from each model consist of 4 daily (0, 6, 12, and 18 UTC) *u* (west–east) and *v* (south–north) wind component (m s^{-1}), geopotential height (m), and temperature (K) values for 12 mandatory pressure levels (1000, 925, 850, 700, 600, 500, 400, 300, 250, 200, 150, and 100 hPa) of the atmosphere from 1980 to 2014. Upper-level

wind speeds (V) for each grid point is calculated from the *u* and *v* wind components extracted from each reanalysis dataset (Equation 1). Seasonal and annual mean wind speeds and geopotential heights were calculated based on the 12 mandatory pressure levels for each grid found within the study area. Sen's slope estimator (Sen 1968) is used to calculate the linear trend of each seasonal and annual upper-level wind grid field used in the study. Mann-Kendall test (Mann 1945; Kendall 1975) is utilized to describe the association between wind speed and time of each individual grid point located in Brazil. Both statistical methods have been used to examine changes in *u* and *v* winds of atmospheric circulations (500 hPa) to help explain near-surface wind trends (Dadaser-Celik and Cengiz 2014; Romanić et al. 2015). The resultant mean seasonal and annual winds trends are analyzed at each mandatory pressure level through a vertical profile and by constructing a three-dimensional model from geographical information system (GIS).

$$V(u,v) = \sqrt{u^2 + v^2} \tag{1}$$

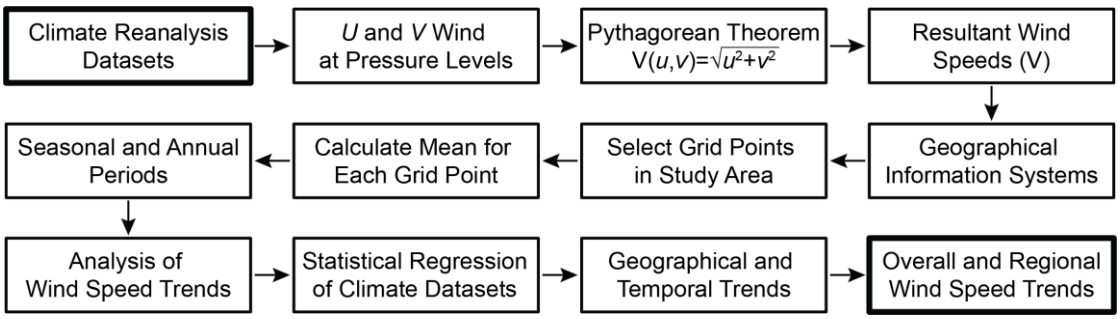

Figure 4.1. Flow diagram showing the methods and datasets used to analyze the geographical and temporal wind speed trend characteristics of Brazil during 1980–2014.

To further quantify any geographic trends, a regional wind speed analysis also was performed to show how the overall vertical wind profiles have changed across each region of Brazil. Regional wind speeds were constructed by selecting grid fields that are within one of the five geographical zones (north, northeast, central-west, southeast, and

south) recognized by Instituto Brasilerio de Geografia e Estatística (IBEG) [Figure 4.2]. Once each grid point was assigned to a region, overall seasonal and annual mean wind speeds were performed for each pressure level at which linear trends were calculated for each region of Brazil

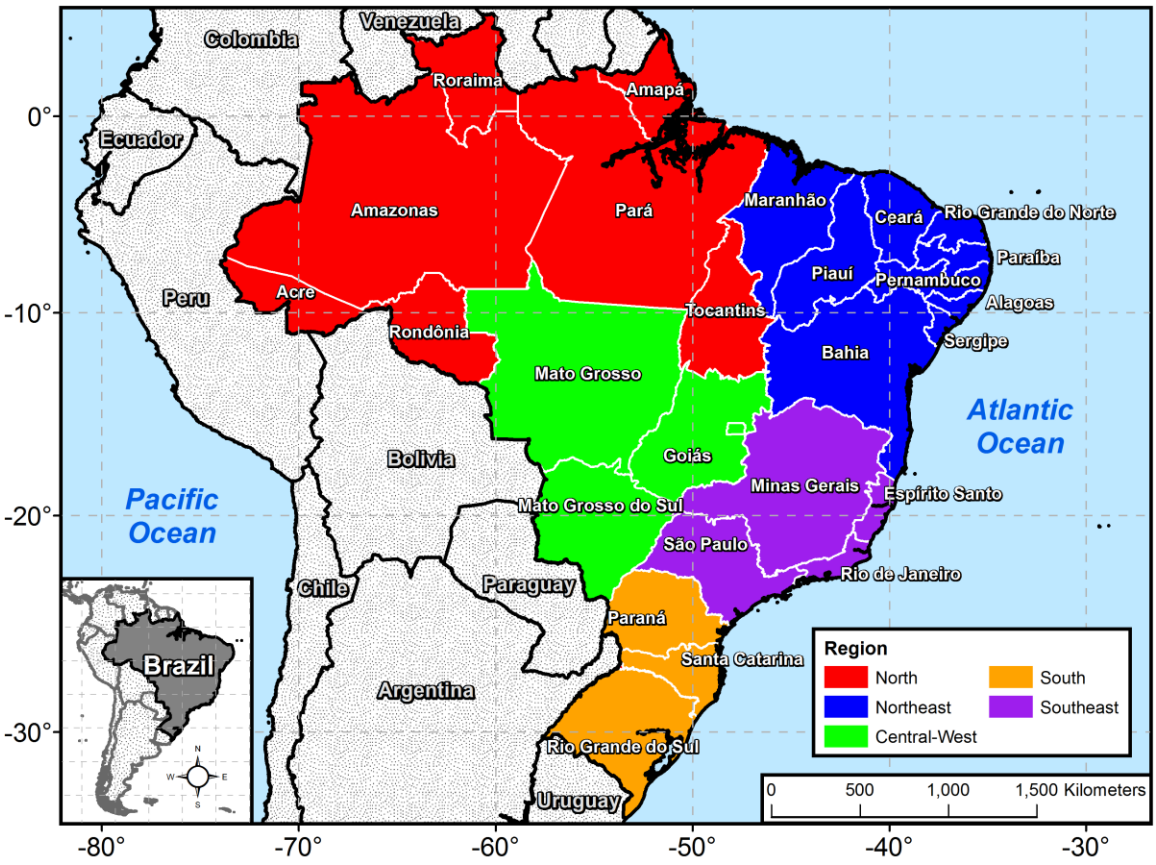

Figure 4.2. Geographic distribution of the five geographical zones (North, Northeast, Central-West, South, and Southeast) of Brazil used to determine the seasonal and annual regional wind trends.

4.3 Results

4.3.1 Overall and Spatial Wind Trends

Figure 4.3 shows the vertical profile of seasonal and annual upper-level wind trends of Brazil for each reanalysis. From these findings, three wind trend patterns are identified for each model. Surface winds (1000 hPa) exhibit decreasing (increasing)

linear trends for Reanalysis 1 and Reanalysis 2 (ERA-Interim). The reason for the differing linear trends is related to the type of surface roughness climatology or scheme used in each reanalysis. Reanalysis 1 and Reanalysis 2 utilize the simple biosphere model (SiB) [Dorman and Sellers 1989], while ERA-Interim employs the Tiled ECMWF Scheme for Surface Exchanges over Land (TESSEL) scheme (Viterbo and Beljaars 1995) to assimilate near-surface *u* and *v* winds. Despite these discrepancies, upper-level winds continue to vertically trend in the same direction before reaching a critical point for each reanalysis. This point in the atmosphere is defined as where the upper-level wind trend shifts direction from its original orientation (i.e., decreasing to increasing) starting from the surface. This shift in upper-level wind trends develops between 700 and 600 hPa for Reanalysis 1, near 850 hPa for Reanalysis 2, and near 925 hPa for ERA-Interim. The conflicting transition points between Reanalysis 1 and Reanalysis 2 occur despite using similar data as a result of the updated physical parameterizations included in Reanalysis 2. Kanamistu et al. (2002) discussed how orography was smoothed in Reanalysis 2 to prevent Gibbs phenomena related to precipitation and sensible and latent heat fluxes near steep topography to occur in the model. Gibbs phenomenon is a jump discontinuity that occurs in a continuous piece-wise Fourier series (Hewitt and Hewitt 1979). This periodic jump observed in the numerical models can have a detrimental effect on properly assessing meteorological variables. Kanamistu et al. (2002) also describes a modification in the planetary boundary layer (PBL) scheme from a localized Richardson number-dependent vertical diffusion process used in Reanalysis 1 to a nonlinear vertical diffusion scheme (Hong and Pan 1996) implemented in Reanalysis 2 to avoid concerns associated with vertical convergence of eddy fluxes (i.e., heat, moisture, and momentum). von

Engeln and Teixeira (2013) further acknowledge that Richardson-based methods are problematic of not adequately characterizing convective turbulence since the Richardson number is derived from localized turbulence and dry atmospheric conditions. These orographic and boundary scheme differences could result in the upper-level wind discrepancies that exist between Reanalysis 1 and Reanalysis 2.

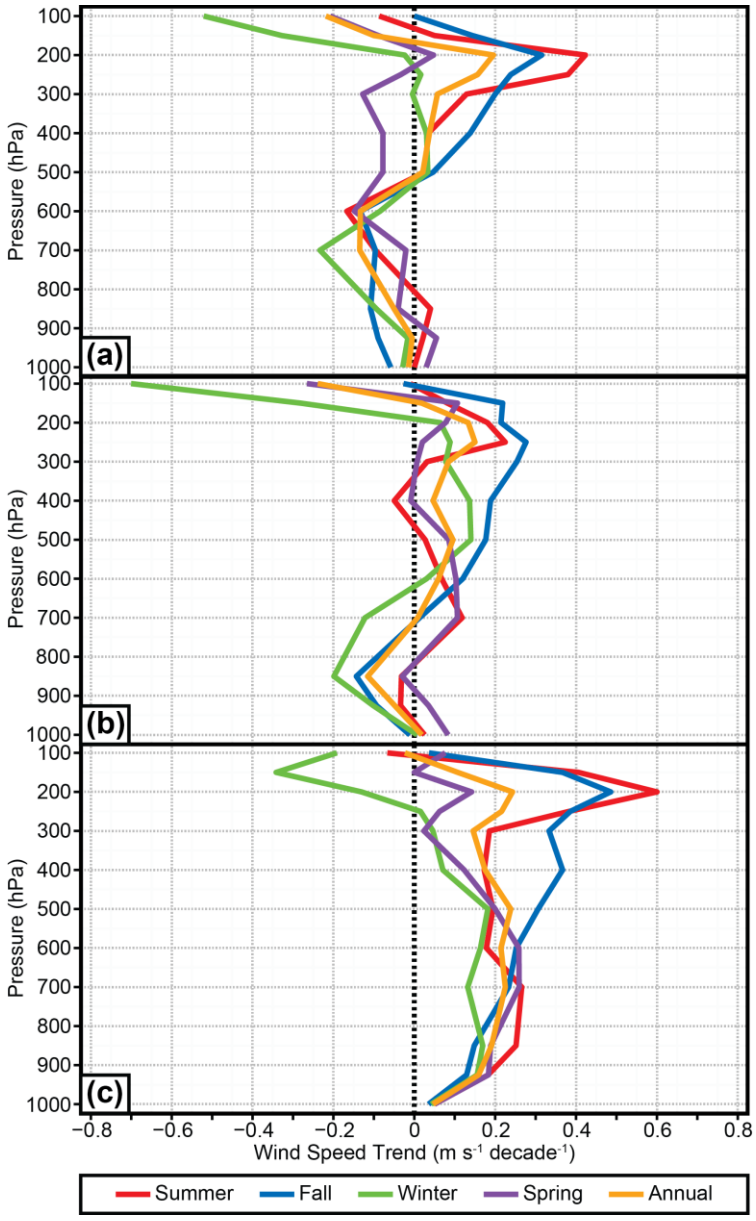

Figure 4.3. Overall vertical wind profile of the seasonal and annual upper-level wind speed trends (m s^{-1} $decade^{-1}$) of Brazil for (a) Reanalysis 1, (b) Reanalysis 2, and (c) ERA-Interim during 1980–2014.

Above this shift, reanalysis models show temporally increasing wind trends until reaching the upper part of the atmosphere, where the highest positive wind trends are documented between 300 and 200 hPa. The largest positive wind trends occur during summer and fall for each model, where wind speeds have increased between 0.2 and 0.6 m s^{-1} $decade^{-1}$ depending upon the climate model. Finally, a sharp change in wind speed is detected above 200 hPa, for which reanalysis datasets show a decrease in wind speed, with mixed results between seasons for the ERA-Interim. This decline in wind speed is associated to temperature changes developing in the upper troposphere and lower stratosphere. Allen and Sherwood (2008) showed that *u* winds decreased across the upper pressure levels (above 200 hPa) of the atmosphere between 5° S and 35°S during 1979–2005, despite an increase in upper-tropospheric wind shear observed. This increase in vertical wind shear develops when the troposphere warms and stratosphere cools, which allows the meridional temperature gradients to be enhanced toward the poles (Lorenz and DeWeaver 2007).

Vautard et al. (2010) suggested that positive upper-level wind trends could not explain the decline in surface wind across North America and Europe. The study identified changes in surface roughness that may attribute to the decreasing trends found in surface winds. Wever (2012) analyzed variations in surface roughness and found that wind speeds decreased on average by 3.1% (0.13 m s^{-1}) per decade due to the doubling of surface roughness in the Netherlands since 1981. This finding of surface roughness change is supported by Bichet et al. (2012), who noted that increasing vegetation roughness length by a factor of 1.5, 2, and 4 decreased average surface winds globally between 1975 and 2005. As expected, this suggests that surface and lower atmospheric

winds of Brazil are interconnected to changes in surface roughness. The results of this analysis show that different land-cover and PBL schemes influence wind trends found in the lower portion of the troposphere (below 850 hPa) for each climate model except for Reanalysis 1 (~700 hPa). Once above this boundary, upper-level wind trends shift or remain constant until reaching the proximity of the jet stream (~300 hPa) for each reanalysis dataset. If upper-level winds were leading to the decline in near-surface and lower-level wind speeds, it would be expected that winds would have weaken throughout vertical profile of the troposphere. It is possible that decreasing trends do exist in the upper-level atmosphere winds, but are geographically located over certain regions of Brazil. Consequently, mechanisms contributing to spatial differences in upper-level trends across Brazil will be examined.

Figures 4.4 and 4.5 show the spatial seasonal and annual mean wind trends based on the 12 pressure levels of the atmosphere for Brazil from 1980 to 2014 from a three-dimensional view. Wind trends correspond to changes in upper tropospheric circulation occurring over South America. During summer (DJF), a zonal pattern of decreasing and increasing wind trends located between 400 and 200 hPa is found between 15° S and 35° S (Figure 4.4a). This geographic configuration is also supported by a positive region found over northeastern Brazil in Reanalysis 1 and Reanalysis 2, which extends into equatorial Brazil for ERA-Interim (Figure 4.5a). The location of these upper-level trends is dynamically-linked to the position of the Bolivian High (BoH) and Nordeste low. The BoH is a warm-core anticyclone that forms over the Altiplano from latent heat released within the Amazon basin and moisture convergence from South Atlantic Convergence Zone (SACZ), while the Nordeste low is a cold-core sinking cyclone that develops

downstream of the Bolivian ridge (Lenters and Cook 1997). As expected, upper-level winds associated with this atmospheric circulation pattern are affected differently under wet and dry conditions (Vuille 1999). The study found that anomalously strong (weak) westerly winds occur in the Altiplano when the BoH weakens (strengthens) is displaced northward (southward) of its climatological position, and is warmer than normal temperatures during dry (wet) periods of the Southern Oscillation Index.

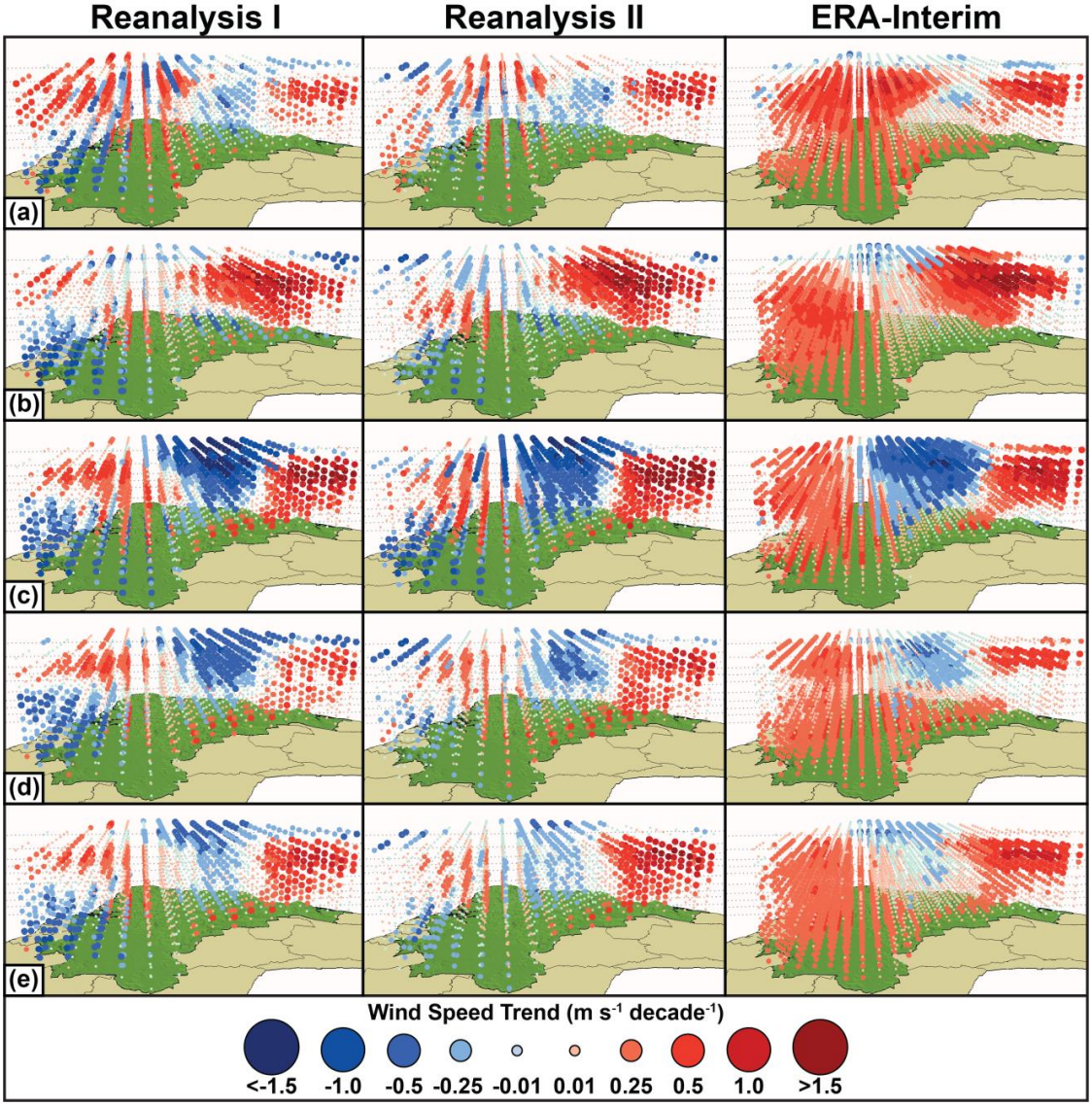

Figure 4.4. Wind speed trends (m s^{-1} $decade^{-1}$) of the mandatory atmospheric pressure levels based on (a) summer (DJF), (b) fall (MAM), (c) winter (JJA), (d) spring (SON), and (e) annual intervals during 1980–2014.

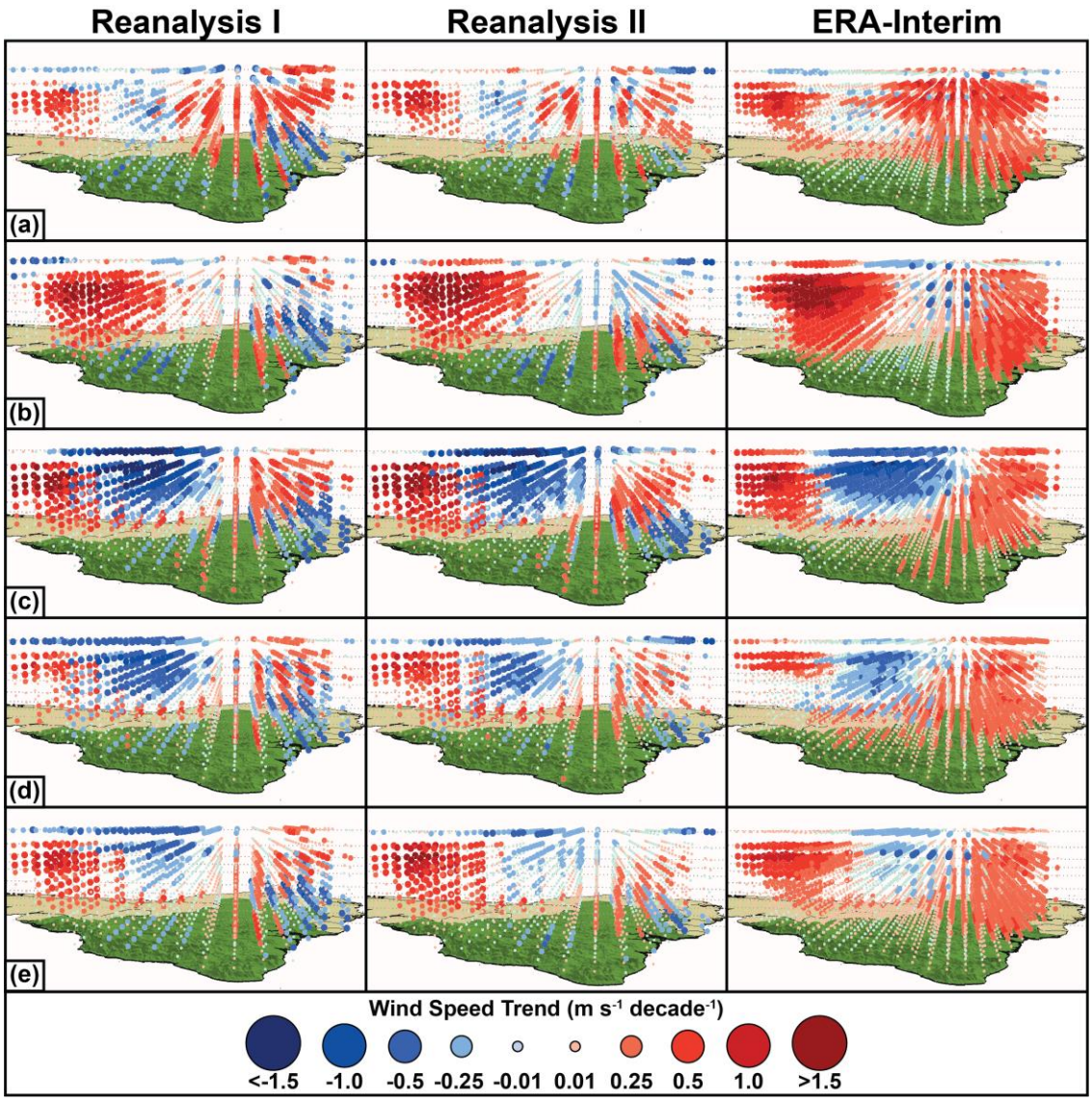

Figure 4.5. As in Figure 4.4 except viewed from Atlantic Ocean.

Figure 4.6 shows that decreasing (increasing) upper-level winds are located between 15° S and 25° S (25° Sand 35° S). It is expected that when the BoH weakens and shifts northward, upper-level wind speeds across central-west and southeastern (southern) Brazil will decrease (increase). Table 4.1 shows a positive trend in the summer mean temperature and geopotential height (latitude) at the core of the BoH. This finding shows that despite increasing temperatures (0.02–0.44 K decade^{-1}) and pressure heights (5.0–8.1 m decade^{-1}) occurring at 250 hPa, it does not necessarily support an

equatorward shift of the BoH. It is possible that the geographic location of the BoH is highly variable during summer. Lenters and Cook (1997) identified five geopotential height (200 hPa) scenarios of the BoH location with respect to Altiplano for eight summer seasons (1985/1986–1992/1993) based on empirical orthogonal function (EOF) analysis. The five EOF locations positioned the BoH over the center (25° S), southwest, southeast, east, and south of Altiplano. This evidence demonstrates that performing a seasonal composite on the spatial location of the BoH will not adequately explain spatial changes occurring with upper-level wind speeds across Brazil.

Table 4.1. Statistical linear regression analysis of summer (DJF) averages of latitude (°), geopotential height (m), and temperature (K) based on the central location of the BoH at 250 hPa for Reanalysis 1, Reanalysis 2, and ERA-Interim. A * indicates the linear trend is statistically significant (p<0.05)

Parameter	Dataset	Slope per decade	Correlation coefficient	p-value
Latitude (°)	*Reanalysis 1*	0.307	0.111	0.356
	Reanalysis 2	-0.014	-0.008	0.955
	ERA-Interim	-0.232	-0.111	0.356
Geopotential Height (m)	*Reanalysis 1*	5.000	0.250	0.038*
	Reanalysis 2	5.450	0.296	0.014*
	ERA-Interim	8.120	0.425	<0.001*
Temperature (K)	*Reanalysis 1*	0.017	0.034	0.787
	Reanalysis 2	0.161	0.270	0.024*
	ERA-Interim	0.437	0.558	<0.001*

It is possible that the thermal expansion of the equatorial and subtropical climates is promoting the increase in geopotential heights across the upper-levels of the atmosphere across Brazil. Figure 4.6 shows a steep decrease in the geopotential heights between the BoH and subtropical jet (STJ) at 250 hPa for each reanalysis dataset. As described earlier, an increase in the geopotential heights and temperature is shown with the BoH during the 35-year study period (Table 2.1). It is expected that as the atmosphere continues to warm, the geopotential height differences developing in the

subtropical and middle latitudes will allow a steeper geopotential gradient to form and result in an increase of wind speeds to occur between 25° S and 35° S.

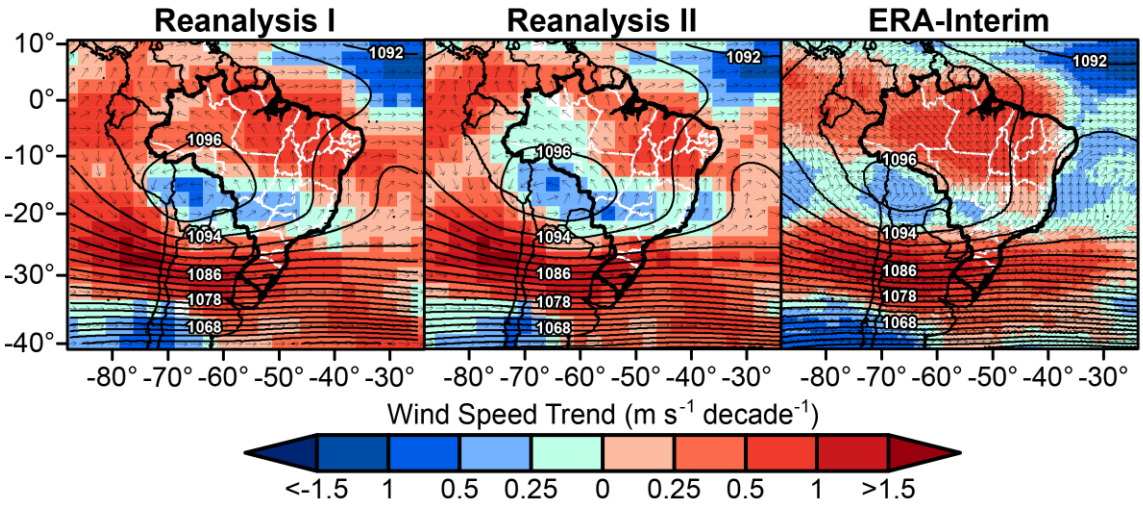

Figure 4.6. Austral summer wind speed trends (m s^{-1} $decade^{-1}$) at 250 hPa overlaid with mean geopotential height (m) and wind direction (°) for the period of 1980 to 2014.

Eventually as the BoH begins to dissipate during fall (MAM), positive and negative upper-level wind trends across southern Brazil move equatorward (Figure 4.4b). A weakening of the Nordeste low is also described over northeastern Brazil for Reanalysis 1 and Reanalysis 2, while the negative wind pattern is located farther off the coast of Brazil for ERA-Interim (Figure 4.5b). This northward shift described by upper-level circulation follows the seasonal cycle of Intertropical Convergence Zone (ITCZ). After the ITCZ migrates past the equator, the STJ over Brazil becomes an important factor for influencing upper-level wind speeds above 400 hPa during winter and spring. Figures 4.4 c–d and 4.5 c–d display the decrease and increase in wind speeds found with respect to the location of the STJ. The boundary separating positive and negative wind trends associated with STJ at 20° S is apparent for each reanalysis. A STJ climatology performed by Koch et al. (2006) documented that the maximum extent of the STJ occur south of 20° S, with the highest distribution developing poleward of 25° S for austral

winter and spring during 1979–1993. Therefore, if the frequency or intensity of the STJ in lower latitudes (>25° S) has changed temporally, it is expected that upper-level winds located between 10° S–20° S across Brazil would decline in each reanalysis. Archer and Calderia (2008) examined the annual mean position and strength of the STJ using ERA-40 data and found that it shifted poleward (-0.06 degrees decade^{-1}) and weakened (-0.41 hPa decade^{-1}) between 1979 and 2001. The study mentioned atmospheric warming and Hadley cell expansion as factors responsible for the latitudinal position and intensity changes occurring with global jets. This thermal heating is related to the location of increasing and decreasing wind trends found along the STJ. The band of decreasing winds is primarily concentrated between 400 and 100 hPa, while the pattern of increasing wind tends to occur above 700 hPa for each model. Allen and Sherwood (2008) explained that increasing meridional temperatures within the upper troposphere (~200 hPa) led to a decline in atmospheric wind speeds for the equatorial zone. Results from this analysis show that geopotential heights (400–200hPa) have increased (decreased) between 10° S and 20° S (>20° S) during austral fall. This change in geopotential height would attribute to the wind speed trends developing across central-west, southern, and southeastern Brazil during 1980–2014.

Several upper-level wind trends related to the position of tropospheric circulations (STJ and BoH) have been identified in this research. However, it is also important to analyze the lower and middle level wind speed trends of equatorial Brazil. ERA-Interim shows positive wind trends across the Amazon basin for each season at the lower levels (850–500 hPa) of the atmosphere (Figure 4.5). Reanalysis 1 (Reanalysis 2) exhibits decreasing wind speeds across the Amazon basin during austral fall and winter (winter

and spring) at 850 hPa but shows a varying amount of seasonal decrease higher above the surface (700–500 hPa). Both models agree, with increasing wind trends across portions of northern and northeastern Brazil during summer and fall below 700 hPa (Figure 4.5a–b). Eventually, the positive wind trend shifts toward the east for all other lower levels of the atmosphere (700–500 hPa). The only exception occurs at 600 hPa, where Reanalysis 1 presents a negative trend of wind speeds across equatorial Brazil for each season. The inconsistencies established between the reanalysis models suggest that other variables not analyzed in the study could attributed to the lower-level wind trends found across equatorial Brazil.

4.3.2 Regional Wind Trends

Figure 4.7 shows the regional wind speed trend magnitudes based on season and annual periods for Brazil. During summer, regional wind trends are minimal across Brazil until a positive pattern develops between 400 and 200 hPa, with the maximum occurring between 250 and 200 hPa (Figure 4.7a). However, reanalysis datasets show different pairings of increasing regional wind trends for austral summer. Reanalysis 1 and Reanalysis 2 depict comparable positive wind speed trends of 0.08–0.70 m s^{-1} $decade^{-1}$ for northern, northeastern, and southern Brazil, while ERA-Interim displays increasing trends, ranging between 0.05 and 0.90 m s^{-1} $decade^{-1}$ for all regions except for southeastern Brazil. The differences observed suggest that atmospheric inputs or model schemes are influencing upper-level wind trends in each model. After an equatorward shift of the ITCZ, wind patterns for central-west, southeastern, and southern Brazil exhibit positive trends between 400 and 100 hPa during fall (Figure 4.7b). The highest

increasing wind trends which are statistically significant (p<0.05) for southeastern and southern Brazil occur between 250 and 200 hPa of each reanalysis dataset.

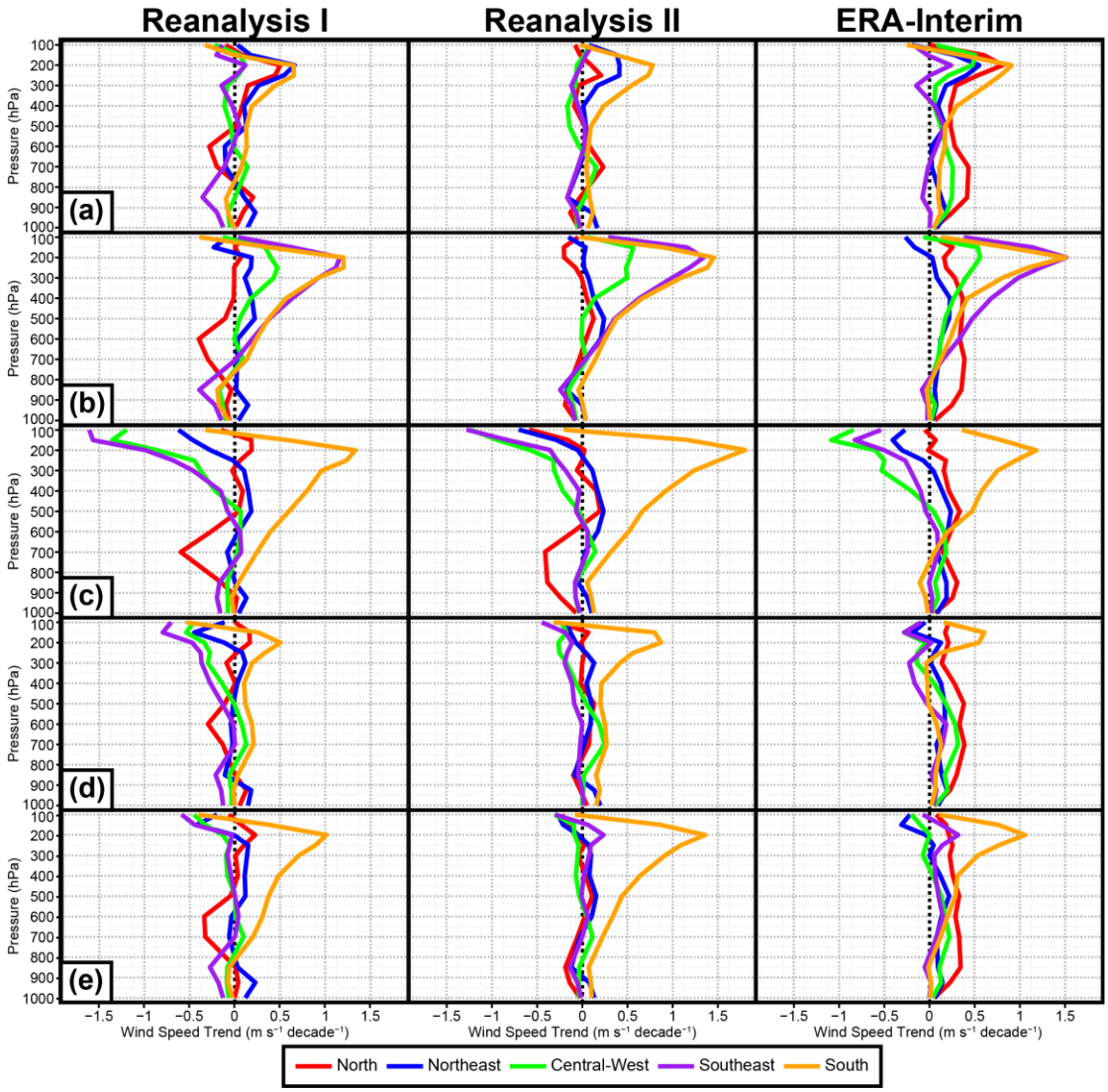

Figure 4.7. As in Figure 4.3 except based on region during (a) summer (DJF), (b) fall (MAM), (c) winter (JJA), (d) spring (SON), and (e) annual.

Figure 4.8 shows how *u* winds have changed across Brazil during fall. A decrease (increase) in *u* winds is observed above (below) 15° S for each dataset. This change in zonal winds is related to modifications of geopotential and temperature gradients. As temperature increases across the tropics, the meridional flow of thermal energy transported toward the subtropical and middle latitudes increases. This additional heating

of the atmosphere increases the meridional temperature and geopotential gradient difference between the tropics and mid-latitudes, which in response allows upper-level westerlies to increase across southern and southeastern Brazil**.** Furthermore, the warming of the atmosphere allows an increase of static stability to occur in the subtropics which results in a poleward shift of baroclinic instability to higher latitudes (Frierson et al. 2007). This change in static stability would increase vertical wind shear and decrease *u* winds across equatorial and subtropical Brazil as described in Figure 4.8.

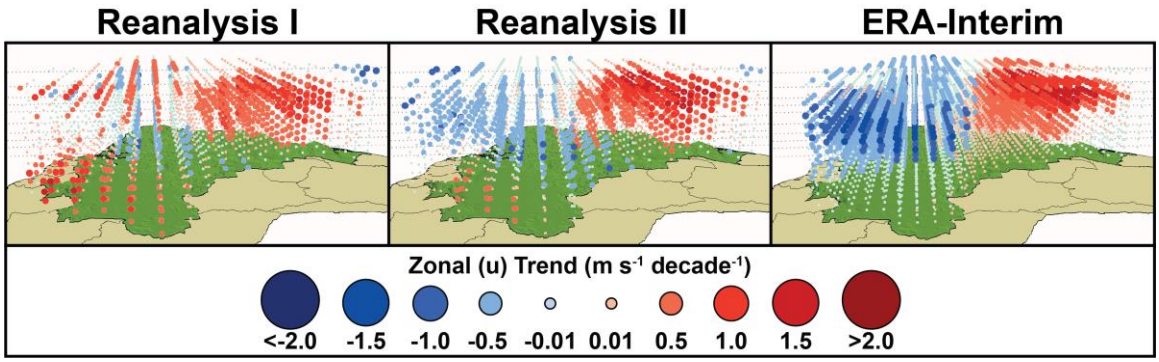

Figure 4.8. Spatial linear trends of the upper-level *u* winds during fall (MAM) for Reanalysis 1, Reanalysis 2, and ERA-Interim between 1980 and 2014.

As winter approaches, wind trends above 500 hPa separate into two groups based on the position of STJ (Figure 4.7c). Points located south (north) of STJ observed increasing (decreasing) winds, with the highest positive (negative) movements developing above 200 (150) hPa for southern (central-west and southeastern) Brazil. The strength of the positive (negative) wind trends found at each maximum (minimum) varies between 1.18 and 1.85 (-1.61 and -0.54) m s^{-1} $decade^{-1}$ among the reanalysis models. This finding supports the geographic interpretation of the upper-level winds described earlier and supports the analysis conducted by Archer and Calderia (2008) on the climatological position of STJ during winter. Eventually, the regional wind trend dissipates as the STJ moves poleward during spring, when upper-level speeds change

between -0.5 and 0.5 m s^{-1} $decade^{-1}$ for each group, with the exception of southeastern Brazil for Reanalysis 2.

4.4 Conclusions

This study analyzed the upper-level wind speed trends characteristics of Brazil from 1980 to 2014 based on three reanalysis datasets. Overall vertical profile show positive seasonal and annual wind trends across the 12 mandatory atmospheric pressure levels for ERA-Interim. Reanalysis 1 and Reanalysis 2 exhibit decreasing wind speed trends at lower levels that eventually transition to increasing trends at upper pressure levels of the atmosphere. The seasonal and annual wind trends are further evaluated at which general patterns are established for each reanalysis. Surface wind trends tend to increase vertically in magnitude at the lower portions of the troposphere due to the type of PBL scheme utilized in each climate model to calculate *u* and *v* winds. Finally, a consensus among the models shows that the highest positive wind trends occur in the upper portion of the atmosphere (400–200 hPa) before returning to a negative trend along the tropopause. This decline in wind speed is attributed to an increase in temperature found in the lower portion of the stratosphere. Allen and Sherwood (2008) showed that an increase of vertical shear from meridional warming of the atmosphere results in the decline of upper-level winds across the tropics.

Other studies have examined upper-level atmospheric circulations to explain changes developing with near-surface wind trends (Jiang et al. 2010; Vautard et al. 2010; Guo et al.2011; Li et al. 2011; Troccoli et al. 2012; Yang et al. 2012; Jaswal and Koppar 2013; Lin et al. 2013; Dadaser-Celik and Cengiz 2014; You et al. 2014; Romanić et al. 2015). As a result, this study constructed and analyzed upper-level wind speed trends

through a three-dimensional model. Results showed that upper-level wind trends are influenced by two synoptic circulations. During summer and fall, wind speed trends observed across northeastern and southern Brazil are affected by the relationship between the BoH and Nordeste low. After the ITCZ shifts northward, wind speed trends are influenced by the position of STJ. Upper-level winds found between 400 and 200 hPa have decreased across central-west and southeastern Brazil, while increases were observed for southern Brazil between 700 and 200 hPa. Recent work suggests that the position and intensity of STJ has declined and shifted poleward during the last century (Archer and Calderia 2008). The southward move of the Southern Hemisphere's STJ over Brazil has also been connected to changes in the atmospheric warming and Hadley cell expansion over the tropics. It is expected as the atmosphere warms, geopotential heights increase in the tropics, which allows a greater gradient to develop between the warm subtropical and colder middle latitudes. This pattern is documented along the boundary of STJ, where an increase (decrease) in wind speeds south (north) of the SJT across southern (central-west and southeastern Brazil) occurred.

A regional comparison of the upper-level wind speed trends confirms the findings of the geographic patterns found across Brazil. The highest (lowest) wind speed trends occur in the upper (lower) portions of the atmosphere between 400 and 200 hPa (1000 and 700 hPa). These results suggest that regional winds located in the lower troposphere are affected by changes in surface roughness rather than in macro-scale atmospheric circulations as supported by Vautard et al. (2010). However, additional research with respect to surface roughness and other climatological variables must be completed before a conclusive statement can be made.

4.5 References

Abhishek A, Lee J-Y, Keener TC, Yang YJ. 2010. Long-term wind speed variations for three Midwestern U.S. cities. *Journal of the Air and Waste Management Association* **60**: 1057–1064. doi: 10.3155/1047-3289.60.9.1057.

Allen RJ, Sherwood SC. 2008. Warming maximum in the tropical upper troposphere deduced from thermal winds. *Nature Geoscience* **1**: 399–403. doi: 10.1038/ngeo208.

Archer CL, Caldeira K. 2008. Historical trends in the jet streams. *Geophysical Research Letters* **35**: L08803. doi: 10.1029/2008GL033614.

Azorin-Molina C, Vicente-Serrano SM, McVicar TR, Jerez S, Sanchez-Lorenzo A, López-Moreno J-I, Revuelto J, Trigo RM, Lopez-Bustins JA, Espírito-Santo F. 2014. Homogenization and assessment of observed near-surface wind speed trends over Spain and Portugal, 1961–2011. *Journal of Climate* **27**: 3692–3712. doi: 10.1175/JCLI-D-13-00652.1.

Bichet A, Wild M, Folini D, Schär C. 2012. Causes for decadal variations of wind speed over land: Sensitivity studies with a global climate model. *Geophysical Research Letters* **39**: L11701. doi: 10.1029/2012GL051685.

Chen L, Li D, Pryor SC. 2013. Wind speed trends over China: Quantifying the magnitude and assessing causality. *International Journal of Climatology* **33**: 2579–2590. doi: 10.1002/joc.3613.

Dadaser-Celik F, Cengiz E. 2014. Wind speed trends over Turkey from 1975 to 2006. *International Journal of Climatology* **34**: 1913–1927. doi: 10.1002/joc.3810.

Dee DP, Uppala SM, Simmons AJ, Berrisford P, Poli P, Kobayashi S, Andrae U, Balmaseda MA, Balsamo G, Bauer P, Bechtold P, Beljaars ACM, van de Berg L, Bidlot J, Bormann N, Delsol C, Dragani R, Fuentes M, Geer AJ, Haimberger L, Healy SB, Hersbach H, Hólm EV, Isaksen L, Kållberg P, Köhler M, Matricardi M, McNally AP, Monge-Sanz BM, Morcrette J-J, Park B-K, Peubey C, de Rosnay P, Tavolato C, Thépaut J-N, Vitart F. 2011. The ERA-Interim reanalysis: Configuration and performance of the data assimilation system. *Quarterly Journal of the Royal Meteorological Society* **137**: 553–597. doi: 10.1002/qj.828.

Donohue RJ, McVicar TR, Roderick ML. 2010. Assessing the ability of potential evaporation formulations to capture the dynamics in evaporative demand within a changing climate. *Journal of Hydrology* **386**: 186–197. doi: 10.1016/j.jhydrol.2010.03.020.

Dorman JL, Sellers PJ. 1989. A global climatology of albedo, roughness length and stomatal resistance for atmospheric general circulation models as represented by the Simple Biosphere Model (SiB). *Journal of Applied Meteorology and Climatology* **28**: 833–855. doi: http://dx.doi.org/10.1175/1520-0450(1989)028<0833:AGCOAR>2.0.CO;2.

Frierson DW, Lu J, Chen G. 2007. Width of the Hadley cell in simple and comprehensive general circulation models. *Geophysical Research Letters* **34**: L18804. doi: 10.1029/2007GL031115.

Fu G, Charles SP, Yu J. 2009. A critical overview of pan evaporation trends over the last 50 years. *Climate Change* **97**: 193–214. doi: 10.1007/s10584-009-9579-1.

----------, Yu J, Zhang Y, Hu S, Ouyang R, Wenbin L. 2011. Temporal variation of wind speed in China for 1961–2007. *Theoretical and Applied Climatology* **104**: 313–324. doi: 10.1007/s00704-010-0348-x.

Guo H, Xu M, Hu Q. 2011. Changes in near-surface wind speed in China: 1969–2005. *International Journal of Climatology* **31**: 349–358. doi: 10.1002/joc.2091.

Hewitt E, Hewitt RE. 1979. The Gibbs-Wilbraham Phenomenon: An episode in Fourier analysis. *Archive for History of Exact Sciences* **21**: 129–160.

Hewston R, Dorling S. 2011. An analysis of observed daily maximum wind gusts in the UK. *Journal of Wind Engineering and Industrial Aerodynamics* **99**: 845–856. doi: http://dx.doi.org/10.1016/j.jweia.2011.06.004.

Hong S-Y, Pan H-L. 1996. Nonlocal boundary layer vertical diffusion in a medium-range forecast model. *Monthly Weather Review* **124**: 2322–2339. doi: http://dx.doi.org/10.1175/1520-0493(1996)124<2322:NBLVDI>2.0.CO;2.

Jaswal AK, Koppar AL. 2013. Climatology and trends in near-surface wind speed over India during 1961–2008. *Mausam* **64**: 417–436.

Jiang Y, Luo Y, Zhao Z, Tao S. 2010. Changes in wind speed over China during 1956–2004. *Theoretical and Applied Climatology* **99**: 421–430. doi: 10.1007/s00704-009-0152-7.

Kalnay E, Kanamitsu M, Kistler R, Collins W, Deaven D, Gandin L, Iredell M, Saha S, White G, Woollen J, Zhu Y, Leetmaa A, Reynolds R, Chelliah M, Ebisuzaki W, Higgins W, Janowiak J, Mo KC, Ropelewski C, Wang J, Jenne R, Joseph D. 1996. The NCEP/NCAR 40-year reanalysis project. *Bulletin of American Meteorological Society* **77**: 437–471. doi: http://dx.doi.org/10.1175/1520-0477(1996)077<0437:TNYRP>2.0.CO;2.

Kanamitsu M, Ebisuzaki W, Woollen J, Yang S-K, Hnilo JJ, Fiorino M, Potter GL. 2002. NCEP–DOE AMIP-II Reanalysis (R-2). *Bulletin of American Meteorological Society* **83**: 1631–1643. doi: http://dx.doi.org/10.1175/BAMS-83-11-1631.

Kendall MG. 1975. Rank correlation methods. 202 pp. Griffin. London, U.K.

Klink K. 1999. Trends in mean monthly maximum and minimum surface wind speeds in the coterminous United States, 1961 to 1990. *Climate Research* **13**: 193–205. doi: 10.3354/cr013193.

Koch P, Wernli H, Davies HC. 2006. An event-based jet-stream climatology and typology. *International Journal of Climatology* **26**: 283–301. doi: 10.1002/joc.1255.

Lenters JD, Cook KH. 1997. On the origin of the Bolivian high and related circulation features of the South American climate. *Journal of Atmospheric Sciences* **54**: 656–677. doi: http://dx.doi.org/10.1175/15200469(1997)054<0656:OTOOTB>2.0.CO;2.

Li X, Zhong S, Bian X, Heilman WE. 2010. Climate and climate variability of the wind power resources in the Great Lakes region of the United States. *Journal of Geophysical Research* **115**: D18107. doi: 10.1029/2009JD013415.

Li Z, Yan Z, Tu K, Liu W, Wang Y. 2011. Changes in wind speed and extremes in Beijing during 1980–2008 based on homogenized observations. *Advances in Atmospheric Sciences* **28**: 408–420. doi: 10.1007/s00376-010-0018-z.

Lim Y-K, Kim K-Y. 2007. ENSO impact on the space-time evolution of the regional Asian summer monsoons. *Journal of Climate* **20**: 2397–2415. doi: http://dx.doi.org/10.1175/JCLI4120.1.

Lin C, Yang K, Qin J, Fu R. 2013. Observed coherent trends of surface and upper-air wind speed over China since 1960. *Journal of Climate* **26**: 2891–2903. doi: http://dx.doi.org/10.1175/JCLI-D-12-00093.1.

Liu Q, Yang Z, Sun T. 2010. The temporal trends of reference evapotranspiration and its sensitivity to key meteorological variables in Yellow River Basin, China. *Hydrological Processes* **24**: 2171–2181. doi: 10.1002/hyp.7649.

Liu X, Luo Y, Zhang D, Zhang M, Liu C. 2011. Recent changes in pan-evaporation dynamics in China. *Geophysical Research Letters* **38**: L13404. doi: 10.1029/2011GL047929.

Liuzzo L, Viola F, Noto LV. 2016. Wind speed and temperature trends impacts on reference evapotranspiration in southern Italy. *Theoretical and Applied Climatology* **123**: 43–62. doi: 10.1007/s00704-014-1342-5.

Lorenz DJ, DeWeaver ET. 2007. Tropopause height and zonal wind response to global warming in the IPCC scenario integrations. *Journal of Geophysical Research* **112**: D10119. doi: 10.1029/2006JD008087.

Lucena AFP, Szklo AS, Schaeffer R, Dutra RM. 2010. The vulnerability of wind power to climate change in Brazil. *Renewable Energy* **35**: 904–912. doi: 10.1016/ j.renene.2009.10.022.

Mann HB. 1945. Nonparametric tests against trend. *Econometrica* **13**: 245–259.

McVicar TR, Roderick ML, Donohue RJ, Li, LT, Van Niel TG, Thomas A. Grieser J, Jhajharia D, Himri Y, Mahowald NM, Mescherskaya AV, Kruger AC, Rehman S, Dinpashoh Y. 2012. Global review and synthesis of trends in observed terrestrial near-surface wind speeds: Implications for evaporation. *Journal of Hydrology* **417**: 182–205. doi: http://dx.doi.org/10.1016/j.jhydrol.2011.10.024.

Moratiel R, Snyder RL, Durán JM, Tarqius AM. 2011. Trends in climatic variables and future reference evapotranspiration in Duero Valley (Spain). *Natural Hazards and Earth System Sciences* **11**: 1795–1805. doi: 10.5194/nhess-11-1795-2011.

Pereira EB, Martins FR, Pes MP, Segundo EID, Lyra AD. 2013. The impacts of global climate changes on the wind power density in Brazil. *Renewable Energy* **49:** 107–110. doi: http://dx.doi.org/10.1016/j.renene.2012.01.053.

Pirazzoli PA, Tomasin A. 2003. Recent near-surface wind changes in the central Mediterranean and Adriatic areas. *International Journal of Climatology* **23**: 963–973. doi: 10.1002/joc.925.

Pryor SC, Barthelmie RJ. 2003. Long-term trends in near-surface flow over the Baltic. *International Journal of Climatology* **23**: 271–289. doi: 10.1002/joc.878.

----------, Ledolter J. 2010. Addendum to "Wind speeds trends over the contiguous United States". *Journal of Geophysical Research* **115**: D10103. doi: 10.1029/ 2009JD013281.

Romanić D, Ćurić M, Jovičić I, Lompar M. 2015. Long-term trends of the 'Koshava' wind during the period 1949–2010. *International Journal of Climatology* **35**: 288–302. doi: 10.1002/joc.3981.

Santos ATS, Silva CMS. 2013. Seasonality, interannual variability, and linear tendency of wind speeds in the northeast Brazil from 1986 to 2011. *The Scientific World Journal*. doi: http://dx.doi.org/10.1155/2013/490857.

Sen PK, 1968. Estimates of the regression coefficient based on Kendall's tau. *Journal of the American Statistical Association* **63**: 1379–1389.

St. George S, Wolfe SA. 2009. El Niño stills winter winds across the southern Canadian Prairies. *Geophysical Research Letters* **36**: L23806. doi:10.1029/2009GL041282.

Tang B, Tong L, Kang S, Zhang L. 2011. Impacts of climate variability on reference evapotranspiration over 58 years in the Haihe river basin of north China. *Agricultural Water Management* **98**: 1660–1670. doi: 10.1016/j.agwat.2011. 06.006.

Troccoli A, Muller K, Coppin P, Davy R, Russell C, Hirsch AL. 2012. Long-term wind speed trends over Australia. *Journal of Climate*, **25**: 170–183. doi: http://dx.doi.org/10.1175/2011JCLI4198.1.

Tuller SE. 2004. Measured wind speed trends on the west coast of Canada. *International Journal of Climatology* **24**: 1359–1374. doi: 10.1002/joc.1073.

Vautard R, Cattiaux J, Yiou P, Thépaut J-N, Ciais P. 2010. Northern Hemisphere atmospheric stilling partly attributed to an increase in surface roughness. *Nature Geoscience* **3**: 756–761. doi: 10.1038/ngeo979.

Viterbo P, Beljaars AC. 1995. An improved land surface parameterization scheme in the ECMWF model and its validation. *Journal of Climate* **8**: 2716 –2748. doi: http://dx.doi.org/10.1175/1520-0442(1995)008<2716:AILSPS>2.0.CO;2.

von Engeln A, Teixeira J. 2013. A planetary boundary layer height climatology derived from ECMWF reanalysis data. *Journal of Climate* **26**: 6575–6590. doi: http://dx.doi.org/10.1175/JCLI-D-12-00385.1.

Vuille M. 1999. Atmospheric circulation over the Bolivian Altiplano during dry and wet periods and extreme phases of the Southern Oscillation. *International Journal of Climatology* **19**: 1579–1600. doi: 10.1002/(SICI)1097-0088(19991130)19:14 <1579::AID-JOC441>3.0.CO;2-N.

Wever N. 2012. Quantifying trends in surface roughness and the effect on surface wind speed observations. *Journal of Geophysical Research* **117**: D11104. doi: 10.1029 /2011JD017118.

Wu R, Hu Z-Z, Kirtman BP. 2003. Evolution of ENSO-related rainfall anomalies in East Asia. *Journal of Climate* **16**: 3742–3758. doi: http://dx.doi.org/10.1175/1520-0442(2003)016<3742:EOERAI>2.0.CO;2.

Xu M, Chang C-P, Fu C, Qi Y, Robock A, Robinson D, Zhang H. 2006. Steady decline of East Asian monsoon winds, 1969–2000: Evidence from direct ground measurements of wind speed. *Journal of Geophysical Research* **111**: D24111. doi: 10.1029/2006JD007337.

Yang S, Lau K-M, Kim K-M. 2002. Variations of the East Asian jet stream and Asian-Pacific-American winter climate anomalies. *Journal of Climate* **15**: 306–325. doi: http://dx.doi.org/10.1175/1520-0442(2002)015<0306:VOTEAJ>2.0.CO;2.

Yang X, Li ZX, Feng Q, He YQ, An WL, Zhang W, Cao WH, Yu TF, Wang YM, Theakstone W. 2012. The decreasing wind speed in southwestern China during 1969–2009 and possible causes. *Quaternary International* **263**: 71–84. doi: http://dx.doi.org/10.1016/j.quaint.2012.02.020.

Yin Y, Wu S, Chen G, Dai E. 2010a. Attribution analyses of potential evapotranspiration changes in China since the 1960s. *Theoretical and Applied Climatology* **101**: 19–28. doi: 10.1007/s00704-009-0197-7.

————, ————, Dai E. 2010b. Determining factors in potential evapotranspiration changes over China in the period 1971–2008. *Chinese Science Bulletin* **55**: 3329–3337. doi: 10.1007/s11434-010-3289-y.

You Q, Fraedrich K, Min J, Kang S ,Zhu X, Pepine N, Zhanga L. 2014. Observed surface wind speed in the Tibetan Plateau since 1980 and its physical causes. *International Journal of Climatology* **34**: 1873–1882. doi: 10.1002/joc.3807.

Zheng X, Liu X, Liu C, Dai X, Zhu R. 2009. Assessing contribution to panevaporation trends in Haihe River Basin, China. *Journal of Geophysical Research* **114**: D24105. doi: 10.1029/2009JD0112203.

Zhou L-T, Wu R. 2010. Respective impacts of the East Asian winter monsoon and ENSO on winter rainfall in China. *Journal of Geophysical Research* **115**: D02107. doi: 10.1029/2009JD012502.

CHAPTER 5
SUMMARY AND CONCLUSIONS

5.1 Overview

Global and regional wind climatologies have shown that surface wind speeds are generally decreasing across the world (Vautard et al. 2010; Bichet et al. 2012; McVicar et al. 2012). McVicar et al. (2012) conducted a comprehensive review of near-surface wind trends globally to show that 82% of all studies found an overall annual decreasing wind trend. The study cautioned that an insufficient amount of research has been conducted for the Latin American countries, especially for Brazil. However, recent studies have analyzed surface wind speed trends across Brazil (Lucena et al. 2010; Pereira et al. 2013; Santos and Silva 2013; Pes et al. 2017). The purpose of those studies was to assess how present and future surface winds will change across northeastern Brazil under different climate scenarios and how it could possibly affect wind energy production. Additionally these studies have focused their efforts on understanding wind speed characteristics for northeastern Brazil. This limited scope of research provides a starting point for wind research across Brazil.

The purpose of this dissertation was to expand upon previous work and analyze how wind speeds changed across Brazil not only from a surface perspective, but at upper levels as well. It is also important to examine how atmospheric features could play a role in influencing surface and upper-level winds across Brazil. To achieve these goals, this dissertation conducted a three-part study, with the motivation of understanding how the geographical and climatological characteristics of surface and upper-level winds have changed across Brazil from 1980 to 2014.

5.2 Statistical Overview

The classic method used in surface and upper-level wind speed climatologies are to examine how the mean wind speed changes for a given a study area through nonparametric linear regression. As a result, this dissertation uses nonparametric linear regression to describe spatial and temporal surface and upper-level wind characteristics of Brazil during 1980–2014 for each *in-situ* and reanalysis dataset.

Mann-Kendall (Mann 1945; Kendall 1975) is a nonparametric rank correlation test used to describe the seasonal and annual temporal relationship of mean wind speeds found in each study. The test assumes that the data is independent and identically distributed (iid) and is not dependent on a normal distribution. Equation (1) depicts the estimation of *S* statistics used in the Mann-Kendall test, where *x* denotes individual data values, *n* is the total number of observations, and sgn *(θ)* is a summation function calculated between sequential data pairs (*i*th and *j*th) of a given time series. Kendall (1975) verified through a proof that the *S* statistic is of normal approximation when $n>10$ and a mean (μ) of zero. The variance (σ) of *S* shown in equation (2) is calculated when rank ties (t_i) exist between x_i and x_j observations. A two-tailed Z-test (Z) is conducted to determine whether the correlation is significant ($p<0.05$) [Equation 3].

$$S = \sum_{i=1}^{n-1} \sum_{j=i+1}^{n} \operatorname{sgn}(x_j - x_i) \tag{1}$$

$$\operatorname{sgn}(\theta) = \begin{cases} +1, & if \quad \theta > 0 \\ 0, & if \quad \theta = 0 \\ -1, & if \quad \theta < 0 \end{cases}$$

$$(\sigma) = \frac{n(n-1)(2n+5) - \sum_{i=1}^{n} t_i (t_i - 1)(2t_i + 5)}{18} \tag{2}$$

$$Z = \begin{cases} \frac{S-1}{\sqrt{\sigma}} & if \quad S > 0 \\ 0 & if \quad S = 0 \\ \frac{S+1}{\sqrt{\sigma}} & if \quad S < 0 \end{cases} \tag{3}$$

Mann-Kendall test only describes the association between the dependent and independent variables and therefore requires additional test to evaluate the slope of a climatological time-series (i.e., wind). Sen's slope estimator (Sen 1968) is another nonparametric test used to detect linear trends based on data pairings. Equation (4) describes how the slope estimators (Q_i) are calculated for each data pairing (x_j and x_k) of the dataset. Sen's slope (β) is then determined from the median value of the slope estimators (N) [Equation 5]. The median value determined from Sen's slope is used to describe the linear seasonal and annual magnitudes found in each study of the dissertation.

$$Q_i = \frac{x_j - x_k}{j - k} \quad for \ j > k \tag{4}$$

$$\beta = \begin{cases} Q_{\frac{N+1}{2}} & if \ N \ is \ odd \\ \frac{1}{2}\left(Q_{\frac{N}{2}} + Q_{\frac{N+2}{2}} \right) & if \ N \ is \ even \end{cases} \tag{5}$$

Several studies have documented wind speed trends for specific quartiles (Pryor et al. 2007; 2009; Pryor and Ledolter 2010; Guo et al. 2011) using ordinary linear regression. However, this type of analysis leaves many unanswered questions pertaining to how wind speeds vary across different percentiles. Therefore, the practicality of using quantile regression in wind climatology research provides a unique opportunity to understand how surface winds change and vary across time and space. The first manuscript (Chapter 2) of the dissertation uses quantile regression to understand how

wind speeds across five percentiles (5%, 25%, 50%, 75%, and 95%) change across Brazil.

Quantile regression (Koenker and Bassett 1978) is an extension of ordinary least squares (OLS), which has the capability to examine changes that occur across different percentiles of a dataset. Consequently, this form of analysis is used with data that is heteroscedastic (i.e., dispersion) in nature. Equation 6 describes the portion of a population [$Q^{(p)}(y_i|x_i)$] that lies below a quantile (p) of the covariates (x_i). It assumes the residual error (ϵ) of the response variable is independent and iid. An exterior point algorithm is used to minimize the error of the coefficients (β_0 and β_1) determined at each quantile (Hao and Naiman 2007). Equation (7) describes how weights are assigned to the entire set of observations based on their location to the regression line. A data observation (y_i) that lies above (below) the fitted quantile regression ($\hat{y}$) is allocated a weight of p (1-p) to determine the sum of distances (d_p) between the regression line and observation points. Similar to OLS, the sum of residuals is used to evaluate the standard error of the slope which helps determine the significance (p<0.05) of each quantile by conducting a Student's t-test.

$$Q^{(p)}(y_i \mid x_i) = \beta_0^{(p)} + \beta_1^{(p)} x_i \tag{6}$$

$$\sum_{i=1}^{n} d_p(y_i, \hat{y}_i) = p \sum_{y_i \geq \beta_0^{(p)} + \beta_1^{(p)} x_i} \left| y_i - \beta_0^{(p)} + \beta_1^{(p)} x_i \right| + (1-p) \sum_{y_i \leq \beta_0^{(p)} + \beta_1^{(p)} x_i} \left| y_i - \beta_0^{(p)} + \beta_1^{(p)} x_i \right| \tag{7}$$

5.3 Summary

5.3.1 Surface Wind Analysis

The purpose of the first manuscript (Chapter 2) was to expand understanding of how near-surface winds (10 m) vary across Brazil based on two *in-situ* and three

reanalysis datasets for the period of 1980 to 2014. Overall seasonal and annual wind speed trends show that variation exists between the datasets. The *in-situ* (INMET and NCEI-ISD) datasets suggest a decreasing and increasing wind trend for each seasonal and annual period. The negative trend pattern found in INMET corresponds to the findings of Santos and Silva (2013). The difference in wind speed trends found between the surface wind measurements is possibly related to two factors: physical environment (location of instrumentation) and quality of the datasets. Wind distribution plots show that INMET stations have a higher probability of observing a wind speed of less than <2 m s^{-1} when compared to NCEI-ISD, which shows a distribution similar to Reanalysis 1.

Climate models exhibited different surface wind trends across Brazil. This variation of seasonal and annual trends is attributed to the type of land-cover and orographic scheme used in each model. Reanalysis 1 and Reanalysis 2 used similar wind data observations to assimilate near-surface winds, but based on the distribution show different shape and scale. This is a result of an updated physical parameterization scheme implemented in Reanalysis 2 (Kanamitsu et al. 2002).

A geographical analysis of the mean and quantile wind trends across Brazil shows two distinct patterns. Surface wind speed trends across portions of coastal, northern, and northeastern Brazil are increasing during 1980–2014. These areas are under the influence of the Intertropical Convergence Zone (ITCZ) and South Atlantic Anticyclone (SAA), which primarily control the daily weather conditions. Vizy and Cook (2016) showed that near-surface winds across the South Atlantic Basin (SAB) have increased despite a poleward shift in the SAA. The study explains that latent heat loss from surface wind movement has allowed a stronger pressure gradient to develop, which in response has

allowed wind speeds to increase across the SAB. These surface winds from the SAA then travel across the SAB and into northeastern Brazil. The decrease in wind speeds across central-west and southeastern Brazil is related to changes in temperature occurring within the interior of Brazil. Santos and Silva (2013) noted that continental heating from the equatorial low weakens the pressure gradient force across these two regions. Studies have also shown that the diurnal temperature range (DTR) has decreased across southern Brazil which has attributed to the decline in sea-level pressure (SLP) [Marengo and Camargo 2008; Sansigolo and Kayano 2010]. Based on these findings, it is important to further evaluate the role of the SAA and ITCZ and its impact on near-surface conditions (wind speed, SLP, and temperature) as the next manuscript (Chapter 3).

5.3.2 South Atlantic Anticyclone Analysis

As previously discussed in Chapter 2, surface winds across northeastern Brazil are influenced by the seasonal relationship between ITCZ and SAA. Therefore, the purpose of the second manuscript (Chapter 3) was to understand how the position of the SAA influences surface winds across Brazil from 1980 to 2014. To perform this analysis, a mean-based algorithm was developed to identify the daily central location of the SAA in the SAB. Next, a linear trend analysis was performed to ascertain how the position of the SAA center has changed over time. It was found that the SAA has shifted poleward during all seasons, but the longitudinal center has shifted westward (eastward) during spring (winter). Previous studies have explained how the role of transient anticyclones and extratropical cyclones moving through the SAB influence the position of the SAA (Ito and Ambrizzi 1999; Degola 2013).

Based on these findings, the study further examined how the position of SAA influences surface conditions across Brazil. As the SAA shifts equatorward, wind speeds across northern (southern) Brazil increased, which is represented by a decrease (increase) in temperature followed by a decrease (increase) in SLP. To further quantify this relationship between surface conditions and SAA, anomalies were calculated to quantify the SAA position changes between the five zones of Brazil as designated by Instituto Brasilerio de Geografia e Estatística (IBEG). It was found that southern Brazil is affected by transient anticyclones, while northern Brazil is influenced by a northward shift in the SAA. This difference in surface features is also supported by the spatial variability of SLP and temperature anomalies for northern and southern Brazil. It was found that SLP is more directly related to wind speed variability in Northern Brazil, while southern Brazil is geographically affected by changes in temperature. A surface wind analysis was conducted to show how the spatial location of the SAA affects wind anomalies across Brazil.

5.3.3 Upper-Level Wind Analysis

The purpose of the final manuscript (Chapter 4) was to examine the upper-level wind characteristics of Brazil based on overall, regional, and geographic perspectives. Overall vertical wind profiles showed that differences exist between surface and upper-level wind trends. This is observed by a shift in the wind speed trends related to the planetary boundary layer (PBL) and vegetation schemes used by each dataset. However, to fully understand the temporal trends of upper-level wind speeds across Brazil, a geographic approach must be used.

Thus, a three-dimensional model was constructed to analyze how wind speeds changed across the atmosphere. Based on this analysis, we were able to identify two major synoptic features: the Bolivian high (BoH) and subtropical jet (STJ) that possibly influence upper-level winds across Brazil. During austral summer and fall, the BoH is the primary feature that controls upper-level winds and if any changes occur with this circulation it could impact wind speeds across Brazil. The temperature and geopotential height associated with the BoH was found to have increased during 1980–2014. This increase in temperature has expanded the upper atmosphere, which has caused a steeper gradient to form between the states of central-west and southern Brazil. This temperature change is related to a thermal expansion that is developing in the tropics (Allen and Sherwood 2008). With this meridional temperature increase, zonal (u) winds across subtropical Brazil are decreasing as a result of increased vertical wind shear. After the BoH dissipates during the fall, the STJ starts to influence upper-level winds between central and southern Brazil. Archer and Calderia (2008) found that the climatological mean of the STJ is weakening and moving poleward during the 20th century. The southward shift has impacted upper-level winds across the states of central-west (southern) Brazil which have decreased (increased) from 1980 to 2014. A regional comparison of these two synoptic features is supported by an increased (decreased) in upper-level wind speeds across the states of southern (central-west) Brazil.

5.4 Conclusions and Future Research

Results from this dissertation deepen understanding of the role of wind for Brazil with respect to surface and upper-level winds. Prior to this study, a limited number of studies have examined wind speed characteristics (Lucena et al. 2010; Pereira et al. 2013;

Santos and Silva 2013; Pes et al. 2017). These studies focused on examining how changes in near-surface winds could potentially affect present and future wind production across northeastern Brazil. This three-part study demonstrated that different wind speed trend patterns exist across Brazil and that various surface and upper-level variables are influencing those atmospheric winds.

This dissertation provided a foundation to ask and answer questions related to changes in wind speed characteristics based on surface and upper-level conditions. However, many questions remain unanswered about how present and future surface and upper-level winds will change based on a changing climate and physical environment. Studies suggest that changes in near-surface winds are attributed to land-cover change (Bichet et al. 2012; Wever 2012) and urbanization (Xu et al. 2006; Li et al. 2011; Yang et al. 2012; Azorin-Molina et al. 2014). Results from this dissertation show that upper-level wind trends differ from surface wind trends based on an overall vertical profile and three-dimensional analysis. Vautard et al. (2010) found that median wind speeds across the Northern Hemisphere have decreased as normalized difference vegetation index (NDVI) becomes more positive. Therefore, it is then important to investigate how changes in land surface type affect surface winds across Brazil. The wind speed changes that are identified in this study for portions of southern and southeastern Brazil may be related to surface land modifications.

Another avenue of interest is conducting an empirical orthogonal function (EOF) analysis on surface winds across the SAB. Lenters and Cook (1997) identified 5 geopotential height (200 hPa) scenarios based on a five-day running sea-level pressure average to identify the upper-level synoptic conditions associated with the BoH. This

type of analysis would be helpful to understand how wind speeds change with respect to the ITCZ and SAA and support the findings conducted on wind speed anomalies based on the position of the SAA in the SAB. The EOF can also be used to investigate upper-level wind speed patterns across the Southern Hemisphere as well.

Studies have examined changes in the upper-level of the atmosphere by conducting a vertical wind or temperature profile. Allen and Sherwood (2008) show that thermal winds across both hemispheres are evolving because of atmospheric warming occurring at the Equator, which is affecting *u* winds between the tropics and middle latitudes. With today's technological advancements, it would be interesting to investigate how the thermal winds across the Southern Hemisphere have changed based on a three-dimensional perspective. It is hypothesized that the decreasing (increasing) wind speeds across equatorial and subtropical (mid-latitude and polar) climates could be further explained by this type of analysis. It would also support the findings of this dissertation on upper-level wind trends across Brazil. Therefore, future research will examine how thermal winds have changed across Brazil.

REFERENCES

Abhishek A, Lee J-Y, Keener TC, Yang YJ. 2010. Long-term wind speed variations for three Midwestern U.S. cities. *Journal of the Air and Waste Management Association* **60**: 1057–1064. doi: 10.3155/1047-3289.60.9.1057.

Allen RJ, Sherwood SC. 2008. Warming maximum in the tropical upper troposphere deduced from thermal winds. *Nature Geoscience* **1**: 399–403. doi: 10.1038/ngeo208.

ANEEL. 2017. Banco de Informacão de Geracão. Available at: National Electricity Regulatory Agency. http://www2.aneel.gov.br/aplicacoes/capacidadebrasil/capacidadebrasil.cfm. [Accessed May 2017].

Archer CL, Caldeira K. 2008. Historical trends in the jet streams. *Geophysical Research Letters* **35**: L08803. doi:10.1029/2008GL033614.

Ashley WS, Black AW. 2008. Fatalities associated with nonconvective high-wind events in the United States. *Journal of Applied Meteorology and Climatology* **47**: 717–725. doi: http://dx.doi.org/10.1175/2007JAMC1689.1.

Azorin-Molina C, Vicente-Serrano SM, McVicar TR, Jerez S, Sanchez-Lorenzo A, López-Moreno J-I, Revuelto J, Trigo RM, Lopez-Bustins JA, Espírito-Santo F. 2014. Homogenization and assessment of observed near-surface wind speed trends over Spain and Portugal, 1961–2011. *Journal of Climate* **27**: 3692–3712. doi: 10.1175/JCLI-D-13-00652.1.

Bandyopadhyay A, Bhadra A, Raghuwanshi NS, Singh R. 2009. Temporal trends in estimates of reference evapotranspiration over India. *Journal of Hydrologic Engineering* **14**: 508–515. doi: http://dx.doi.org/10.1061/(ASCE)HE.1943-5584.0000006.

Barthel F, Neumayer E. 2012. A trend analysis of normalized insured damage from natural disasters. *Climatic Change* **113**: 215–237. doi 10.1007/s10584-011-0331-2.

Bichet A, Wild M, Folini D, Schär C. 2012. Causes for decadal variations of wind speed over land: Sensitivity studies with a global climate model. *Geophysical Research Letters* **39**: L11701. doi: 10.1029/2012GL051685.

Black AW, Ashley WS. 2010. Nontornadic convective wind fatalities in the United States. *Natural Hazards* **54**: 355–366. doi: 10.1007/s11069-009-9472-2.

Blender R, Schubert M. 2000. Cyclone tracking in different spatial and temporal resolutions. *Monthly Weather Review* **128**: 377–384. doi: 10.1175/1520-0493(2000)128<0377:CTIDSA>2.0.CO;2.

Brázdil R, Chromá K, Dobrovolný P, Tolasz R. 2009. Climate fluctuations in the Czech Republic during the period 1961–2005. *International Journal of Climatology* **29**: 223–242. doi: 10.1002/joc.1718.

Burn DH, Hesch NM. 2007. Trends in evaporation for the Canadian Prairies. *Journal of Hydrology* **336**: 61–73. doi: http://doi.org/10.1016/j.jhydrol.2006.12.011.

Castro JS, Camargo R, Marone E, Sepúlveda. 2015. Using the mean pressure gradient and NCEP/NCAR reanalysis to estimate the strength of the South Atlantic Anticyclone. *Dynamics of Atmospheres and Oceans* **71**: 83–90. doi: http://doi.org/10.1016/j.dynatmoce.2015.06.003.

Changnon SA. 2009. Temporal and spatial distributions of wind storm damages in the United States. *Climatic Change* **94**: 473–482. doi: 10.1007/s10584-008-9518-6.

Chen L, Li D, Pryor SC. 2013. Wind speed trends over China: Quantifying the magnitude and assessing causality. *International Journal of Climatology* **33**: 2579–2590. doi: 10.1002/joc.3613.

CRESESB. 2001. Atlas do Potencial Eólico Brasileiro. Rio de Janeiro. Available at: Centro de Referência para Solar e Eólica Sérgio Brito. http://www.cresesb.cepel.br/publicacoes/download/atlas_eolico/Atlas%20do%20Potencial%20Eolico%20Brasileiro.pdf/. [Accessed May 2017].

Dadaser-Celik F, Cengiz E. 2014. Wind speed trends over Turkey from 1975 to 2006. *International Journal of Climatology* **34**: 1913–1927. doi: 10.1002/joc.3810.

Davenport AG. 1963. The relationship of wind structure to wind loading. *Proceedings of Conference: Wind Effects on Buildings and Structures*. National Physical Laboratory. London, England. 19–82.

Davis RB. Hayden D, Gay W, Phillips, Jones G. 1997. The North Atlantic subtropical anticyclone. *Journal of Climate* **10**: 728–744. doi: http://dx.doi.org/10.1175/1520-0442(1997)010<0728:TNASA>2.0.CO;2.

Dee DP, Uppala SM, Simmons AJ, Berrisford P, Poli P, Kobayashi S, Andrae U, Balmaseda MA, Balsamo G, Bauer P, Bechtold P, Beljaars ACM, van de Berg L, Bidlot J, Bormann N, Delsol C, Dragani R, Fuentes M, Geer AJ, Haimberger L, Healy SB, Hersbach H, Hólm EV, Isaksen L, Kållberg P, Köhler M, Matricardi M, McNally AP, Monge-Sanz BM, Morcrette J-J, Park B-K, Peubey C, de Rosnay P, Tavolato C, Thépaut J-N, Vitart F. 2011. The ERA-Interim reanalysis: Configuration and performance of the data assimilation system. *Quarterly Journal of the Royal Meteorological Society* **137**: 553–597. doi: 10.1002/qj.828.

DeGaetano AT. 1998. Identification and implications of biases in U.S. surface wind observation, archival, and summarization methods. *Theoretical and Applied Climatology* **60**: 151–162. doi: 10.1007/s007040050040.

Degola TSD. 2013. Impactos e variabilidade do Anticiclone Subtropical do Atlântico Sul sobre o Brasil no clima presente e em cenários futuros. Institute of Astronomy, Geophysics and Atmospheric Sciences, University of São Paulo, São Paulo, pp. 91.

Donohue RJ, McVicar TR, Roderick ML. 2010. Assessing the ability of potential evaporation formulations to capture the dynamics in evaporative demand within a changing climate. *Journal of Hydrology* **386**: 186–197. doi: 10.1016/j.jhydrol.

Dorman JL, Sellers PJ. 1989. A global climatology of albedo, roughness length and stomatal resistance for atmospheric general circulation models as represented by the Simple Biosphere Model (SiB). *Journal of Applied Meteorology and Climatology* **28**: 833–855. doi: http://dx.doi.org/10.1175/1520-0450(1989)028<0833:AGCOAR>2.0.CO;2.

Frierson DW, Lu J, Chen G. 2007. Width of the Hadley cell in simple and comprehensive general circulation models. *Geophysical Research Letters* **34**: L18804. doi: 10.1029/2007GL031115.

Fu G, Charles SP, Yu J. 2009. A critical overview of pan evaporation trends over the last 50 years. *Climate Change* **97**: 193–214. doi: 10.1007/s10584-009-9579-1.

----------, Yu J, Zhang Y, Hu S, Ouyang R, Wenbin L. 2011. Temporal variation of wind speed in China for 1961–2007. *Theoretical and Applied Climatology* **104**: 313–324. doi: 10.1007/s00704-010-0348-x.

Gao G, Chen D, Ren G, Chen Y, Liao Y. 2006. Spatial and temporal variations and controlling factors of potential evapotranspiration in China: 1956–2000. *Journal of Geographical Sciences* **16**: 3–12.

Garreaud RD. 2000. Cold air incursions over subtropical South America: Mean structure and dynamics. *Monthly Weather Review* **128**: 2544–2559. doi: http://dx.doi.org/10.1175/1520-0493(2000)128<2544:CAIOSS>2.0.CO;2.

Good SA, Corlett GK, Remedios JJ, Noyes EJ, Llewellyn-Jones DT. 2007. The global trend in sea surface temperature from 20 years of Advanced Very High Resolution Radiometer data. *Journal of Climate* **20**: 1255–1264. doi: http://dx.doi.org/10.1175/JCLI4049.1.

Gordon C, Cooper C, Senior CA, Banks H, Gregory JM, Johns TC, Mitchell JFB, Wood A. 2000. The simulation of SST, sea ice extents and ocean heat transports in a version of the Hadley Centre coupled model without flux adjustments. *Climate Dynamics* **16**: 147–168. doi: 10.1007/s003820050010.

Greene SJ, Chatelain M, Morrissey M, Stadler S. 2012. Estimated changes in wind speed and wind power density over the western High Plains, 1971–2000. *Theoretical and Applied Climatology* **109**: 507–518. doi: 10.1007/s00704-012-0596-z.

Griffin BJ, Kohfeld KE, Cooper AB, Boenisch G. 2010. Importance of location for describing typical and extreme wind speed behavior. *Geophysical Research Letters* **37**: L22804. doi: 10.1029/2010GL045052.

Grodsky SA, Carton JA. 2003. The intertropical convergence zone in the South Atlantic and the Equatorial cold tongue. *Journal of Climate* **16**: 723–733. doi: http://dx.doi.org/10.1175/1520-0442(2003)016<0723:TICZIT>2.0.CO;2.

Guo H, Xu M, Hu Q. 2011. Changes in near-surface wind speed in China: 1969–2005. *International Journal of Climatology* **31**: 349–358. doi: 10.1002/joc.2091.

Hao L, Naiman DQ. 2007. Quantile Regression. *Series: Quantitative Applications in the Social Sciences*. Liao, TF (ed.). Thousand Oaks, CA. 136 pp.

Harman JR. 1987. Mean monthly North American anticyclone frequencies, 1950–79. *Monthly Weather Review* **115**: 2840–2848. doi: http://dx.doi.org/10.1175/1520-0493(1987)115<2840:MMNAAF>2.0.CO;2.

Hastenrath S. 1976. Variations in low-latitude circulation and extreme climatic events in the Tropical Americas. *Journal of the Atmospheric Sciences* **33**: 202–215. doi: http://dx.doi.org/10.1175/1520-0469(1976)033<0202:VILLCA>2.0.CO;2.

----------. 1985. Regional circulation systems. *Climate and Circulation of the Tropics*. Reidel, D (ed.). Dordrecht. 107–209.

Hastings DA, Dunbar PK, Elphingstone GM, Bootz M, Murakami H, Maruyama H, Masaharu H, Holland P, Payne J, Bryant NA, Logan TL, Muller J-P, Schreier G, MacDonald JS. 1999. The Global Land One-kilometer Base Elevation (GLOBE) Digital Elevation Model, Version 1.0. *National Oceanic and Atmospheric Administration. National Geophysical Data Center*. Boulder, CO. http://www.ngdc.noaa.gov/mgg/topo/globe.html.

Hewitt E, Hewitt RE. 1979. The Gibbs-Wilbraham Phenomenon: An episode in Fourier analysis. *Archive for History of Exact Sciences* **21**: 129–160.

Hewston R, Dorling S. 2011. An analysis of observed daily maximum wind gusts in the UK. *Journal of Wind Engineering and Industrial Aerodynamics* **99**: 845–856. doi: http://dx.doi.org/10.1016/j.jweia.2011.06.004.

Holt E, Wang J. 2012. Trends of wind speed at wind turbine height of 80 m over the contiguous United States using the North American Regional Reanalysis (NARR). *Journal of Applied Meteorology and Climatology* **51**: 2188–2202. doi:10.1175/JAMC-D-11-0205.1.

Hong S-Y, Pan H-L. 1996. Nonlocal boundary layer vertical diffusion in a medium-range forecast model. *Monthly Weather Review* **124**: 2322–2339. doi: http://dx.doi.org/10.1175/1520-0493(1996)124<2322:NBLVDI>2.0.CO;2.

Hundecha Y, St-Hilaire A, Ouarda TBMJ, El Adlouni S, Gachon P. 2008. A nonstationary extreme value analysis for the assessment of changes in extreme annual wind speed over the Gulf of St. Lawrence, Canada. *Journal of Applied Meteorology and Climatology* **47**: 2745–2759. doi: http://dx.doi.org/10.1175/2008JAMC1665.1.

Ito ERK, Ambrizzi T. 1999. Um estudo Climatológico do Anticiclone Subtropical do Atlântico Sul e sua influência em Sistemas Frontais. Institute of Astronomy, Geophysics and Atmospheric Sciences, University of São Paulo, São Paulo, pp 126.

----------, ----------. 2000. Climatologia da posição da alta subtropical do atlântico sul para os meses de inverno. Congresso Latino Americao e Iberico de Meteorologia, Metorologia Brasileria além do ano 2000. Rio de Janeiro. *Sociedade Brasileira de Meteorologia*. 860–865.

Jakob D. 2010. Challenges in developing a high-quality surface wind-speed data-set for Australia. *Australian Meteorological and Oceanographic Journal* **60**: 227–236.

Jaswal AK, Koppar AL. 2013. Climatology and trends in near-surface wind speed over India during 1961–2008. *Mausam* **64**: 417–436.

Jiang Y, Luo Y, Zhao Z, Tao S. 2010. Changes in wind speed over China during 1956–2004. *Theoretical and Applied Climatology* **99**: 421–430. doi: 10.1007/s00704-009-0152-7.

Jones DA, Simmonds I. 1994. A climatology of Southern Hemisphere anticyclones. *Climate Dynamics* **10**: 333–348. doi: 10.1007/BF00228031.

Jönsson P, Fortuniak K. 1995. Interdecadal variations of surface wind direction in Lund, Southern Sweden, 1741–1990. *International Journal of Climatology* **15**: 447–461. doi: 10.1002/joc.3370150407.

Justus CG, Hargraves WR, Mikhail A, Graber D. 1978. Methods for estimating wind speed frequency distributions. *Journal of Applied Meteorology* **17**: 350–353. doi: http://dx.doi.org/10.1175/1520-0450(1978)017<0350:MFEWSF>2.0.CO;2.

Kahn ME. 2005. The death toll from natural disasters: the role of income, geography, and institutions. *The Review of Economics and Statistics* **87**: 271–284. doi: 10.1162/0034653053970339.

Kalnay E, Kanamitsu M, Kistler R, Collins W, Deaven D, Gandin L, Iredell M, Saha S, White G, Woollen J, Zhu Y, Leetmaa A, Reynolds R, Chelliah M, Ebisuzaki W, Higgins W, Janowiak J, Mo KC, Ropelewski C, Wang J, Jenne R, Joseph D. 1996. The NCEP/NCAR 40-year reanalysis project. *Bulletin of American Meteorological Society* **77**: 437–471. doi: http://dx.doi.org/10.1175/1520-0477(1996)077<0437:TNYRP>2.0.CO;2.

Kanamitsu M, Ebisuzaki W, Woollen J, Yang S-K, Hnilo JJ, Fiorino M, Potter GL. 2002. NCEP–DOE AMIP-II Reanalysis (R-2). *Bulletin of American Meteorological Society* **83**: 1631–1643. doi: http://dx.doi.org/10.1175/BAMS-83-11-1631.

Kendall MG. 1975. Rank correlation methods. 202 pp. Griffin. London, U.K.

Kim J, Palk K. 2015. Recent recovery of surface wind speed after decadal decrease: A focus on South Korea. *Climate Dynamics* **45**: 1699–1712. doi: 10.1007/s00382-015-2546-9.

Klink K. 1998. Complementary use of scalar, directional and vector statistics with an application to surface winds. *The Professional Geographer* **50**: 3–13. doi: 10.1111/0033-0124.00099.

----------. 1999a. Climatological mean and interannual variance of United States surface wind speed, direction and velocity. *International Journal of Climatology* **19**: 471–488. doi: 10.1002/(SICI)1097-0088(199904)19:5<471::AID-JOC367>3.0.CO;2-X.

----------. 1999b. Trends in mean monthly maximum and minimum surface wind speeds in the coterminous United States, 1961 to 1990. *Climate Research* **13**: 193–205. doi: 10.3354/cr013193.

----------. 2002. Trends and interannual variability of wind speed distributions in Minnesota. *Journal of Climate* **15**: 3311–3317. doi: http://dx.doi.org/10.1175/1520-0442(2002)015<3311:TAIVOW>2.0.CO;2.

Koch P, Wernli H, Davies HC. 2006. An event-based jet-stream climatology and typology. *International Journal of Climatology* **26**: 283–301. doi: 10.1002/joc.1255.

Koenker R, Bassett G. 1978. Regression Quantiles. *Econometrica* **46**: 33–50.

Lenters JD, Cook KH. 1997. On the origin of the Bolivian high and related circulation features of the South American climate. *Journal of Atmospheric Sciences* **54**: 656 –677. doi: http://dx.doi.org/10.1175/15200469(1997)054<0656:OTOOTB>.

Li X, Zhong S, Bian X, Heilman WE. 2010. Climate and climate variability of the wind power resources in the Great Lakes region of the United States. *Journal of Geophysical Research* **115**: D18107. doi: 10.1029/2009JD013415.

Li Z, Yan Z, Tu K, Liu W, Wang Y. 2011. Changes in wind speed and extremes in Beijing during 1980–2008 based on homogenized observations. *Advances in Atmospheric Sciences* **28**: 408–420. doi: 10.1007/s00376-010-0018-z.

Lim Y-K, Kim K-Y. 2007. ENSO impact on the space-time evolution of the regional Asian summer monsoons. *Journal of Climate* **20**: 2397–2415. doi: http://dx.doi.org/10.1175/JCLI4120.1.

Lin C, Yang K, Qin J, Fu R. 2013. Observed coherent trends of surface and upper-air wind speed over China since 1960. *Journal of Climate* **26**: 2891–2903. doi: http://dx.doi.org/10.1175/JCLI-D-12-00093.1.

Liu Q, Yang Z, Sun T. 2010. The temporal trends of reference evapotranspiration and its sensitivity to key meteorological variables in Yellow River Basin, China. *Hydrological Processes* **24**: 2171–2181. doi: 10.1002/hyp.7649.

Liu X, Luo Y, Zhang D, Zhang M, Liu C. 2011. Recent changes in pan-evaporation dynamics in China. *Geophysical Research Letters* **38**: L13404. doi: 10.1029/2011 GL047929.

Liuzzo L, Viola F, Noto LV. 2016. Wind speed and temperature trends impacts on reference evapotranspiration in southern Italy. *Theoretical and Applied Climatology* **123**: 43–62. doi: 10.1007/s00704-014-1342-5.

Lorenz DJ, DeWeaver ET. 2007. Tropopause height and zonal wind response to global warming in the IPCC scenario integrations. *Journal of Geophysical Research* **112**: D10119. doi: 10.1029/2006JD008087.

Lott JN, Vose RS, Del Greco SA, Ross TR, Worley S, Comeaux JL. 2008. The integrated surface database: Partnerships and progress. Preprints 24th Conference on Interactive Information Processing Systems for Meteorology, Oceanography, and Hydrology New Orleans, LA. *American Meteorological Society*: Paper 131387.

Lucena AFP, Szklo AS, Schaeffer R, Dutra RM. 2010. The vulnerability of wind power to climate change in Brazil. *Renewable Energy* **35**: 904–912. doi: 10.1016/ j.renene.2009.10.022.

Lupo AR, Nocera JJ, Bosart LF, Hoffman EG, Knight DJ. 2001. South American cold surges: Types, composites, and case studies. *Monthly Weather Review* **129**: 1021 –1041. doi: http://dx.doi.org/10.1175/1520-0493(2001)129<1021:SACSTC >2.0.CO;2.

Mächel H, Kapala A, Flohn, H. 1998. Behaviour of the centres of action above the Atlantic since 1881. Part I: Characteristics of seasonal and interannual variability. *International Journal of Climatology* **18**: 1–22. doi: 10.1002/(SICI)1097-0088(199801)18:1<1::AID-JOC225>3.0.CO;2-A.

Mann HB. 1945. Nonparametric tests against trend. *Econometrica* **13**: 245–259.

Mantua NJ, Hare SR, Zhang Y, Wallace JM, Francis RC. 1997. A Pacific Interdecadal Climate Oscillation with impacts on salmon production. *Bulletin of the American Meteorological Society* **78**: 1069–1079. doi: http://dx.doi.org/10.1175/1520-0477(1997)078<1069:APICOW>2.0.CO;2.

Marengo JA, Ambrizzi T, Kiladis G, Liebmann B. 2002. Upper-air wave trains over the Pacific Ocean and wintertime cold surge in tropical-subtropical South America leading to freezes in southern and southeastern Brazil. *Theoretical and Applied Climatology* **73**: 223–242. doi: 10.1007/s00704-001-0669-x.

----------, Camargo CC. 2008. Surface air temperature trends in Southern Brazil for 1960–2002. *International Journal of Climatology* **28**: 893–904. doi: 10.1002/ joc.1584.

Martin-Vide J, Lopez-Bustins J-A. 2006. The Western Mediterranean Oscillation and rainfall in the Iberian Peninsula. *International Journal of Climatology* **26**: 1455–1475. doi: 10.1002/joc.1388.

McVicar TR, Van Niel TG, Li LT, Roderick ML, Rayner DP, Ricciardull L, Donohue RJ. 2008. Wind speed climatology and trends for Australia, 1975–2006: Capturing the stilling phenomenon and comparison with near-surface reanalysis output. *Geophysical Research Letters* **35**: L20403. doi: 10.1029/2008GL035627.

----------, Roderick ML. 2010. Atmospheric science: Winds of change. *Nature Geoscience* **3**: 747–748. doi: 10.1038/ngeo1002.

----------, Roderick ML, Donohue RJ, Li, LT, Van Niel TG, Thomas A. Grieser J, Jhajharia D, Himri Y, Mahowald NM, Mescherskaya AV, Kruger AC, Rehman S, Dinpashoh Y. 2012. Global review and synthesis of trends in observed terrestrial near-surface wind speeds: Implications for evaporation. *Journal of Hydrology* **417**: 182–205. doi: http://dx.doi.org/10.1016/j.jhydrol.2011.10.024.

Mearns LO, Gutowki W, Jones R, Leung R, McGinnis S, Nunes A, Qian Y. 2009. A regional climate change assessment program for North America. *Eos Transactions* **90**: 311–311 doi: 10.1029/2009EO360002.

Mesinger F, DiMego G, Kalnay E, Mitchell K, Shafran PC, Ebisuzaki W, Jović D, Woollen J, Rogers E, Berbery EH, Ek MB, Fan Y, Grumbine R, Higgins W, Li H, Lin Y, Manikin G, Parrish D, Shi W. 2006. National American Regional Reanalysis. *Bulletin of American Meteorological Society* **87**: 343–360. doi: 10.1175/BAMS-87-3-343.

Moratiel R, Snyder RL, Durán JM, Tarqius AM. 2011. Trends in climatic variables and future reference evapotranspiration in Duero Valley (Spain). *Natural Hazards and Earth System Sciences* **11**: 1795–1805. doi: 10.5194/nhess-11-1795-2011.

Moscati MCL, Gan MA. 2007. Rainfall variability in the rainy season of semiarid zone of northeast Brazil (NEB) and its relation to wind regime. *International Journal of Climatology* **27**: 493–512. doi: 10.1002/joc.1408.

Murray RJ, Simmonds I. 1991. A numerical scheme for tracking cyclone centres from digital data. Part I: Development and operation of the scheme. *Australian Meteorological Magazine* **39**: 155–166.

Palutikof JP. 2003. Analysis of Mediterranean climate data: Measured and modelled. *Mediterranean Climate: Variability and Trends*. Bolle, H-J. (ed.). Springer-Verlag. Berlin. 125–132.

Pereira EB, Martins FR, Pes MP, Segundo EID, Lyra AD. 2013. The impacts of global climate changes on the wind power density in Brazil. *Renewable Energy* **49:** 107–110. doi: 10.1016/j.renene.2012.01.053.

Pes MP, Pereira EB, Marengo JA, Martins FR, Heineman D, Schmidt M. 2017. Climate trends on the extreme winds in Brazil. *Renewable Energy* **109**: 110–120. doi: http://doi.org/10.1016/j.renene.2016.12.101.

Pezza AB, Ambrizzi T. 2005. Dynamical conditions and synoptic tracks associated with different types of cold surge over tropical South America. *International Journal of Climatology* **25**: 215–241. doi: 10.1002/joc.1080.

Pirazzoli PA, Tomasin A. 1999. Recent abatement of easterly winds in the northern Adriatic. *International Journal of Climatology* **19**: 1205–1219. doi: 10.1002/(SICI)1097-008(199909)19:11<1205::AID-JOC405>3.0.CO;2-D.

----------, ----------. 2003. Recent near-surface wind changes in the central Mediterranean and Adriatic areas. *International Journal of Climatology* **23**: 963–973. doi: 10.1002/joc.925.

Prohaska F. 1976. The climate of Argentina. *World Survey of Climatology, Volume 12, Climates of Central and South America*. Schwerdtfeger, W (ed.). Amsterdam. 13–112.

Pryor SC, Barthelmie RJ, Riley ES. 2007. Historical evolution of wind climates in the USA. *Journal of Physics: Conference Series* **75**: 012065. doi:10.1088/1742–6596/75/1/012065.

----------, ----------, Young, DT, Takle ES, Arritt RW, Flory D, Gutowski WJ, Nunes A, Roads J. 2009. Wind speed trends over the contiguous United States. *Journal of Geophysical Research* **114**: D14105. doi:10.1029/2008JD011416.

----------, ----------. 2003. Long-term trends in near-surface flow over the Baltic. *International Journal of Climatology* **23**: 271–289. doi: 10.1002/joc.878.

----------, Ledolter J. 2010. Addendum to "Wind speeds trends over the contiguous United States". *Journal of Geophysical Research* **115**: D10103. doi: 10.1029/2009J D013281.

Ratisbona LR. 1976. The climate of Brazil. *World Survey of Climatology, Volume 12, Climates of Central and South America*. Schwerdtfeger, W (ed.). Amsterdam. 405–451.

Reboita MS, Gan MA, Rocha RP, Ambrizzi T. 2010. Precipitation regimes in South America: A bibliography review. *Revista Brasileira de Meteorologia* **25**: 185–204. doi: http://dx.doi.org/10.1590/S0102-77862010000200004.

----------, da Rocha RP, Ambrizzi T, Gouveia CD. 2015. Trend and teleconnection patterns in the climatology of extratropical cyclones over the Southern Hemisphere. *Climate Dynamics* **45**: 1929–1944. doi: 10.1007/s00382-014-2447-3.

Romanić D, Ćurić M, Jovičić I, Lompar M. 2015. Long-term trends of the 'Koshava' wind during the period 1949–2010. *International Journal of Climatology* **35**: 288–302. doi: 10.1002/joc.3981.

----------, Hangan H, Ćurić M. 2016. Wind climatology of Toronto based on the NCEP/NCAR reanalysis 1 data and its potential relation to solar activity. *Theoretical and Applied Climatology* **In press**: 1–17. doi: 10.1007/s00704-016-2011-7.

Ropelewski CF, Jones PD. 1987. An extension of the Tahiti–Darwin Southern Oscillation Index. *Monthly Weather Review* **115**: 2161–2165. doi: 10.1175/1520-0493(1987)115<2161%3AAEOTTS>2.0.CO%3B2.

Sahsamanoglou HS. 1990. A contribution to the study of action centres in the North Atlantic. *International Journal of Climatology* **10**: 247–261. doi: 10.1002/joc.3370100303.

Sansigolo CA, Kayano MT. 2010. Trends of seasonal maximum and minimum temperatures and precipitation in Southern Brazil for 1913–2006 period. *Theoretical and Applied Climatology* **101**: 209–216. doi: 10.1002/joc.3370100303.

Santos ATS, Silva CMS. 2013. Seasonality, interannual variability, and linear tendency of wind speeds in the northeast Brazil from 1986 to 2011. *The Scientific World Journal*. doi: http://dx.doi.org/10.1155/2013/490857.

Satyamurty P, Nombre CA, Silva Dias PL. 1998. South America, *Meteorology of the Southern Hemisphere*. Koroly, DJ, Vincent DG (eds.). Boston, Massachusetts, 119–139.

Schmidlin TW. 2009. Human fatalities from wind-related tree failures in the United States, 1995-2007. *Natural Hazards* **50**: 13–25. doi: 10.1007/s11069-008-9314-7.

Schoen JM, Ashley WS. 2011. A climatology of fatal convective wind events by storm type. *Weather and Forecasting* **26**: 109–121. doi: http://dx.doi.org/10.1175/2010WAF2222428.1

Schwerdtfeger W. 1976. Introduction. *World Survey of Climatology, Volume 12, Climates of Central and South America*. Schwerdtfeger, W (ed.). Amsterdam. 1–11.

Sen PK, 1968. Estimates of the regression coefficient based on Kendall's tau. *Journal of the American Statistical Association* **63**: 1379–1389.

Shenbin C, Yunfeng L, Thomas A. 2006. Climatic change on the Tibetan Plateau: Potential evapotranspiration trends from 1961–2000. *Climatic Change* **76**: 291–319. doi: 10.1007/s10584-006-9080-z.

Silva VPR. 2004. On climate variability in northeast of Brazil. *Journal of Arid Environments* **58**: 575–596. doi: http://doi.org/10.1016/j.jaridenv.2003.12.002.

Sinclair M. 1996. A climatology of anticyclones and blocking for the Southern Hemisphere. *Monthly Weather Review* **124**: 245–263. doi: http://dx.doi.org/10.1175/1520-0493(1996)124<0245:ACOAAB>2.0.CO;2.

----------. 1997. Objective identification of cyclones and their circulation intensity, and climatology. *Weather and Forecasting* **12**: 595–612. doi: http://dx.doi.org/10.1175/1520-0434(1997)012<0595:OIOCAT>2.0.CO;2.

Skansi MM, Brunet M, Sigró J, Aguilar E, Groening JAA, Bentancur OJ, Geier YRC, Amaya RLC, Jácome H, Ramos AM, Rojas CO, Pasten AM, Mitro SS, Jiménez CV, Martínez R, Alexander LV, Jones PD. 2013. Warming and wetting signals emerging from analysis of changes in climate extreme indices over South America. *Global and Planetary Change* **100**: 295 – 307. doi: https://doi.org/10.1016/j.gloplacha.2012.11.004.

Sprenger M, Martius O, Arnold J. 2013. Cold surge episodes over southeastern Brazil – At potential vorticity perspective. *International Journal of Climatology* **33**: 2758–2767. doi: 10.1002/joc.3618.

St. George S, Wolfe SA. 2009. El Niño stills winter winds across the southern Canadian Prairies. *Geophysical Research Letters* **36**: L23806. doi: 10.1029/2009GL041282.

Sun X, Cook KH, Vizy EK. 2017. The south Atlantic subtropical high: Climatology and interannual variability. *Journal of Climate* **30**: 3279–3296. doi: http://dx.doi.org/10.1175/JCLI-D-16-0705.1.

Taljaard JJ. 1967. Development, distribution and movement of cyclones and anticyclones in the Southern Hemisphere during the IGY. *Journal of Applied Meteorology and Climatology* **6**: 973–987. doi: http://dx.doi.org/10.1175/1520-0450(1967)006<0973:DDAMOC>2.0.CO;2.

----------. 1972. Synoptic Meteorology of the Southern Hemisphere. *Meteorology of the Southern Hemisphere*. Newton, CW (ed.). Boston, Massachusetts. 139–211.

Tang B, Tong L, Kang S, Zhang L. 2011. Impacts of climate variability on reference evapotranspiration over 58 years in the Haihe river basin of north China. *Agricultural Water Management* **98**: 1660–1670. doi: 10.1016/j.agwat.2011.06.006.

Teissereng de Bort L. 1883. Etude sur l'hiver de 1879–80 et re-cherches sur la position des centres d'action de l'atmosphere dans les hivers anormaux. *Bureau Central Meteorologique de France. Annales, 1881*, **4**: 17–62.

Troccoli A, Muller K, Coppin P, Davy R, Russell C, Hirsch AL. 2012. Long-term wind speed trends over Australia. *Journal of Climate*, **25**: 170–183. doi: http://dx.doi.org/10.1175/2011JCLI4198.1.

Tuller SE. 2004. Measured wind speed trends on the west coast of Canada. *International Journal of Climatology* **24**: 1359–1374. doi: 10.1002/joc.1073.

Vautard R, Cattiaux J, Yiou P, Thépaut J-N, Ciais P. 2010. Northern Hemisphere atmospheric stilling partly attributed to an increase in surface roughness. *Nature Geoscience* **3**: 756–761. doi: 10.1038/ngeo979.

Vincent LA, Petterson TC, Barros VR, Marino MB, Rusticucci M, Carrasco G, Ramirez E, Alves LM, Ambrizzi T, Berlato MA, Grimm AM, Marengo JA, Molion LC, Moncunill DF, Rebello E, Anunciação YMT, Quintana-Gomes J, Santos JL, Baez J, Coronel G, Garcia J, Trebejo I, Bidegain M, Haylock MR, Karoly D. 2005. Observed trends in indices of daily temperature extremes in South America 1960–2000. *Journal of Climate* **18**: 5011–5023. doi: http://dx.doi.org/10.1175/JCLI3589.1.

Viterbo P, Beljaars AC. 1995. An improved land surface parameterization scheme in the ECMWF model and its validation. *Journal of Climate* **8**: 2716 –2748. doi: http://dx.doi.org/10.1175/1520-0442(1995)008<2716:AILSPS>2.0.CO;2.

Vizy EK, Cook KH. 2016. Understanding long-term (1982–2013) multi-decadal changes in the equatorial and subtropical South Atlantic climate. *Climate Dynamics* **46**: 2087–2113. doi: 10.1007/s00382-015-2691-1.

von Engeln A, Teixeira J. 2013. A planetary boundary layer height climatology derived from ECMWF reanalysis data. *Journal of Climate* **26**: 6575–6590. doi: http://dx.doi.org/10.1175/JCLI-D-12-00385.1.

Vuille M. 1999. Atmospheric circulation over the Bolivian Altiplano during dry and wet periods and extreme phases of the Southern Oscillation. *International Journal of Climatology* **19**: 1579–1600. doi:10.1002/(SICI)1097 0088(19991130)19:14 WAF2222428.1.

Waliser DE, Gautier C. 1993. A Satellite-derived climatology of the ITCZ. *Journal of Climate* **6**: 2162–2174. doi: http://dx.doi.org/10.1175/15200442(1993)006<2162:ASDCOT>2.0.CO;2.

Wallace JM, Gutzler DS. 1981. Teleconnections in the geopotential height field during the Northern Hemisphere winter. *Monthly Weather Review* **109**: 784–812. doi: http://dx.doi.org/10.1175/1520-0493(1981)109<0784:TITGHF>2.0.CO;2.

Wan H, Wang, XL, Swail VR. 2010. Homogenization and trend analysis of Canadian near-surface wind speeds. *Journal of Climate* **23**: 1209–1225. doi: http://dx.doi.org/10.1175/2009JCLI3200.1.

Wernli H, Schwierz C. 2006. Surface cyclones in the ERA-40 Dataset (1958–2001). Part I: Novel identification method and global climatology. *Journal of Atmospheric Sciences* **63**: 2486–2507. doi: http://dx.doi.org/10.1175/JAS3766.1.

Wever N. 2012. Quantifying trends in surface roughness and the effect on surface wind speed observations. *Journal of Geophysical Research* **117**: D11104. doi: 10.1029/2011JD017118.

Whittaker LM, Horn LH. 1984. Northern Hemisphere extratropical cyclone activity for four mid-season months. *International Journal of Climatology* **4**: 297–310. doi: 10.1002/joc.3370040307.

Wu R, Hu Z-Z, Kirtman BP. 2003. Evolution of ENSO-related rainfall anomalies in East Asia. *Journal of Climate* **16**: 3742–3758. doi: http://dx.doi.org/10.1175/1520-0442(2003)016<3742:EOERAI>2.0.CO;2.

Xu M, Chang C-P, Fu C, Qi Y, Robock A, Robinson D, Zhang H. 2006. Steady decline of East Asian monsoon winds, 1969–2000: Evidence from direct ground measurements of wind speed. *Journal of Geophysical Research* **111**: D24111. doi: 10.1029/2006JD007337.

Yang S, Lau K-M, Kim K-M. 2002. Variations of the East Asian jet stream and Asian-Pacific-American winter climate anomalies. *Journal of Climate* **15**: 306–325. doi: http://dx.doi.org/10.1175/1520-0442(2002)015<0306:VOTEAJ>2.0.CO;2.

Yang X, Li ZX, Feng Q, He YQ, An WL, Zhang W, Cao WH, Yu TF, Wang YM, Theakstone W. 2012. The decreasing wind speed in southwestern China during 1969–2009 and possible causes. *Quaternary International* **263**: 71–84. doi: http://dx.doi.org/10.1016/j.quaint.2012.02.020.

Yin Y, Wu S, Chen G, Dai E. 2010a. Attribution analyses of potential evapotranspiration changes in China since the 1960s. *Theoretical and Applied Climatology* **101**: 19–28. doi: 10.1007/s00704-009-0197-7.

————, ————, Dai E. 2010b. Determining factors in potential evapotranspiration changes over China in the period 1971–2008. *Chinese Science Bulletin* **55**: 3329–3337. doi: 10.1007/s11434-010-3289-y.

You Q, Kang S, Flügel W-A, Pepin N, Yan Y, Huang J. 2010. Decreasing wind speed and weakening latitudinal surface pressure gradients in the Tibetan Plateau. *Climate Research* **42**: 57–64. doi: https://doi.org/10.3354/cr00864.

————, Fraedrich K, Min J, Kang S ,Zhu X, Pepine N, Zhanga L. 2014. Observed surface wind speed in the Tibetan Plateau since 1980 and its physical causes. *International Journal of Climatology* **34**: 1873–1882. doi: 10.1002/joc.3807.

Zarrin A, Ghaemi H, Azadi M, Farajzadeh M. 2010. The spatial pattern of summertime subtropical anticyclones over Asia and Africa: A climatological review. *International Journal of Climatology* **30**: 159–173. doi: 10.1002/joc.1879.

Zhao Z, Luo Y, Jiang Y. 2011. Is global strong wind declining?. *Advances in Climate Change Research* **2**: 225–228. doi: 10.3724/SP.J.1248.2011.00225.

Zheng X, Liu X, Liu C, Dai X, Zhu R. 2009. Assessing contribution to panevaporation trends in Haihe River Basin, China. *Journal of Geophysical Research* **114**: D24105. doi: 10.1029/2009JD0112203.

Zhou L-T, Wu R. 2010. Respective impacts of the East Asian winter monsoon and ENSO on winter rainfall in China. *Journal of Geophysical Research* **115**: D02107. doi: 10.1029/2009JD012502.

Zishka KM, Smith PJ. 1980. The climatology of cyclones and anticylones over North America and surrounding ocean environs for January and July, 1950–77. *Monthly Weather Review* **108**: 387–401. doi: http://dx.doi.org/10.1175/1520-0493(1980)108<0387:TCOCAA>2.0.CO;2.

Zuo H, Li D, Hu Y, Bao Y, Lü S. 2005. Characteristics of climate trends and correlation between pan-evaporation and environmental factors in the last 40 years over China. *Chinese Science Bulletin* **50**: 1235–1241. doi: 10.1007/BF03183699.

VITA

Joshua M. Gilliland was born in May 1986 and raised in Hartford, Ohio. He graduated from The Ohio State University in June 2009, where he earned a Bachelor of Science degree in Geography with a concentration in Atmospheric Sciences and a minor in Earth Sciences with a focus in Environmental Studies. Upon graduation, Josh enrolled at Western Kentucky and earned his Master of Science degree in Geosciences, with a graduate certificate in Geographical Information Sciences (GIS) in August 2011. His master thesis entitled, "A climatology of high-wind events associated with post-tropical cyclones in United States" examined the surface wind characteristics of post-tropical cyclones for the United States during 1951–2009. In 2012, Josh enrolled in the Department of Geography and Anthropology at Louisiana State University to pursue the Doctor of Philosophy degree in Geography. Since 2013, Josh has been an instructor for the Disaster Science Management (DSM) program through the Department of Geography and Anthropology at Louisiana State University. His current research interests are in physical geography, post-tropical (extratropical) meteorology, climatological assessment of high-wind events in North America, analyzing wind speed characteristics of South America, hazard mitigation, and GIS applications in atmospheric sciences and climatology.